OXFORD UNIVERSITY PRESS
AMEN HOUSE E.C. 4
LONDON EDINBURGH GLASGOW
LEIPZIG NEW YORK TORONTO
MELBOURNE CAPETOWN BOMBAY
CALCUTTA MADRAS SHANGHAI
HUMPHREY MILFORD
PUBLISHER TO THE
UNIVERSITY

CONSTITUTION OF ATOMIC NUCLEI AND RADIOACTIVITY

BY

G. GAMOW

OXFORD
AT THE CLARENDON PRESS
1931

PRINTED IN GREAT BRITAIN

To the
CAVENDISH LABORATORY
CAMBRIDGE

PREFACE

THE aim of this book is to give as complete an account as possible of our present experimental and theoretical knowledge of the nature of atomic nuclei. The book is written from the theoretical point of view and no details of experimental methods are given. References are given to the experimental papers from which numerical data are taken, but not to theoretical work. I am glad to express my thanks to PROF. N. BOHR and to my friends H. CASIMIR, F. HOUTERMANS, L. LANDAU, and N. F. MOTT for valuable advice concerning different questions treated in the book; also to MISS B. SWIRLES for the difficult work of revising the manuscript for publication in English.

G. G.

INSTITUTE FOR THEORETICAL PHYSICS,
COPENHAGEN.
1 *May* 1931.

CONTENTS

VALUES OF PHYSICAL CONSTANTS viii

I. THE CONSTITUENT PARTS AND ENERGY OF NUCLEI . 1–29
- § 1. Introduction 1
- 2. Classification of Nuclei 5
- 3. Energy of Binding of Nuclei (Mass Defect) . . . 13
- 4. Relative Abundance of Different Nuclei . . . 21
- 5. Nuclear Spin and Magnetic Moment 23

II. SPONTANEOUS DISINTEGRATION OF NUCLEI . 30–56
- § 1. Decay-constant and the Energy of Disintegration . . 30
- 2. General Features of α-disintegration 36
- 3. Penetration of Particles through Potential Barriers . . 38
- 4. General Theory of α-disintegration 42
- 5. Application to the Real Nuclei 47
- 6. Comparison with Experiments 50
- 7. General Features of β-disintegration 52

III. EXCITED STATES AND ELECTRO-MAGNETIC RADIATION OF NUCLEI 57–82
- § 1. Spectra of γ-rays 57
- 2. Fine Structure of α-particles and γ-rays . . . 63
- 3. Long Range α-particles and γ-rays 69
- 4. Probability of γ-emission 74
- 5. Secondary Electrons ejected from the Atom during Disintegration 76
- 6. The Anomalous Absorption of γ-rays 79

IV. ARTIFICIAL TRANSFORMATION OF NUCLEI . 83–114
- § 1. Anomalous Scattering of α-particles 83
- 2. General Theory of Inelastic Collisions . . . 86
- 3. Excitation of Nuclei by Collision with α-particles . . 91
- 4. Transformation of Nuclei by Collision with α-particles . 96
- 5. Comparison with Experiment. 99
- 6. Balance of Energy in Artificial Transformations . . 111

PERIODIC TABLE OF ELEMENTS . . . *at end*

VALUES OF PHYSICAL CONSTANTS*

Velocity of light .	$c = (2\cdot99796 \pm 0\cdot00004) \times 10^{10}$ cm. sec^{-1}.
Quantum constant .	$\hbar = \frac{h}{2\pi} = (1\cdot0420 \pm 0\cdot0013) \times 10^{-27}$ erg. sec.
Elementary charge .	$e = (4\cdot770 \pm 0\cdot005) \times 10^{-10}$ abs. E.S.U.
Mass of electron .	$m_e = (9\cdot035 \pm 0\cdot010) \times 10^{-28}$ gr.
Mass of proton . .	$m_p = (1\cdot6609 \pm 0\cdot0017) \times 10^{-24}$ gr.
Mass of α-particle .	$m_\alpha = (6\cdot598 \pm 0\cdot002) \times 10^{-24}$ gr.
Magnetic moment of electron . .	$\mu_e = (0\cdot9175 \pm 0\cdot0013) \times$
Magnetic moment of proton . . .	$\mu_p = (0\cdot4967 \pm 0\cdot0010) \times 10^{-23}$ erg. gauss^{-1}.
Radius of normal H-orbit . . .	$a_0 = (0\cdot5285 \pm 0\cdot004) \times 10^{-8}$ cm.
Reciprocal of fine-structure-constant .	$\frac{1}{\alpha} =$

To transfer:	**multiply by:**
Electron Volts into *Ergs* .	$\times 1\cdot5911 \times 10^{-12}$
into *Electron Volts* .	$\times 0\cdot6285 \times 10^{+12}$
Mass-Units $\left(\frac{He}{4}\right)$ into	$\times 1\cdot483 \times 10^{-3}$
rgs into *Mass-Units* $\left(\frac{He}{4}\right)$ . .	$\times 0\cdot6743 \times 10^{+3}$
Mass-Units $\left(\frac{He}{4}\right)$ into *Electron Volts*	$\times 0\cdot9321 \times 10^{+9}$
Electron Volts into *Mass-Units* $\left(\frac{He}{4}\right)$	$\times 1\cdot0729 \times 10^{9}$

Wave-length of light

$$\frac{1\cdot9628 \times 10^{-16}\ \text{cm.}}{\text{Energy of quanta (in ergs)}} \qquad \frac{1\cdot2336 \times 10^{-4}\ \text{cm.}}{\text{Energy of quanta (in volts)}}$$

$$\begin{cases} 1\ \text{X.U.} = 10^{-11}\ \text{cm.} \\ 1\ \text{Å} \quad = 10^{-8}\ \text{cm.} \\ 1\ \text{inch} = 2\cdot54\ \text{cm.} \end{cases}$$

R. T. Birge, *Phys. Rev.*, Suppl. I, 1, 1929.

THE CONSTITUENT PARTS AND THE ENERGY OF ATOMIC NUCLEI

§ 1. Introduction.

Since the nuclear model of the atom was first suggested by E. Rutherford in 1911 physical research has been mainly occupied with the investigation of the motion of the extra-nuclear electrons which are responsible for the main physical and chemical properties of the atom. In the work of N. Bohr and his school the quantum theory of atomic constitution has been brilliantly developed, and is now, with the help of the quantum mechanics of Heisenberg and Schrödinger, practically completed.

It very early became clear that the nucleus itself is not an elementary particle, but in its turn has a rather complicated structure. The discovery of radioactivity and its interpretation, due to Rutherford, as the spontaneous disintegration of atomic nuclei, show that the nuclei of heavy elements are not stable and can change into the nuclei of lighter elements, with the liberation of immense amounts of energy. Still later Rutherford succeeded in producing artificial disintegration of the usually stable nuclei of certain light elements by bombarding them with fast particles.

In accordance with the concepts of modern physics we assume that all nuclei are built up of elementary particles—protons and electrons. There is also no doubt that a very important part in the nuclear structure is played by α-particles, which are constructed from four protons and two electrons; the ejection of these particles is observed in the disintegration of heavy unstable nuclei. The extraordinarily large energy of binding of α-particles is responsible for the fact that even when there is strong interaction within the nucleus, the α-particles may be treated as individuals and do not split up into separate protons and electrons. The fact that the masses of different nuclei are always very nearly whole numbers, if we take as basis the mass of the helium nucleus,* seems to indicate that heavy nuclei are mainly constructed from α-particles. It gives rise to the classification of atomic nuclei into four classes, corresponding to the mass-numbers $4n$, $4n+1$, $4n+2$, $4n+3$, where n is an integer. In the

---

This does not hold if the H-nucleus is used as basis.

nuclei of the first type all the protons are supposed to be packed up into α-particles, while in the nuclei of the other types, one, two, or three '*loose protons*' are present, not packed into α-particles and therefore comparatively weakly bound. Here also we must distinguish between the '*loose nuclear electrons*' and those which are bound in the nuclear α-particles.

When we know the mass and charge of the nucleus it is easy to estimate the total number of α-particles, loose protons, and loose electrons in it. However, as we shall see later, it is not certain that all possible protons are packed into α-particles; there is quite definite evidence that in heavy nuclei there can be more than three loose protons without the formation of a new α-particle.* Nevertheless, we may retain the old classification for the formal description and systematization of the different types of nuclei.

It might seem that the structure of the nucleus could be explained in the same way as that of the atom by applying the principles of quantum mechanics, as developed so far, but this is only partially true. We can easily estimate from the dimensions of nuclei that the heavy constituents of the nucleus, protons, and α-particles have inside the nucleus velocities small compared with the velocity of light, and may, therefore, be expected to obey the laws of the unrelativistic quantum mechanics. This expectation is fulfilled; as we shall see later, no fundamental difficulties arise in the treatment of the heavy constituent parts of the nucleus by quantum mechanics.

∾ This is no longer true of the nuclear electrons. From Heisenberg's uncertainty principle we can estimate the uncertainty of the momentum p of an electron in the nucleus. This is defined by the relation

$$\Delta p > \frac{\hbar}{\Delta q} \tag{1}$$

where Δq is the uncertainty of a co-ordinate of the electron and $\hbar$ the quantum constant. The uncertainty of the co-ordinate is certainly smaller than the nuclear radius r_0, which, as we shall see later, can be taken to be of the order of magnitude 10^{-12} cm. Substituting these numerical values we have

$$\Delta p > \frac{\hbar}{\ } \cdot 10^{-15} \text{ erg. sec. cm}^{-1}.$$

---

* See an unpublished article by H. Casimir: 'Sind alle Tetraprotiden Alphiden?'.

∾ These signs mark the more speculative passages about nuclear electrons.

As is well known, we can apply non-relativistic mechanics if the momentum is small compared with the quantity mc, where m is the mass of the particle and c the velocity of light. For the proton and electron we have respectively:

$$m_p c = 4{\cdot}95\,.\,10^{-14}\ \text{erg. sec. cm}^{-1}.$$

and

$$m_e c = 1{\cdot}8\,.\,10^{-17}\ \text{erg. sec. cm}^{-1}.$$

Thus we see that for the nuclear proton the relativity correction may be practically neglected as the momentum is about fifty times smaller than $m_p c$. On the other hand, the motion of a nuclear electron must be treated relativistically since the velocity is practically equal to the velocity of light.*

The treatment of relativistic motion in quantum mechanics has presented very great difficulties up to now. Attempts have been made to generalize the non-relativistic quantum mechanics. Relativistically invariant wave-equations have been proposed by Dirac and have been successfully applied to the description of electron spin and many features of the relativistic motion of electrons in the atom. Nevertheless, Dirac's equations are not the complete solution of the problem; they can be successfully applied to the extra-nuclear electrons where the relativity corrections are small, but fail completely if applied to nuclear electrons. The difficulties arise particularly in connexion with the so-called 'states of negative energy'. Already in classical mechanics it was known that the relativistic equations of motion have two classes of solution, corresponding to positive and negative values of the 'Ruhenergie' $+mc^2$ or $-mc^2$; this is often interpreted as 'positive or negative mass'. The particles with negative total energy (or negative mass) would have very peculiar properties and have never been observed. For such particles the force and acceleration are directed in opposite directions. If two electrons, one of 'positive' and the other of 'negative mass', meet, then the first will be repelled and the second attracted to the other one; both electrons will fly away one behind the other with infinitely increasing velocity, giving an amusing picture of electronic races. In classical mechanics the two classes of solution are completely independent, and we can avoid the difficulty simply by assuming that the solutions with 'negative mass' do not correspond to any physical reality, so that we need only consider the solutions with positive mass. In wave mechanics, however, both types of solution are not completely separated, and transitions from one type of solution to the other are possible. From Dirac's equations we get that the probability for an electron of positive mass to jump spontaneously to a level of negative energy ($+mc^2 \rightarrow -mc^2$), with radiation of the difference of energy, is large, and the ordinary electron of positive mass would not exist for more than 10^{-11} sec. We notice here that this paradox appears to have certain analogies in nature. The so-called cosmic rays consist of light quanta* which have energies of the order of magnitude $m_p c^2$, as estimated from the absorption coefficient. If this is correct we must consider the possibility of the spontaneous annihilation of a proton and electron in which the total rest-energy is emitted in the form of very hard radiation; the probability of such a process must, however, be very small.

---

* From $p = mv \dfrac{1}{\sqrt{\left[1-\left(\frac{v}{c}\right)^2\right]}}$, where v is the velocity of the particle, we get for a nuclear electron $\dfrac{v}{c} = 0{\cdot}9998$.

This difficulty becomes particularly clear if we try to treat the problem of the reflection of a parallel beam of electrons at a high potential barrier by means of Dirac's equations. Suppose the electrons of given kinetic energy E to fall on a barrier due to a sudden rise of potential from zero up to a certain value U_0. If $U_0 > E$, we should expect all the electrons to be reflected from barrier. The solution of Dirac's equations for this simple problem shows that this is only true for values of U_0 below a certain value. If is greater than $E+2m_0c^2$, it is possible for an electron to penetrate into the potential barrier, changing the sign of its mass, and escape as a particle of 'negative mass' (Klein's paradox). The probability of this is great and a large percentage of the incident electrons would pass the potential barrier. From these considerations it follows, for example, that an electron could never stay in the nucleus. If we try to treat in this way the problem of an electron in a deep potential hole of the dimensions of

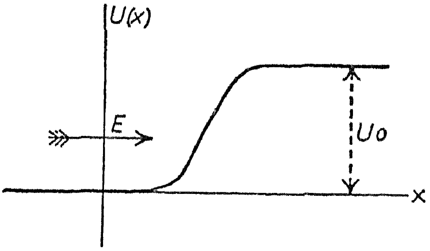

FIG. 1

---

* The question whether the cosmic rays consist of radiation or of very fast electrons is not, however, at present settled.

the nucleus we shall find that, although the electron has not sufficient energy to leave the hole as a particle of positive mass, it will nevertheless immediately escape by changing the sign of its mass.

In addition to these formal difficulties of relativistic quantum mechanics there are experimental facts which show that the problem can hardly be solved by some simple modification of the ordinary wave-equation. The usual ideas of quantum mechanics absolutely fail in describing the behaviour of nuclear electrons; it seems that they may not even be treated as individual particles (p. 27), and also the concept of energy seems to lose its meaning (p. 52). The problem of finding the equation of motion for a particle moving with a velocity comparable with that of light evidently cannot be solved without taking into account that also the interaction of particles is propagated with finite velocity c, that is, without first developing a quantum electrodynamics. These problems are also closely connected with the fundamental question of the origin of the discrete masses and charges of the elementary particles. We must hope that the future development of theoretical physics will enable us to answer these important questions and give a complete explanation of these obscure phenomena.

We should expect that, owing to the strong interaction between the nuclear electrons and the heavier constituents of the nucleus, it would be impossible to investigate theoretically any of the nuclear processes. Fortunately this is not so. For some unknown reason, although the electrons in the nucleus behave in a peculiar and obscure way, this does not affect very much the laws governing the motion of the nuclear α-particles and protons; we can treat nuclear processes involving only α-particles and protons independently of the presence of the nuclear electrons.

§ 2. Classification of Nuclei.

In the system of atomic nuclei each nucleus can be characterized by its mass and its electric charge. We have already seen that the masses of all nuclei are very nearly whole numbers if we take as basis the He-nucleus ($M_{He} = 4{\cdot}0000$). The charge is always an integral multiple of the charge of an electron. Thus we can ascribe to each nucleus two whole numbers, the *mass-number*, M, and the *charge-number*, Z. It is evidently possible to have several nuclei with the same charge but different mass (*isotopes*), and of the same mass but different charge (*isobares*).

We have now, mainly due to the investigations of Aston, very full information about the different nuclei. In Table I the complete list of nuclei known at present is given, arranged according to the charge-number.

TABLE I[1]

[The radioactive nuclei are marked by *; the round brackets indicate uncertain values]

Element.	Charge-number Z.	Mass-[2] number A.	Relative[3] abundance of isotopes.	Element.	Charge-number Z.	Mass-[2] number A.	Relative[3] abundance of isotopes.
H	1	1	100	O	8	16	c.100
He	2	4	100			17[7]	<0·03
Li	3	6	6			18[7]	~0·15
		7	94	F	9	19	
Be	4	8[4]	<0·1	Ne	10	20	
		9	c.100			21	
B	5	10	22			22	
		11	78	Na	11	23	
C	6	12	c.100	Mg	12	24	
		13[5]	<0·1			25	
N	7	14	c.100			26	
		15[6]	~0·1	Al	13	27	

---

[1] In recent letters to *Nature* (vol. cxxvi, p. 913 (1930); vol. cxxvii, pp. 233, 591 (1931)) Aston gives the isotopic constitution of Tungsten, Osmium, Ruthenium, and Rhenium:

W. Mass-Numbers: 182; 183; 184; 186.
Relat. abundance: 22·6; 17·2; 30·1; 30·0.
Mass-Numbers: 186; 187; 188; 189; 190; 192.
Relat. abundance: 1·0; 0·6; 13·5; 17·3; 25·1; 42·6.
Ru. Mass-Numbers: 96; (98); 99; 100; 101; 102; 104.
Relat. abundance: 5; (?); 12; 14; 22; 30; 17.
Rh. Mass-Numbers: 185; 187.
Relat. abundance: 38; 62.

[2] Aston, *Phil. Mag.*, vol. xlix, p. 1191 (1925).

[3] Aston, *Proc. Roy. Soc.*, A, vol. cxxvi, p. 511 (1930); vol. cxxx, p. 302 (1931); *Nature*, vol. cxxiii, p. 313 (1929).

When there are only two isotopes the relative percentage can be easily estimated from the chemical weight.

[4] Watson and Parker, *Phys. Rev.*, vol. xxxvii, p. 167 (1931).

[5] King and Bridge, *Nature*, vol. cxxiv, p. 182 (1929); *Astr. Journal*, vol. lxxii, p. 19 (1930).

[6] Meiring Naude, *Phys. Rev.*, vol. xxxvi, p. 333 (1930).

[7] Giauque and Johnston, *Nature*, vol. cxxiii, p. 318 (1929); vol. cxxiii, p. 831 (1929). Childs and Mecke, *Zs. f. Phys.*, Bd. 68, p. 362 (1931).

I (*cont.*)

Element.	Charge-number Z.	Mass-[1] number A.	R abundance of i
Si	14	28	
		29	
		30	
P	15	31	
S	16	32	
		33	
		34	
Cl	17	35	
		37	41
		39[3]	<1
Ar	18	36	
		40	
K	19	39	94·8
		41*	
Ca	20	40	
		44	
Sc	21	45	
Ti	22	48	
		(50)	
V	23	51	
Cr	24	50	4·9
		52	81·6
		53[4]	10·4
		54	
Mn	25	55	
Fe	26	54	
		56	
Co	27	59	
Ni	28	58	
		60	
Cu	29	63	
		65	
Zn	30	64	48·0
		65	2·5
		66	
		67	5·3
		68	17·1
		69	0·85
		70	0·38
Ga	31	69	
		71	

Element.	Charge-number Z.	Mass-[1] number A.	Relative[2] abundance of isotopes.
Ge	32	70	
		71	
		72	
		73	
		74	
		75	
		76	
		77	
As	33	75	
Se	34	74	
		76	
		77	
		78	
		80	
		82	
Br	35	79	
		81	
Kr	36	78	0·4
		80	2·5
		82	11·8
		83	11·8
		84	56·8
		86	16·7
Rb	37	85	
		87*	
Sr	38	86	
		88	
Y	39	89	
Zr	40	90	
		92	
		94	
		96	
Mo	42	92	14·2
		94	10·2
		95	15·5
		96[5]	17·8
		97	9·6
		98	23·0
		100	9·8
Ag	47	107	
		109	

[1], [2] See p. 6, nn. 2 and 3.

[3] Hettner and Böhme, *Naturwiss.*, Bd. 19, p. 252 (1931).

[4] Aston, *Nature*, vol. cxxvi, p. 200 (1930).

[5] Ibid., p. 348 (1930).

TABLE I (*cont.*)

Element.	Charge-number Z.	Mass-(1 number A.	Relative(3 abundance of isotopes.	Element.	Charge-	number	abun- of
Cd	48	110		Hg	80	200	23·8
		111				201	13·7
		112				202	29·3
		113				204	6·8
		114		Tl	81	203	30
		116				205	70
In	49	115				207*	
Sn	50	112	1·07			208*	
		114	0·74			210*	
		115	0·44	Pb	82	206	86·8
		116	14·19			207	9·3
		117	9·81			208	3·9
		118	21·48			(209)	
		119	11·02			210*	
		120	27·04			211*	
		121	2·96			212*	
		122	5·03			214*	
		4	6·19	Bi	83	209	
Sb	51	121				210*	
		123				211*	
Te	52	126				212*	
		128				214*	
		130		Po	84	210*	
I	53	127				211*	
Xe	54	124	0·1			212*	
		126	0·1			214*	
		128	2·3			215*	
		129	27·1			216*	
		130	4·2			218*	
		131	20·7				
		132	26·4	Em	86	220*	
		134	10·3			222	
		136	8·8	Ra	88	223*	
Cs	55	133				224*	
Ba	56	(136)				226*	
		138				228*	
La	57	139		Ac	89	227*	
Ce	58	140				228*	
		142		Th	90	227*	
Pr	59	141				228*	
Nd	60	142				230*	
		144				232*	
		(145)				234*	
		146		Pa	91	231*	
		196	0·1			234*	
		198	9·9				
		199	16·4	U	92	238*	

See p. 6, nn. 2 and 3.

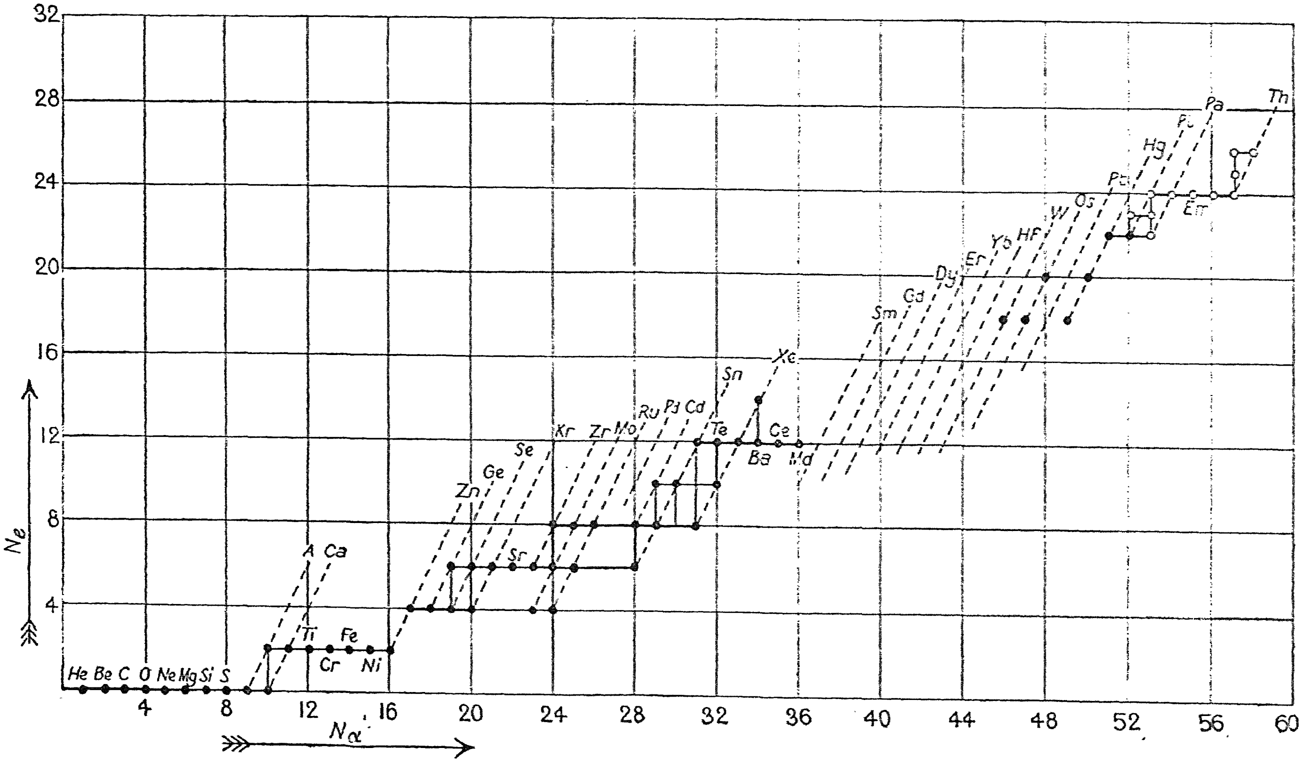

FIG. 2*a*. Number of loose electrons in the nuclei of 4*n*-type.

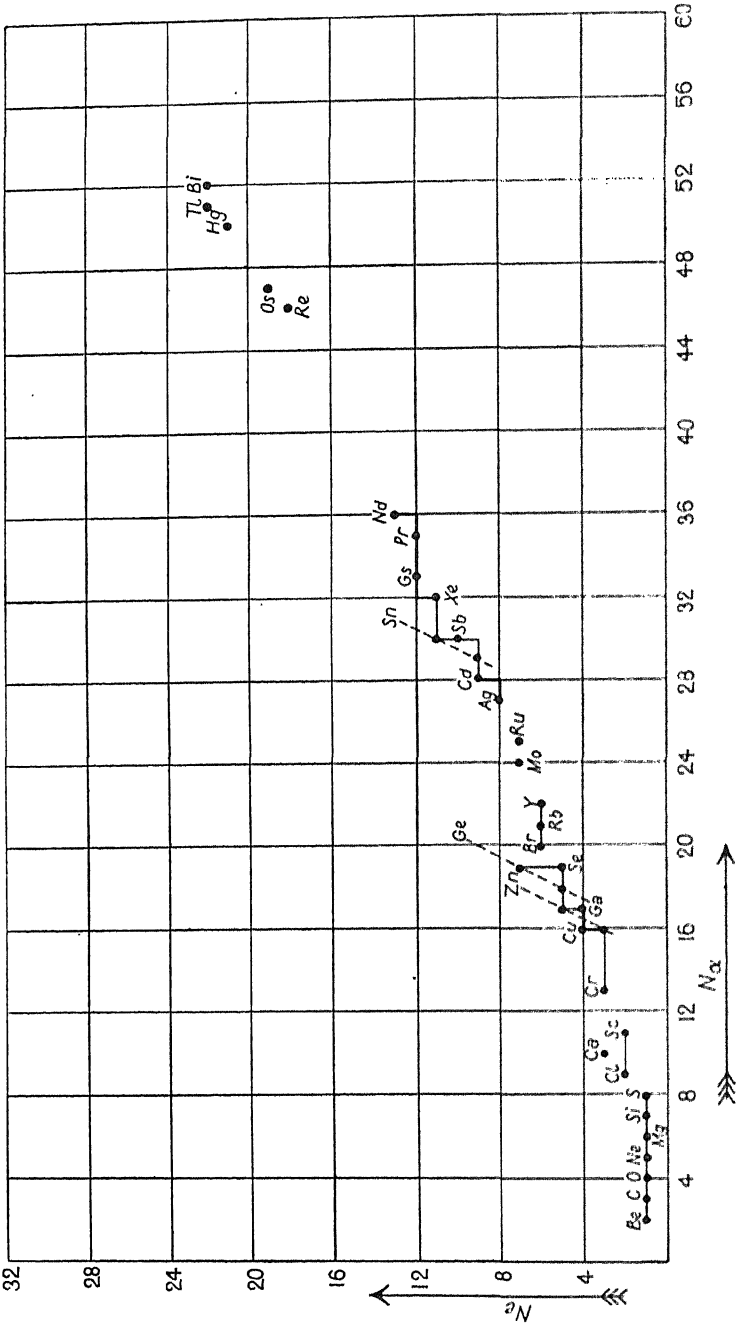

FIG. 2b. Number of loose electrons in the nuclei of $4n-1$-type.

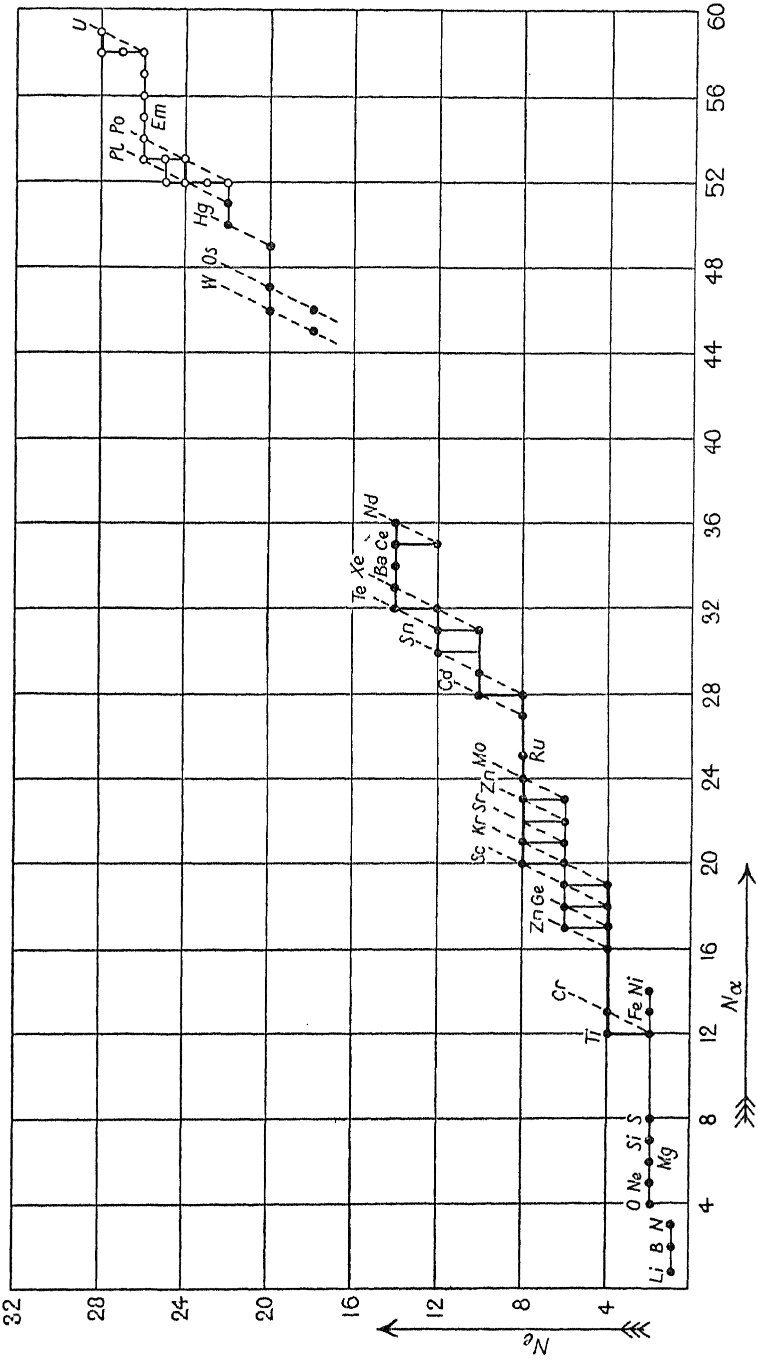

FIG. 2*c*. Number of loose electrons in the nuclei of $4n+2$-type.

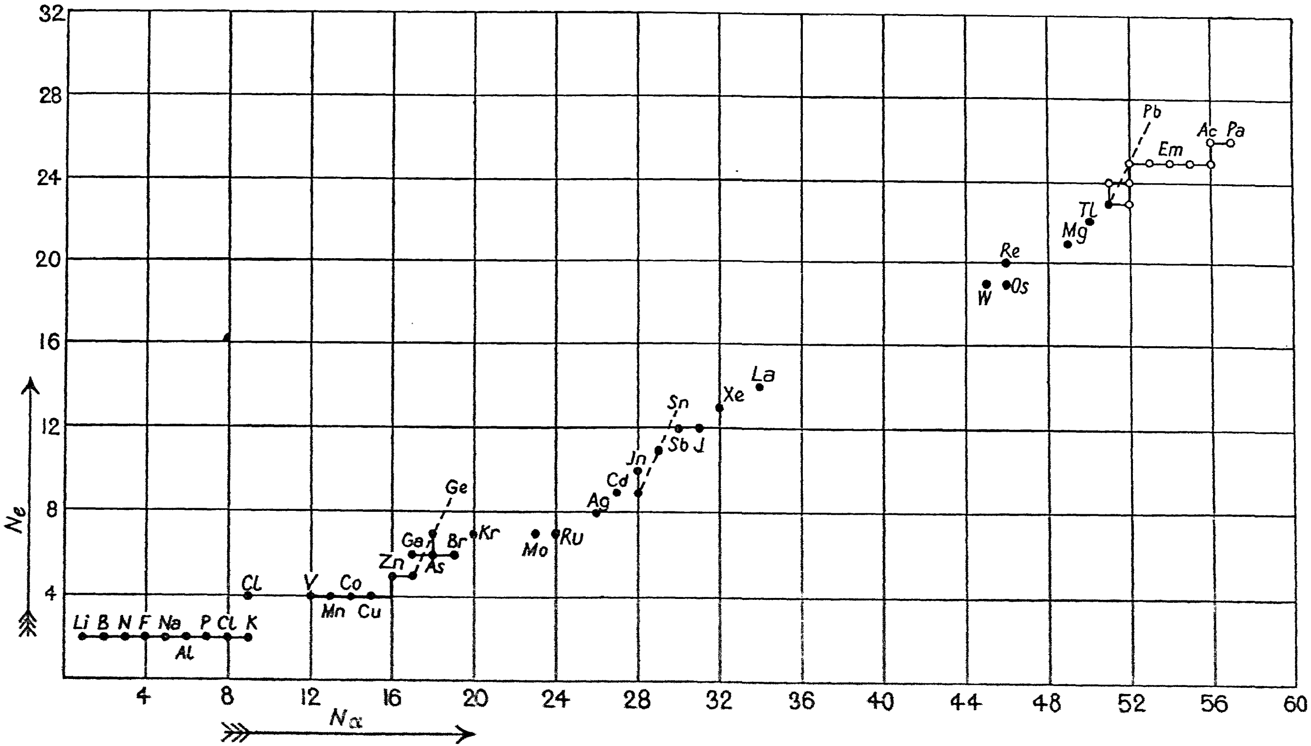

FIG. 2*d*. Number of loose electrons in the nuclei of $4n+3$-type.

From the mass- and charge-number of a given nucleus we can easily calculate the number of α-particles, N_α, of loose protons, N_p, and of loose electrons, N_e, from which the nucleus is constructed, if we make the hypothesis that there are never more than three protons. The result is shown in Fig. 2*a, b, c, d*, where the number of loose electrons in the nuclei of the four different classes is plotted against the number of α-particles. The figure is especially regular for nuclei of the $4n$-type. The number of nuclear electrons bound to the α-aggregate is always even, a new pair appearing at certain points. At such points we have two isobares with charge-numbers differing by two.

At those points where the new electron-shell is built up we may expect the existence of nuclei with very loosely bound and possibly unstable electrons; it is quite possible that the natural β-activity of certain light elements (K, $Z = 19$, $A = 39; 41$, and Rb, $Z = 37$, $A = 85; 87$), situated just near the jumps of the curves (Fig. 2), is connected with this instability.

§ 3. Energy of Binding of Nuclei (Mass-defect).

As complex nuclei are stable they must have a certain negative energy of binding, $-E$. According to the general principles of the theory of relativity, the mass of the nucleus is not equal to the sum of the masses of its constituent parts, but less than this by an amount:

$$\Delta M = \frac{E}{c^2} \qquad (2)$$

where c is the velocity of light. This *mass-defect* of complex nuclei can actually be deduced from the accurate measurements of atomic weight, carried out largely by Aston. For example, the mass of an α-particle, constructed from four protons ($m_H = 1{\cdot}6609 \times 10^{-24}$ gr.) and two electrons ($m_e = 9{\cdot}035 \times 10^{-28}$ gr.) is actually only $6{\cdot}598 \times 10^{-24}$ gr., whereas

$$4m_H + 2m_e = 6{\cdot}645 \times 10^{-24} \text{ gr.} \qquad (2')$$

The difference, $0{\cdot}047 \times 10^{-24}$ gr., corresponds to the energy of binding $42{\cdot}3 \times 10^{-6}$ erg. The large value of this energy helps us to understand why α-particles figure in the nucleus as indivisible units. In calculating the mass-defect of other complex nuclei, we shall treat them as constructed from α-particles as units, protons (not more than three), and electrons.

The exact values of the atomic weights of the elements investigated up till now, and the energies of binding calculated from them, are shown in Table II, A, B, C, D, and in Fig. 3, where the mass-defect of the four different types of nuclei is plotted against the number of α-particles.

TABLE II A

Nuclei of $4n$*-type.*

Name of the nucleus.	Charge number Z.	Number of α-particles N_α.	Number of loose electrons N_e.	Exact[1] atomic weight A.	Binding energy			Probable
					E in Mass-Units.	$E \times 10^{-6}$ volt.		
He_4	2	1	0	4·0000	—			
C_{12}	6	3	0	11·9971	0·0029	2·7	4·3	
O_{16}	8	4	0	15·9914	0·0086	8·2	12·7	
Ne_{20}	10	5	0	19·9892	0·0108	10	16·0	
A_{36}	18	9	0	35·957	0·043	40	64	
A_{40}	18	10	2	39·949	0·051	48	76	
Cr_{52}	24	13	2	51·920	0·080	75	119	
Zn_{64}	30	16	2	63·903	0·097	91	144	
Kr_{80}	36	20	4	79·883	0·117	109	174	
Kr_{84}	36	21	6	83·883	0·117	109	174	
Mo_{100}	42	25	8	99·891	0·109	102	162	
Sn_{112}	50	28	6	111·858	0·142	133	211	±50
Sn_{116}	50	29	8	115·852	0·148	138	219	
Sn_{120}	50	30	10	119·847	0·153	143	227	
Sn_{124}	50	31	12	123·842	0·158	147	234	
Xe_{124}	54	31	8	123·867	0·133	124	197	
Xe_{128}	54	32	10	127·863	0·137	128	203	
Xe_{132}	54	33	12	131·859	0·141	131	209	
Xe_{136}	54	34	14	135·855	0·145	135	215	
Hg_{196}	80	49	18	195·910	0·090	84	133	
Hg_{200}	80	50	20	199·908	0·092	86	136	
Hg_{204}	80	51	22	203·906	0·094	87	139	±90
Pl_{208}	82	52	22	207·905	0·095	89	141	

TABLE II B

Nuclei of $4n+1$-

Name of the nucleus.	Charge number Z.	Number of α-particles N_α.	Number of loose electrons N_e.	Exact atomic weight A.	Binding energy			error
					E in Mass-Units.	$E \times 10^{-6}$ volt.	$E \times 10^{6}$ erg.	
C_{13}	6	3	1	12·87	0·011	10·7	16·3	
Cl_{37}	17	9	2	36·960	0·047	44	70	±
Br_{81}	35	20	6	80·882	0·125	116	186	±30
Sn_{117}	50	29	9	116·853	0·154	143	228	±52
Sn_{121}	50	30	11	120·846	0·161	150	239	±53
Hg_{201}	80	50	21	200·908	0·099	92	147	±89

---

[1] Atomic weights are calculated on the basis He → 4·0000. The exact values are taken from Aston's paper: *Proc. Roy. Soc.*, A, vol. cxv, p. 487 (1927); and from his later publications (see references to the Table I). The value for O^{18} is from spectroscopic measurements of the bands of O_2 by Mecke and Wurm, *Zs. f.* Bd. 61, p. 37 (1930); the recent measurements of Babcock and Birge, Phys. vol. xxxvii, p. 233 (1931), give a considerably lower value: 0·018 M.U.

TABLE II C

Nuclei of $4n+2$-type.

Name of the nucleus.	Charge number Z.	Number of α-particles N_α.	Number of loose electrons N_e.	Exact atomic weight A.	Binding energy			Probable error in 10^{-6} erg.
					E in Mass-Units.	$E\times 10^{-6}$ volt.	$E\times 10^{6}$ erg.	
Li_6	3	1	1	6·009	0·006	5·6	8·9	±3·7
B_{10}	5	2	1	10·008	0·007	6·5	10·4	±3·8
N_{14}	7	3	1	14·000	0·015	14	22	±6
O_{18}	8	4	2	(17·981)	(0·034)	(31)	(49)	±18
Ne_{22}	10	5	2	21·993	0·022	21	33	±8
Ni_{58}	28	14	2	57·911	0·104	97	154	±27
Kr_{78}	36	19	4	77·884	0·131	122	194	±36
Kr_{82}	36	20	6	81·883	0·132	123	196	±31
Kr_{86}	36	21	8	85·883	0·132	123	196	±33
Mo_{98}	42	24	6	97·892	0·123	114	182	±30
Sn_{114}	50	28	8	113·856	0·159	148	236	±50
Sn_{118}	50	29	10	117·850	0·165	154	245	±53
Sn_{122}	50	30	12	121·845	0·170	159	252	±55
Xe_{126}	54	31	10	125·865	0·150	140	222	±56
Xe_{130}	54	32	12	129·861	0·154	143	228	±58
Xe_{134}	54	33	14	133·857	0·158	147	234	±59
Hg_{198}	80	49	20	197·909	0·106	99	157	±89
Hg_{202}	80	50	22	201·907	0·108	101	160	±90
Pl_{206}	82	51	22	205·905	0·110	103	163	±92

TABLE II D

Nuclei of

Name of the nucleus.	Charge number Z.	Number of α-particles N_α.	Number of loose electrons N_e.	Exact atomic weight A.	Binding energy			Probable error in 10^{-6} erg.
					E in Mass-Units.	$E\times 10^{-6}$ volt.	$E\times 10^{6}$ erg.	
Li_7	3	1	2	7·008	0·014	13	21	±4
B_{11}	5	2	2	11·005	0·017	16	25	±4
F_{19}	9	4	2	18·990	0·032	30	47	±6
P_{31}	15	7	2	30·966	0·056	52	83	±12
Cl_{35}	17	8	2	34·964	0·058	54	86	±13
As_{75}	33	18	6	74·894	0·128	120	190	±28
Br_{79}	35	19	6	78·886	0·136	127	202	±30
Kr_{83}	36	20	7	82·882	0·140	131	208	±31
Sn_{115}	50	28	9	114·854	0·168	157	249	±53
Sn_{119}	50	29	11	118·849	0·173	162	257	±55
I_{127}	53	31	12	126·864	0·158	147	234	±56
Xe_{131}	54	32	13	130·860	0·162	151	240	±58
Hg_{199}	80	49	21	198·909	0·113	106	168	±89
Pl_{207}	82	51	23	206·905	0·117	109	174	±92

We see that the energy decreases with increasing complexity of the nucleus, reaching a minimum for N_α about equal to 30. This minimum gives rise to a serious difficulty in the interpretation of nuclear stability. For if the curve as marked by the experimental

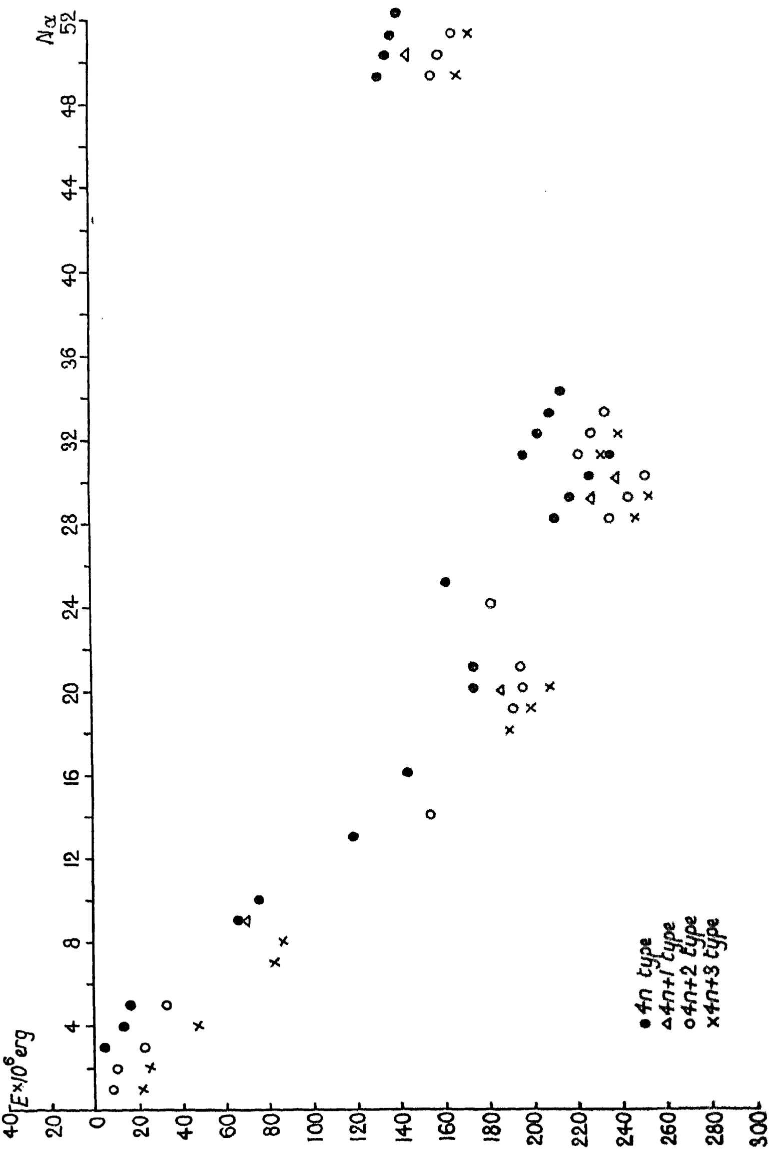

FIG. 3. Mass-defect curve (relative to α-particles).

points goes up again for nuclei of mass-number greater than 120 ($N_\alpha > 30$) we have to expect spontaneous α-disintegration for elements of atomic mass greater than 120, as the ejection of an α-particle is accompanied by the liberation of energy. The rate of such transformations, which can be approximately estimated from the known energy-difference, would be rather rapid, and the radioactivity of these elements should be easily observed. Actually, as we know, none of the elements with atomic weight between 120 and 208 is found to be radioactive.

We shall investigate more carefully the question of the contribution of the different constituents of the nucleus to the total energy of binding and the precise shape of the mass-defect curve, marked in this region ($120 < M < 208$) only very roughly by the few known experimental points. We shall at first treat the nucleus built from a number N_α of α-particles only. This holds for the first ten elements of atomic mass $4n$. For the heavier elements, as shown by Fig. 2, a certain number of free nuclear electrons is always present. To explain the possibility of a stable configuration of positively charged α-particles we must assume some attractive forces which come into play only for a close approach of two α-particles and overbalance at short distances the forces due to electrostatic repulsion. We have experimental evidence of the presence of these forces from the investigations of the anomalous scattering of α-particles in helium for very close collisions. The important point for the development of a nuclear model, constructed from a number of α-particles, is the question of the quantum numbers to be ascribed to the different α-particles. The solution of this question is simple; all α-particles in the nucleus must be considered to be in the same state of lowest energy. This is due to the fact that the Pauli exclusion principle, which requires the electrons in the atom to be distributed in different shells, is not applicable to α-particles since they have an even charge. It can be shown from general principles of quantum mechanics that the Pauli principle need only be applied to a collection of similar particles, each constructed from a certain number of protons and electrons, when the total number of protons and electrons in each is an odd number, or, in other words, when the resultant charge of each particle is odd.* Since the number of α-particles on the same level is unlimited, we should expect that in an unexcited nucleus all the α-particles are in the same state of lowest energy, that is, on the first quantum level.

---

* Recently the validity of these theoretical considerations as applied to the nuclei has become doubtful (see p. 27). We can, however, be sure that the Bose statistics

In examining such a collection of particles, all with equal energies and attracting each other with forces decreasing very rapidly with the distance, without a predominating central body, we have a problem different from that of the extra-nuclear structure. The behaviour of such an aggregate must be rather similar to that of a small drop of liquid, where no forces act on a particle inside the drop, but very strong forces come into play when the particle approaches the boundary (surface tension). Although no exact theory of such an aggregate can be worked out at present (due partly to our ignorance of the law of force at small distances and partly to mathematical difficulties in the treatment of such a complex system), the general properties of such a model for the nucleus may be easily obtained. First of all we may expect that the volume of such an aggregate would be almost proportional to the number of particles, so that the nuclear radius would vary approximately as the cube root of the mass-number; this conclusion agrees more or less with the experimental evidence. The potential inside such a model must be more or less constant inside the nucleus and increase sharply at the boundary, the distribution forming a 'potential hole' of the shape shown in Fig. 4a.

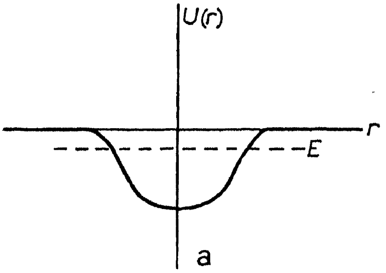

FIG. 4a

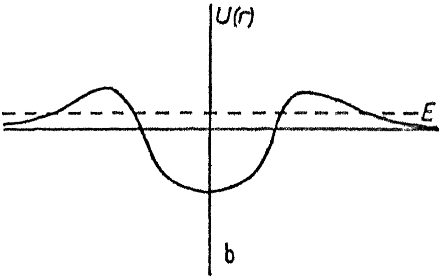

FIG. 4b

The total energy of such a model is roughly proportional to the total number N_α of α-particles. We must now take into account the additional energy due to the Coulomb forces. These forces will not

---

must be applied for α-particles, from direct experimental evidence: the investigations of helium-band-spectra have shown that the nuclei in the helium-molecule must be described by symmetrical wave-functions (p. 26).

change very much the distribution of potential inside the nucleus where the attractive forces predominate. The effect of the repulsive forces is to reduce the value of the potential at greater distances from the centre, giving rise to a 'potential barrier' (Fig. 4 *b*).

The additional energy due to the electrostatic energy of the particles can be estimated as the energy of a sphere of radius $r_0 \sim R_0 \sqrt[3]{(N_\alpha)}$ ($R_0 = 2{\cdot}2 \times 10^{-13}$ cm.) and charge $+2eN_\alpha$. Thus we have for the total energy of the model,

$$E \sim -CN_\alpha + \frac{(2eN_\alpha)^2}{r_0} \sim -CN_\alpha + \frac{(2e)^2}{R_0} N_\alpha^{5/3}. \tag{3}$$

For small values of N_α this formula gives negative decreasing energies; for a certain N_α it reaches a minimum, so that a nucleus constructed from a larger number of α-particles would be unstable. As we have already said, this formula may be applied only to the first ten nuclei of the $4n$-type which, according to the usual theory, are the only ones constructed entirely of α-particles. If we choose the coefficient C so as to fit the mass-defects of the first few elements, we find that the curve reaches a minimum round about $N_\alpha = 20$, so that an aggregate of a greater number of α-particles would be unstable; this is not important, however, as for the actual nuclei of heavier elements ($N_\alpha > 10$) the loose electrons must be taken into account in the discussion of stability.

We do not at present know much about the properties of electrons inside the nucleus and we must be prepared to meet with difficulties; therefore we can hardly expect at present to understand all the peculiarities of the energy-curve as they doubtless depend on the properties of the nuclear electrons. However, certain possibilities may be discussed, the validity of which depends entirely on the degree to which the usual concept of energy may be applied to electrons inside the nucleus.

We have seen that for $N_\alpha = 10$ the first stable electron-level appears in the nucleus, two electrons being bound to the original α-aggregate. As such a combination of α-particles and two electrons is stable for $N_\alpha > 10$, its energy-curve must lie beneath the curve for the bare α-aggregate. The two curves are represented in Fig. 5 crossing one another near $N_\alpha = 10$. The next electron-shell appears at $N_\alpha = 16$, so that the curve $N_\alpha + 4e$ must cross the previous curve near this point. The lowest parts of the curves (shown by black circles) represent stable nuclei, while the inside branches give either unstable elements with two electrons ready to escape (left-hand branches) or the 'ionized' nuclei ready to absorb one or more pairs of electrons (right-hand branches). We see that, owing to the addition of electrons, the stable (descending) part of the curve can be continued much further than for a bare α-aggregate.

The most interesting part of the experimental energy-curve is the ascending branch, for $N_\alpha > 30$. It seems that the nuclei in this region must inevitably be unstable. For this region, however, the experimental knowledge is rather scanty, as most of the mass-defects and even isotopic numbers have not yet been measured. The only moderately accurate values are those for Hg and Pb, which show the general increase of the energy for $N_\alpha > 30$. We can try to account for the existence of stable nuclei in this region, in spite of the average increase of the energy, by assuming that the energy-curves are of the type shown in Fig. 5 (Region II). We see that the nucleus 'A' can eject neither an α-particle (transformation to 'C') nor two electrons (transformation to 'B'), since both processes are endothermic and cannot occur spontaneously without the introduction of external

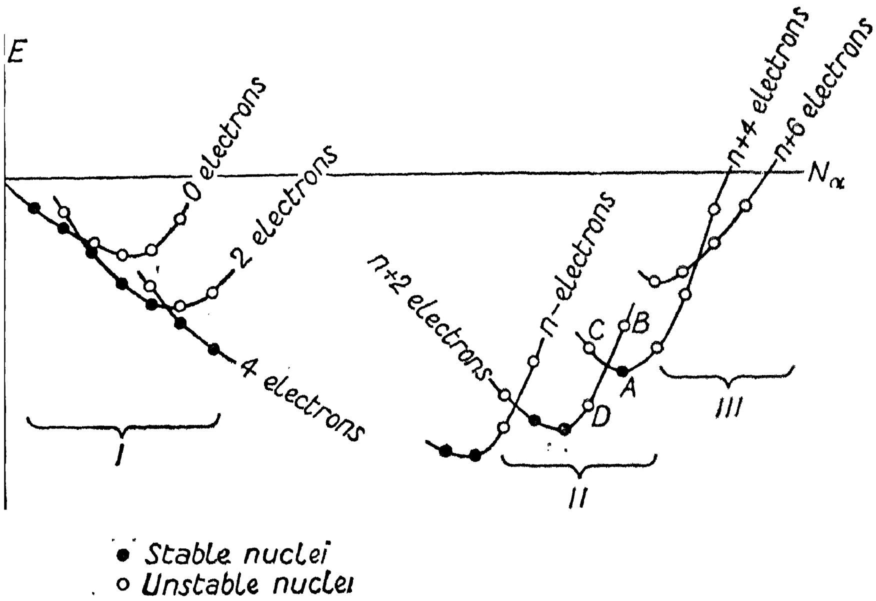

FIG. 5. Hypothetical shape of mass-defect curve.

energy. The only possible transformation is to 'D' with simultaneous ejection of an α-particle and two electrons, but, as it is easy to see, the probability of such a double disintegration is extremely small. We may expect some gaps in the series of isotopic numbers corresponding to the unstable region; unfortunately, the isotopes in this region have not been investigated sufficiently completely, and we cannot, therefore, give any experimental proofs of the accuracy of these deductions.

In the region of radioactive elements the mass-defect curve can be drawn without difficulty, as the differences of the energy of binding of successive radioactive nuclei can be directly estimated from the known energy liberated in each α- or β-transformation. If we draw the curves for nuclei containing the same number of free electrons it will be seen that there are three ascending branches, crossing one another near the β-disintegrating products. It is seen from the figure that there is a possibility of a single transformation with liberation of energy, from one curve to another at the joints. This differs from the state of affairs in the Region II, where the only possibility is a highly improbable double disintegration.

§ 4. Relative Abundance of Different Nuclei.

Another interesting question connected with the general constitution of atomic nuclei is that of the relative abundance of different types of nuclei in the universe; this gives us information about the relative stability of different nuclei. The abundance of different elements depends not only on the special properties of their nuclei but also on the cosmological factors governing the origin of the elements. The chemical analysis of the universe (in practice of the earth's crust and of meteorites) gives us only the abundance of different chemical elements. As most elements are a mixture of several isotopes, a knowledge of the proportions of different isotopes of a given element is necessary in order to know the relative abundance of different kinds of nuclei. In Fig. 6 the logarithm of the abundance of different nuclei is plotted against the mass-number. We see that nuclei of the type $4n$ occur much more frequently than nuclei of other types (Harkins's rule). The rarest are the nuclei of the type $4n+1$, which is evidently connected with the fact that, as we have seen from the mass-defect curves, the proton in nuclei of this type is very loosely bound. Considerations based on the relative abundance of the elements are

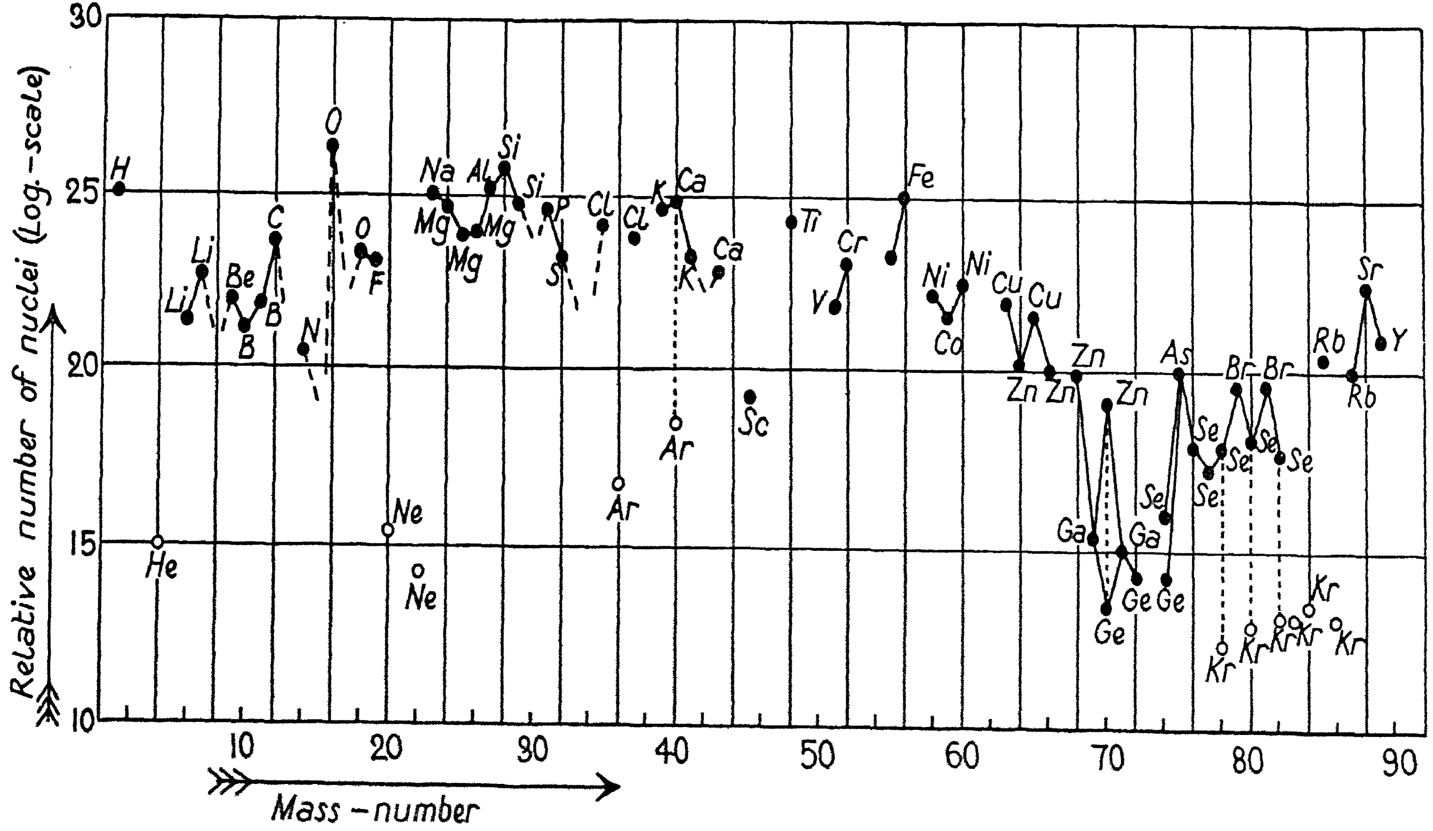

Fig. 6. Relative abundance of different nuclei (in earth-crust).

interesting, but not of very great importance for the theory of nuclear constitution, as the observed abundance depends also on astronomical and geological factors.

§ 5. Nuclear Spin and Magnetic Moment.

If we treat the nucleus as a whole, the most important characteristics, besides the mass- and charge-numbers, are its properties of symmetry and its angular momentum and magnetic properties. We know that the 'position' of an elementary particle (proton or electron) is characterized by four quantities: three space co-ordinates, x, y, z, and the spin co-ordinate σ $(= \pm\frac{1}{2})$.

According to Pauli's exclusion principle, the wave-functions describing the motion of a system of identical elementary particles must be anti-symmetrical in all four co-ordinates of the particles.

For example, if we have a system of two electrons, as in the helium atom, the corresponding wave-functions may be divided into two classes. The wave-function may be symmetrical in the space co-ordinates and anti-symmetrical in the spin co-ordinates, so that the electrons have spins in opposite directions; or it may be anti-symmetrical in the space co-ordinates and symmetrical in the spin co-ordinates, so that the electrons have spins in the same direction.

If now we have a system of identical complex particles, each constructed from a certain number of elementary particles (for example, atomic nuclei), we cannot know *a priori* whether the wave-functions describing the system should be symmetrical or anti-symmetrical in the co-ordinates of the complex particles, that is, whether the Einstein-Bose or Fermi-Dirac statistics should be applied.

It can be shown from the general principles of quantum mechanics that the wave-functions must be anti-symmetrical or symmetrical according as the number of elementary particles in each complex particle is odd or even. The angular momentum 'i' of such a complex particle must also be an odd or even multiple of the angular momentum, $\frac{1}{2}$, of an elementary particle (assuming that the quantum mechanics holds for the elementary particles).

For example, consider a molecule constructed from two identical atoms. The wave-functions corresponding to the different quantum states of the molecule must be anti-symmetrical in the co-ordinates of the atomic electrons; if the nuclei have no spin the wave-function must be either symmetrical or anti-symmetrical in the space co-ordinates of the nuclei, according to the type of the nucleus. From the analysis of the band-spectra of such molecules it is always possible to find out the kind of symmetry in the co-ordinates of the nuclei. If the nucleus has a spin i, solutions either symmetrical or anti-symmetrical in the space-coordinates of the nuclei may exist, just as for the helium atom considered above. The observed band-spectra may be divided into two classes, corresponding to parallel or anti-parallel nuclear spins. As each of these possibilities may be realized in several ways, we should expect the two types of bands to have intensities proportional to the statistical weights. *Simple considerations show that there are more solutions corresponding to the case of parallel spins than to that of anti-parallel spins. The intensity ratio of the two kinds of bands is*

$$\frac{W\uparrow\uparrow}{W\uparrow\downarrow}=\frac{i+1}{i} \tag{5}$$

where 'i' is the value of the nuclear spin. As the intensity of the bands can only be estimated very roughly experimentally, the formula (5) will help us to determine the nuclear spin only when the spin is small, and consequently the alternate lines of the band have sufficiently different intensities. If the band-spectrum of such an element is analysed, we can determine whether the solution corresponding to parallel spins is also symmetrical in the space co-ordinates of the nuclei or not, that is, whether the nuclei obey the Einstein-Bose or the Fermi-Dirac statistics.

Another more valuable method for determining the nuclear spin consists in the study of the hyperfine structure of atomic spectra. As the spin of the nucleus can be orientated in different ways relative to the orbital motion of the electrons, each simple energy-level of the ordinary scheme will be split up into a number of sub-levels very close together. We shall see later that the magnetic moment of the nucleus is much less than that of the electron; consequently the separation of the energy-levels will be considerably less than that due to the electronic spin (fine-structure) and can only be observed by using very powerful spectroscopic apparatus. Let j be the total angular momentum of the electrons (constructed from the orbital momenta and the spin), and i the angular momentum of the nucleus. The resultant angular momentum $f=j+i$ may have different values corresponding to the relative orientations of the vectors j and i.

Applying the rules of addition of quantum vectors we see that f can take a set of values

$$\begin{aligned} &f_0 = j+i, f_1 = j+i-1, \ldots, f_{2i} = j-i \qquad (j \geqslant i) \\ &f_0 = i+j, f_1 = i+j-1, \ldots, f_{2j} = i-j \qquad (j \leqslant i). \end{aligned} \tag{6}$$

Thus, owing to the nuclear spin, each simple energy-level will be split into $2i+1$ *or* $2j+1$ *sub-levels according as* $i \leqslant j$ *or* $i \geqslant j$. The relative distances between the different sub-levels can be estimated, assuming that the additional energy due to the interaction of the nuclear and electronic spins is proportional to the scalar product $(i \,.\, j)$. Simple calculations show that *the relative energy differences between neighbouring hyperfine structure-levels are given by the interval rule*

$$f_0 : f_1 : f_2 : \ldots : f_{min}+1$$

where f_r *is defined by the formulae* (6).*

The most direct method of determining the nuclear spin is the investigation of the splitting of spectral lines in a very strong magnetic field, when the Paschen-Back effect takes place.† *In such strong fields the nuclear spin 'i' will be orientated independently of 'j', and each component of the ordinary Zeeman triplet will be split into* $2i+1$ *components. This defines the nuclear spin directly without requiring any knowledge of the angular momenta of the atomic electrons.* Owing to experimental difficulties the nuclear spin has been investigated for a few elements only. The results obtained from band-spectra on the one hand and from hyperfine structure on the other do not always agree. These inconsistencies may be due to the uncertainty of the experimental data, or to the wrong interpretation of the observed facts; there is also the possibility that we meet here new factors not taken into account in the previous discussion (see p. 29). We must hope that experimental work in the near future will help to rid the

---

* As an example of the application of these rules we give the analysis of the hyperfine structure of Pr, for which the energy-level $^6K_7$ corresponding to $j = 7$ is shown to be split into six close sub-levels with relative energy differences 19·0 : 16·7 : 14·4 : 12·7 : 10·4. As the number of sub-levels is less than $2j+1 (= 15)$ we conclude that in this case $i < j$ and the relation $2i+1 =$ gives directly $i = \frac{5}{2}$. For these values of j and i the functions f become

$$\frac{19}{2} : \frac{17}{2} : \frac{15}{2} : \frac{13}{2} : \frac{11}{2}$$

in good agreement with the observed values.

† In strong magnetic fields the complex splitting of the lines (anomalous effect) degenerates into the simple splitting into three lines (normal Zeeman effect). This is known as the Paschen-Back effect.

theory of contradictions. Table III shows the results obtained from the analysis of the intensity-change in the band-spectra of the different elements investigated.

TABLE

Name of the element.	Nuclear constituent parts.	Kind of symmetry.	Nuclear spin 'i'	
			from bands.	from hyperfine structure.
H	$0\alpha+1p+0e$	antisymmetrical	$\frac{1}{2}$	
He	$1\alpha+0p+0e$	symmetrical	0	
Li	$1\alpha+2p+1e$ $1\alpha+3p+2e$		>1	$0;\ \frac{3}{2}$
C	$3\alpha+0p+0e$		0	
N	$3\alpha+2p+1e$	symmetrical (!)	$\frac{2}{2}$	
O	$4\alpha+0p+0e$		0	
F	$4\alpha+3p+2e$		$\frac{1}{2}$	
Na	$5\alpha+3p+2e$		$\sim\frac{5}{2}$	$>\frac{1}{2}$
Cl	$8\alpha+3p+2e$ $9\alpha+1p+2e$		$\sim\frac{5}{2}$	
Mn	$13\alpha+3p+4e$			$\sim\frac{5}{2}$
Br	$19\alpha+3p+6e$ $20\alpha+1p+6e$			$\sim\frac{3}{2}$
Rb	$21\alpha+1p+6e$ $21\alpha+3p+8e$			>0
Cd	$27\alpha+2p+8e$ $27\alpha+3p+9e$ $28\alpha+0p+8e$ $28\alpha+1p+9e$ $28\alpha+2p+10e$ $29\alpha+0p+12e$			$0;\ \frac{1}{2}$
Sb	$30\alpha+1p+10e$ $30\alpha+3p+12e$			$\sim\frac{5}{2}$
I	$31\alpha+3p+12e$		$>\frac{5}{2}$	
Cs	$33\alpha+1p+12e$			>0
La	$34\alpha+3p+14e$			$\frac{7}{2}$
Pr	$35\alpha+1p+12e$			$\frac{5}{2}$
Tl	$50\alpha+3p+22e$ $51\alpha+1p+22e$			$\frac{1}{2};\ \frac{1}{2}$
Pb	$51\alpha+2p+22e$ $51\alpha+3p+23e$ $52\alpha+0p+22e$			$0;\ \frac{1}{2}$
Bi	$52\alpha+1p+22e$			$\frac{9}{2}$

---

[1] For literature about estimation of nuclear spin from hyperfine structure band-intensity change see Goudsmit and Pauling, *Structure of Line-spectra*, Chap. XI (1930), and Kronig, *Band Spectra and Molecular Structure*, Chap. III (1930). For the most recent references see Schüler and Keyston, *Zs. f. Phys.*, Bd. 68, p. 174 (1931).

From the results obtained we see that protons have the same spin ($\frac{1}{2}$) as electrons, and obey the Fermi-Dirac statistics. On the other hand α-particles (helium nuclei) have no spin, and obey the Einstein-

Bose statistics, as we should expect for a particle constructed from an even number of electrons and protons.*

∾ A difficulty arises over nitrogen: since the nucleus contains an odd number of elementary particles (14 protons and 7 electrons) we should expect the wave-functions to be anti-symmetrical (see p. 23). Experiment, however, seems to show positively that the wave-functions of the nuclei in the nitrogen molecule are symmetrical. This is in striking disagreement with the theory. *It seems to show that the nuclear electrons do not count in the statistics of the system*; either, for some reason as yet unknown, the nuclear electrons must be described by symmetrical wave-functions, or we must give up the idea of assigning space co-ordinates to the electrons inside the nucleus. At present nitrogen is the only element for which this difficulty has arisen, but it seems probable that it is true in general that *the statistics of the nucleus depend only on the total number of protons in it.* We see that there is not enough experimental material for us to draw any definite conclusions about the spin of the nucleus. It seems, however, that *nuclei with an even number of protons always have an even spin (e.g. He, C, N, O), while those with an odd number of protons have an odd spin. This indicates that the nuclear electrons do not make any contribution to the total angular momentum of the nucleus.* It is possible that these two facts—that the electrons do not affect either the statistics or the total spin of the nucleus—are connected by a theorem of quantum mechanics, as yet unproved, that the statistical properties of a complex particle are uniquely determined by its angular momentum. ∾

From the study of the angular momentum of the nucleus we may try to draw conclusions about the number of loose protons in the nucleus. As the α-particle itself has no spin we should expect all the nuclear α-particles to be in the lowest energy-level with zero angular momentum; the observed nuclear spin must be ascribed to the angular momenta and spins of the protons. In the Li-nucleus, for example, on the hypothesis that all possible protons are packed into α-particles, we must assume three loose protons. If we suppose two of them to be on the first nuclear-level with orbital angular momentum $j = 0$, their spins must be in opposite directions and the resulting momentum vanishes. The third proton must be on the next level with $j = 1$, and we get the right value for the spin of the Li-nucleus if we suppose that the spin of this proton is orientated parallel to the orbital angular momentum. A similar interpretation of the spins of other nuclei meets with difficulties which are especially serious for heavy elements. For example, the Bi-nucleus has a spin $i = \frac{9}{2}$, for which we have to account by means of one proton alone, since the Bi-nucleus is of the $4n+1$ type. This seems to indicate that all possible protons are not packed into α-particles and there are 5 or perhaps even 9 loose protons. On the other hand the Tl-nucleus, which differs from that of Bi by one α-particle, has a spin $i = \frac{1}{2}$. This should mean that if an α-particle is added to the Tl-nucleus, for example by capture with radiation, the α-particle will be split up into its constituent parts.

---

* The fact that α-particles are described by symmetrical wave-functions may be taken as an experimental proof that they are complex particles, since, according to the general principles of quantum mechanics, an elementary particle must always have a spin.

The absolute value of the separation of the sub-levels in the hyperfine structure depends on the value of the magnetic moment of the nucleus, or more exactly on the projection of the magnetic moment on the direction of the nuclear spin. The additional energy of an extra-nuclear electron due to the magnetic moment of the nucleus can be found by the general theory of perturbations to be

$$\Delta E = \tfrac{8}{3}\pi\mu_e\mu_p\, g(i)[f(f+1)-i(i+1)-\tfrac{3}{4}]\Psi^2(0) \tag{7}$$

for an S-term ($l = 0$) and

$$\Delta E = \frac{l(l+1)}{j(j+1)}\mu_e\mu_p\, g(i)[f(f+1)-i(i+1)-j(j+1)]\int\frac{1}{\sqrt{3}}\Psi\overline{\Psi}\,dv \tag{7'}$$

for higher terms ($l > 0$). Here l, j are the orbital angular momentum and the total angular momentum of the electron, i is the nuclear spin, and f the resultant angular momentum of the nucleus and electron together; f takes different values for different sub-levels (see p. 25). The magnetic moment of the nucleus is taken to be $g(i)\,\mu_p$, where $\mu_p = \frac{\mu_e}{1840}$ is the magnetic moment of the proton. We may call μ_p a proton magneton; $g(i)$, from analogy with atomic may be called Landé's factor for the nucleus. In order to calculate ΔE from the formulae (7, 7′) a knowledge of the wave-function Ψ for the term in question is necessary. For atoms with more than one electron these solutions cannot be written in an analytical form, and must be calculated by some numerical method such as Hartree's. As the formulae (7, 7′) are very sensitive to small variations of Ψ, no great accuracy can be expected from these calculations. The evaluation of $g(i)$ from the measured separation of the hyperfine structure-levels has been done up to now only for a very few nuclei. The results are given in Table IV.

TABLE

Values of $g(i)$ for different nuclei

$i =$	$\frac{1}{2}$	$\frac{2}{2}$	$\frac{3}{2}$	$\geqslant 1$
Element.				
Li$^{(2}$	—	—	2·1	—
Na$^{(3}$	2·1	2·9	3·1	4·1
Rb$^{(3}$	1·1	1·4	1·6	2·2
Cs$^{(3}$	0·9	1·2	1·4	1·9

[1] For the alkali metals for which the calculations have been made, the value of the nuclear spin i is not known (except Li). This is why in Table IV the values of $g(i)$ are calculated for different values of i.

[2] Breit, *Phys. Rev.*, vol. xxxvi, p. 1262 (1930).

[3] Fermi, *Zs. f. Phys.*, Bd. 60, p. 320 (1930).

∾ The fact that the separation of the hyperfine structure-levels is always much smaller than the separation of the ordinary fine structure-levels, due to the spin of the extra-nuclear electrons, shows that *the electrons lose their magnetic moment in the nucleus or at least that it has no apparent effect.* ∾

Besides the magnetic moment there are other factors which may influence the separation of the hyperfine structure-levels. Among such factors is a possible electrical moment of the nucleus and also the quantum-mechanical resonance between the nucleus and the extra-nuclear electrons.* However, the fact that for most elements investigated the relative distances of the sub-levels obey the interval rule (6, 6′), so that the additional energy is proportional to the nuclear spin, seems to show that the factor of greatest importance in explaining hyperfine structure is the magnetic moment of the nucleus. There are too few data at present available for us to draw any more definite conclusions about the regularities of the magnetic moments of different nuclei.

---

* See Fermi, Solvay Congress (1930); Schüler and Keyston, *Naturwiss.*, Bd. 19 p. 320 (1931).

II

SPONTANEOUS DISINTEGRATION OF NUCLEI

§ 1. Decay-constant and the Energy of Disintegration.

We have already seen that in radioactive disintegration two different kinds of particles, α and β, are emitted. In the α-disintegration the charge-number of the nucleus decreases by two and the mass-number by four; in the β-disintegration the charge-number is increased by one and the mass-number remains unchanged. In both cases the resulting nucleus belongs to the same nuclear class (see p. 1) as the original one, so that we may naturally divide the radioactive bodies into four independent families. Actually, only three of these families are known: the Thorium family $(4n)$; the Uranium family $(4n+2)$; and the Actinium family $(4n+3)$. The failure to detect a radioactive family of the type $4n+1$ is evidently due to the very rare occurrence of elements of this type in general. Each radioactive family, starting from a certain heavy element, undergoes a succession of α- and β-transformations leading to a certain stable final product on the boundary of the stable elements. The stable products of the three known families all have (accidentally?) the same charge-number and are isotopes of lead. In the figure the schemes of the known radioactive families are shown:

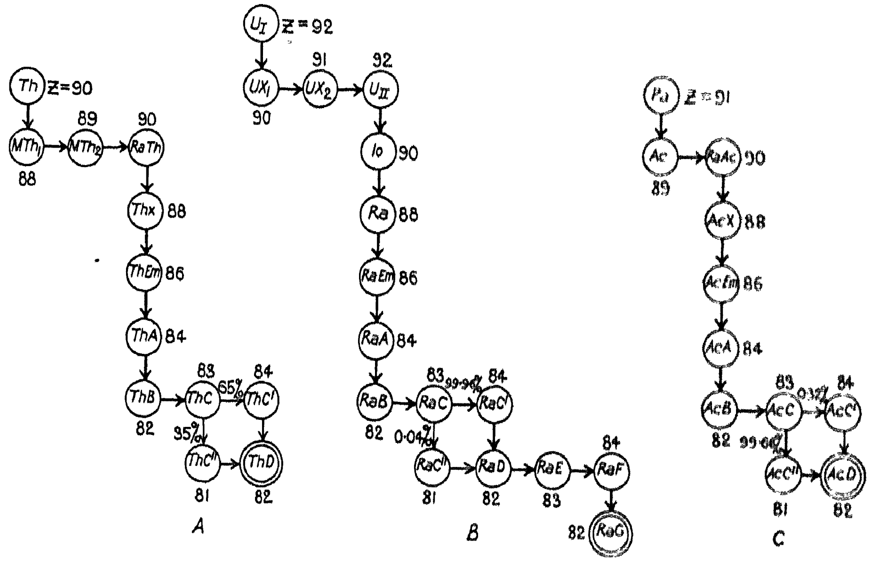

. 7. Schemes of radioactive families.

We notice that a continuous series of α-transformations is sometimes interrupted by two successive β-transformations. The forking of radioactive families observed usually in C-products, when two different kinds of disintegration are possible for the nucleus, is especially interesting. The percentage of nuclei undergoing one transformation or the other is defined by the relative probabilities of these two processes.

One of the most important characteristics of a decaying nucleus is its *decay constant* (usually denoted by λ), giving the probability of disintegration per unit time. If N_0, N are the numbers of not yet disintegrated nuclei at times t_0 and t, the number of disintegrations in the interval $(t, t+dt)$ will be given by

$$-dN = \lambda N dt. \tag{1}$$

Integrating, we have $$N = e^{-\lambda(t-t_0)}N_0, \tag{1'}$$

which gives the exponential decrease of the amount of the radioactive body in question. The decay constant λ has a quite definite value for each radioactive body, and varies within very wide limits from 10^{-18} sec^{-1}. to $> 10^{+5}$ sec^{-1}., the average life, λ^{-1} varying from thousands of millions of years to a small fraction of a second.

When multiple decay occurs, the observed decay constant is constructed from the constants of the individual disintegrations. If λ_α and λ_β are the probabilities of the two kinds of disintegration, we have for the total number of disintegrated atoms

$$-dN = \lambda_\alpha N dt + \lambda_\beta N dt = (\lambda_\alpha + \lambda_\beta) N dt, \tag{2}$$

which shows that the resulting decay constant will be simply the sum of the two individual constants. The relative numbers of atoms disintegrated in the two ways is evidently given by

$$N_\alpha = \frac{\lambda_\alpha}{\lambda_\alpha + \lambda_\beta} N \quad \text{and} \quad N_\beta = \frac{\lambda_\beta}{\lambda_\alpha + \lambda_\beta} N. \tag{2'}$$

If we measure the total decay constant $\lambda_{\alpha\beta}$ and the relative percentages of the two different kinds of particles, α and β, we can easily calculate the individual decay constants from the formulae:

$$\lambda_\alpha = \frac{\lambda_{\alpha\beta}}{1 + \dfrac{N_\beta}{N_\alpha}}; \qquad \lambda_\beta = \frac{\lambda_{\alpha\beta}}{1 + \dfrac{N_\alpha}{N_\beta}} \tag{2''}$$

The decay constants of different radioactive bodies are given in the fourth columns of Tables II and IV.

Another important characteristic of radioactive decay is the *energy of disintegration*. The energy can be emitted from the decaying nucleus either in the form of kinetic energy of α- or β-particles or in the form of electro-magnetic radiation (γ-rays).

The energy of the α-particles can be directly estimated by measuring the deviation of a beam of α-particles in a known magnetic field (magnetic spectra). In this way it has been shown that the beam of α-particles emitted by a given radioactive body is extremely homogeneous, all the particles having exactly the same velocity. Recently the existence of several weak but well-defined groups other than the main one has been proved for some elements; we shall return to this question in the next chapter. As a standard of the energy of α-particles those from RaC′ are used, since their velocity was measured with special care by Briggs and found to be $1{\cdot}923 \, . \, 10^9$ cm./sec. The direct estimation of the energy of α-particles by the method of magnetic deflection has been done up to the present for only a few radioactive elements; the most reliable data are shown in Table I.

TABLE I

Name of the element.	Velocity of α-particles $V_\alpha \times 10^{-9}$ $\frac{\text{cm.}}{\text{sec.}}$.	Energy of α-particles $E_\alpha 10^6$ erg.	Energy of disintegration.	
			$E \times 10^6$ erg.	$E \times 10^{-6}$ volt
ThC′ [1]	2·059	13·99	14·26	8·97
RaC′ [2]	1·923	12·20	12·43	7·82
ThCα_0 [1]	1·710	9·65	9·83	6·18
ThCα_1 [1]	1·704	9·58	9·76	6·14
RaA [1]	1·693	9·46	9·64	6·07
RaF [3]	1·592	8·36	8·52	5·36

[1] C. Rosenblum, *C. R.*, vol. cxc, p. 1124 (1930) (see also § 2, Chap. III).

[2] G. H. Briggs, *Proc. Roy. Soc.*, A, vol. cxiv, p. 371 (1927); vol. cxviii, p. 557 (1928).

[3] Laurence, *Proc. Roy. Soc.*, A, vol. cxxii, p. 543 (1929).

In most experimental work it is usual to express the energy of α-particles by their power to penetrate through matter. If a beam of α-particles passes through matter, the particles gradually lose their energy in collisions with the atomic electrons and will be stopped at a certain distance. The intensity of the beam does not decrease exponentially, as in absorption of electro-magnetic waves, but stays approximately constant up to a certain distance where it decreases abruptly. At the end of the beam there is a straggling, the length of each individual track having an error-distribution round a certain value R_0. This average distance of penetration is called the *mean range* of the α-particle in a given substance under given conditions. Ranges are usually given in centimetres for standard air, that is, air at 15° C. and 760 mm. pressure. In most older work the so-called *extrapolated ranges* are given, defined by the intersection of the tangent at the steepest place of the curve with the range axis. In modern work, using differential electric counters, the mean ranges are always directly found. To calculate the mean range from the extrapolated range we must know the breadth of the straggling curve. Using the experimental data on this subject* we find that the mean range in standard air can be calculated from the extrapolated range, using the formula

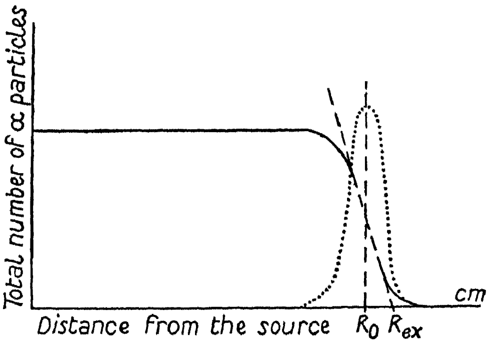

FIG. 8

$$R_0 = R_{ex} - 0{\cdot}044\sqrt{(R_{ex})}\text{ cm.} \tag{3}$$

The relation between the range and the energy of α-particles was initially studied by Geiger, who found the empirical relation that the range varies very nearly as the energy to the power of 3/2. Taking the mean range and the energy of the α-particles from RaC′ to be 6·854 cm. and 12·20 . 10^{-6} erg., we may write Geiger's relation in the form

$$E = [3{\cdot}382\,.\,10^{-6}R_0^{2/3} + \delta(R_0)]\text{ erg.,} \tag{4}$$

where $\delta(R_0)$ is a small correction vanishing for $R_0 = 6{\cdot}8$ cm. In Fig. 9 the deviations $\delta(R_0)$ are shown for elements for which the energy of the α-particles has been found directly by magnetic deviation. In calculating the energy from the range we must use the formula (4), taking the small correction directly from Fig. 9. Practically all elements have a range in between the experimental points in Fig. 9, and the small correction can be obtained fairly accurately by interpolation. For the calculation of the energy for the so-called long-range particles emitted by certain radioactive elements we must extrapolate the curve for greater ranges. The extrapolated part in Fig. 9 is calculated from the formula taken from Bohr's theory of the stopping-power of matter for α-particles:

---

* G. H. Briggs, *Proc. Roy. Soc.*, A, vol. cxiv, p. 313 (1927).

$$R_0 = \frac{AE^2}{\log(BE^{\frac{1}{2}})}.$$

The values of the coefficients $A = 2{\cdot}211.10^{10}$, $B = 865$ are chosen to fit the curve with the experimental points for RaC′ and ThC′. As the result of extrapolation the energies given by the curve for long ranges cannot be very reliable.

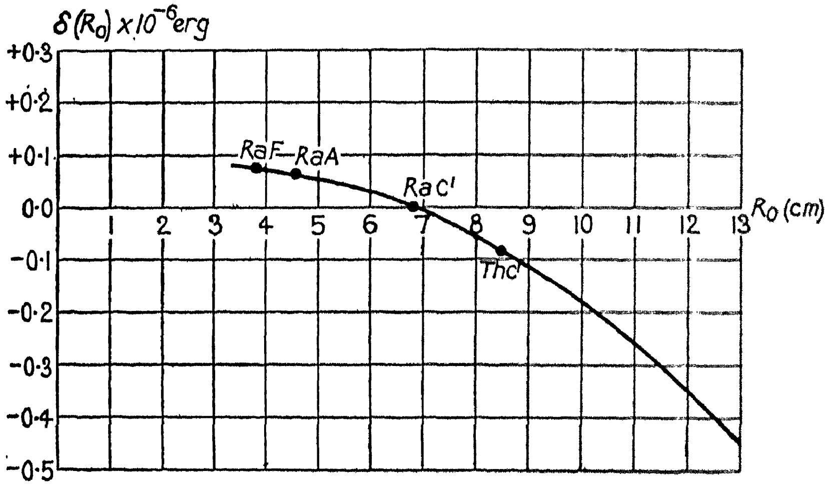

FIG. 9

The most complete list of extrapolated ranges of α-particles of different elements was given by Geiger; in this book we shall take these as standard values (see Table II). The corresponding values of the mean ranges, calculated according to (4), and the corresponding energies are given in the next two columns of the same table. To know the *total energy* of α-disintegration we must also take into account the kinetic energy of the recoil atom; the total energies are given in the last column of Table II.

If we compare the energies of different α-disintegrations with the corresponding decay constants we perceive a very interesting regularity; the decay constant increases very rapidly with increasing energy of disintegration. Plotting $\log\lambda$ against the energy of

TABLE II

Name of the element.	Mass-number M.	Charge-number Z.	Decay[1] const. λ sec^{-1}.	R_{ex} (cm.) (15°C.; 760 mm.)	R_0 (cm.) (15°C.; 760 mm.)	Velocity of α-particles $V_\alpha \times 10^{-9}$ $\frac{\text{cm.}}{\text{sec.}}$	Energy of α-particles $E_\alpha \times 10^6$ erg.	Energy of disintegration (with recoil).	
								$E \times 10^6$ erg.	$E \times 10^{-6}$ volt.
Th	232	90	1·33 . 10^{-18}	2·59 [2]	2·52	1·39	6·34	6·45	4·06
RaTh	228	90	1·16 . 10^{-8}	4·019 [3]	3·930	1·603	8·48	8·63	5·43
ThX	224	88	2·20 . 10^{-6}	4·354 [3]	4·261	1·647	8·95	9·11	5·73
ThEm	220	86	1·27 . 10^{-2}	5·063 [3]	4·963	1·731	9·89	10·07	6·33
ThA	216	84	4·78	5·683 [3]	5·577	1·798	10·67	10·87	6·84
ThCa_0	212	83	1·54 . 10^{-5} [4]	4·787 [3]	4·691	**1·710** [6]	**9·65**	**9·83**	**6·18**
ThCa_1			5·11 . 10^{-5} [4]			**1·704** [6]	**9·58**	**9·76**	**6·14**
ThC′	212	84		8·617 [3]	8·487	**2·059** [6]	**13·99**	**14·26**	**8·97**
U_1	238	92	4·8 . 10^{-18}	2·70 [7]	2·63	1·41	6·56	6·67	4·19
U_{11}	234	92		3·28 [7]	3·20	1·50	7·43	7·56	4·75
Io	230	90	2·9 . 10^{-13}	3·194 [3]	3·115	1·487	7·30	7·43	4·67
Ra	226	88	1·373 . 10^{-11}	3·389 [3]	3·307	1·515	7·57	7·71	4·85
RaEm	222	86	2·097 . 10^{-6}	4·122 [3]	4·032	1·617	8·63	8·79	5·53
RaA	218	84	3·78 . 10^{-3}	4·722 [3]	4·626	**1·693** [6]	**9·46**	**9·64**	**6·07**
RaCa_0	214	83	1·34 . 10^{-7} [4]	4·145	4·055 [5]	1·620	8·66	8·82	5·55
RaCa_1			0·44 . 10^{-7} [4]	3·958	3·868 [5]	1·595	8·40	8·55	5·38
RaC′	214	84	4·2 . 10^{+5}	6·971 [3]	6·854	**1·923** [6]	**12·20**	**12·43**	**7·82**
RaF	210	84	5·88 . 10^{-8}	3·925 [3]	3·837	**1·592** [6]	**8·36**	**8·52**	**5·36**
Pa	235	91	1·80 . 10^{-12}	3·673 [3]	3·588	1·557	8·00	8·14	5·12
RaAc	231	90	4·24 . 10^{-7}	4·676 [3]	4·580	1·686	9·38	9·55	6·01
AcX	227	88	7·16 . 10^{-7}	4·369 [3]	4·276	1·649	8·97	9·13	5·74
AcEm	223	86	1·77 . 10^{-1}	5·789 [3]	5·682	1·808	10·97	11·17	7·03
AcA	219	84	4·74 . 10^{+2} [4]	6·584 [3]	6·470	1·888	11·76	11·98	7·53
AcCa_0	215	83	4·39 . 10^{-3} [4]	5·511	5·411 [5]	1·780	10·46	10·65	6·70
AcCa_1			0·96 . 10^{-3}	5·091	4·991 [5]	1·734	9·92	10·10	6·35
AcC′	215	84		6·49 [8]	6·38	1·88	11·65	11·87	7·46

---

[1] E. Rutherford, J. Chadwick and C. D. Ellis, *Radiations from Radioactive Substances* (Cambridge, 1930). For the value of λ for RaC′ see Jacobsen, *Phil. Mag.* vol. xlvii, p. 23 (1924); Barton, *Phil. Mag.*, vol. ii, p. 1273 (1926).

[2] G. H. Henderson and J. L. Nickerson, *Phys. Rev.*, vol. xxxvi, p. 1344 (1930).

[3] Geiger, *Zs. f. Phys.*, Bd. 8, p. 45 (1922).

[4] The decay constants are calculated from the total α-decay constant of C-products and the relative intensities of α-fine structure components.

[5] E. Rutherford, F. A. B. Ward, and C. E. Wynn-Williams, *Proc. Roy. Soc.*, A, vol. cxxix, p. 211 (1930).

[6] See references for Table I.

[7] Laurence, *Phil. Mag.*, vol. v, p. 1028 (1928).

[8] L. F. Bates and J. S. Rogers, *Proc. Roy. Soc.*, A, vol. cv, p. 37 (1924).

disintegration E we get almost straight lines, different for the different radioactive families but parallel to each other (Fig. 10). This regularity is known as the Geiger-Nuttall rule. As we can see from the figure, there are certain deviations from this rule; for example, the point for AcX does not lie on the smooth curve. It has also been shown that the points on the Geiger-Nuttall graph do not actually lie on a straight line but are much better represented by a curve slightly concave to the E axis.

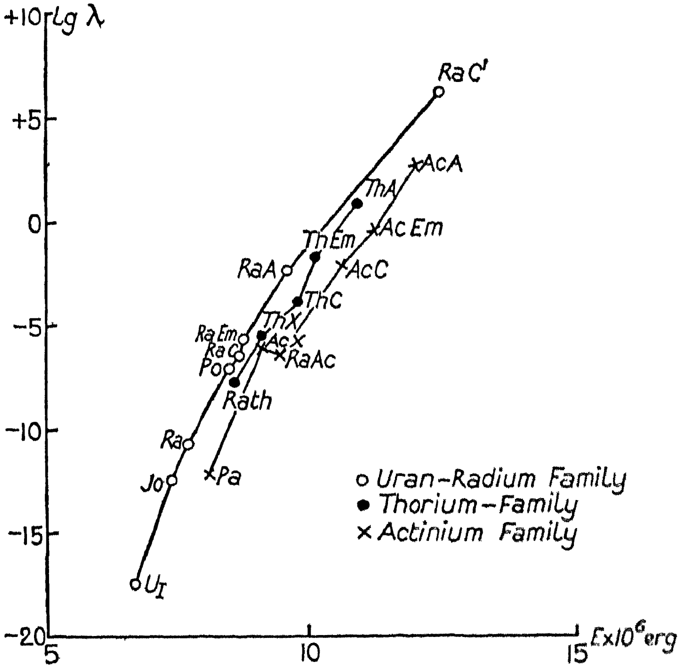

FIG. 10. Geiger-Nuttall diagram.

§ 2. General Features of α-disintegration.

To understand the extremely long periods of life of radioactive bodies, and their connexion with the energy of disintegration, we must investigate more closely the process of ejection of radioactive particles. Very important information concerning the process of α-decay was given by Rutherford's experiments on the scattering of fast α-particles in radioactive substances. It is known that experiments of this kind with light nuclei make it possible to detect the deviations from the Coulomb law of force at small distances, and so give information about the forces acting in the nucleus. On the other hand, when Rutherford bombarded atoms of Uranium with very rapid α-particles from Thorium C′, he could not observe any deviations from the Coulomb law, although the α-particles approached the nucleus up to distances of 3.10^{-12} cm. This shows that the attractive forces come into play only at much smaller distances, a region which cannot be reached by bombarding heavy nuclei with the fastest α-particles we have in our laboratories. This negative, and at first sight not very important, result gives rise to a difficulty, the solution of which will lead us to a complete theory of α-disintegration.

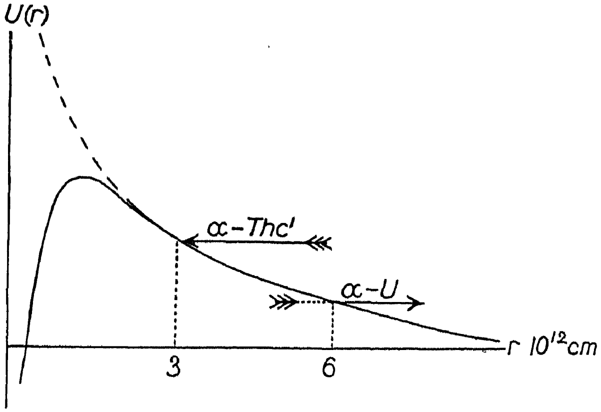

Fig. 11

The diagrammatical representation of the potential distribution near the Uranium nucleus is given in Fig. 11. With decreasing distance from the nucleus the potential energy increases at first up to a distance certainly smaller than 3.10^{-13} cm. and reaches a value certainly greater than

$$2Ze^2 \qquad \frac{2\,.\,92(4{\cdot}77)^2\,.\,10^{-20}}{10^{-12}} = 13\,.\,10^{-6}\text{ erg.}$$

For smaller distances the attractive forces come into play and the potential energy-curve drops down towards the centre of the nucleus. In this region α-particles may stay under the action of attractive forces. The difficulty mentioned above is that the Uranium nucleus sends out rather slow α-particles with energy $6{\cdot}6\,.\,10^{-6}$ ergs—only about half that of the Thorium C′ α-particles. Now how can such an α-particle get out from the nucleus if it has to cross on its way a potential barrier which is certainly higher than the total energy of the α-particle itself ? It seems that the α-particle must stay for ever inside the nucleus, since it has not enough energy to jump over the barrier. This paradox, which seems very difficult on the classical theory, disappears, from the point of view of the wave mechanics.

The apparently paradoxical fact of a particle passing through such a barrier can be explained on account of the wave character of the new quantum mechanics, and has a complete analogy in the wave theory of light. It is well known that if a beam of light falls on the boundary between two media with its angle of incidence greater than the critical angle, then, according to geometrical optics, all the light is reflected and no disturbance enters the second medium. From the point of view of wave optics the process of total reflection of light is much more complicated; some vibrations penetrate into the second medium, their amplitude decreasing very rapidly (exponentially) with the distance from the boundary. Already, at a distance of several wave-lengths from the boundary, the disturbance is very small. Exactly the same effect must be expected for the de Broglie waves describing the flow of material particles falling on a potential barrier. A small fraction of the de Broglie waves will penetrate any finite potential barrier, which means that it is possible to observe the particles on the other side of it. In this way we can explain the possibility of α-particles escaping from radioactive nuclei and the existence of very long periods of decay.

§ 3. Penetration of Particles Through Potential Barriers.

We shall now develop formulae for the coefficient of transparency of potential barriers. Suppose a particle of energy E falls (from the right) on the potential barrier represented by an arbitrary potential function $U(r)$. We suppose that the function $U(r)$ is in a certain region (x_1, x_2) greater than the total energy of the particle and approaches the constant values $U_{-\infty}$ and $U_{+\infty}$ on either side of this region. We write the Schrödinger wave-equation in the form

$$\frac{\partial^2\psi(x,t)}{\partial x^2}+\frac{2mi}{\hbar}\frac{\partial\psi(x,t)}{\partial t}-\frac{2m}{\hbar^2}U(x)\psi(x,t)=0 \tag{5}$$

where m is the mass of the particle and $\hbar$ quantum constant. As the potential energy $U(x)$ is independent of the time, the solution can be written in the form

$$\psi(x,t)=\Psi(x)e^{-\frac{i}{\hbar}Et} \tag{6}$$

and $\Psi(x)$ must satisfy the equation

$$\frac{d^2\Psi}{dx^2}+\frac{2m}{\hbar^2}[E-U(x)]\Psi = 0. \tag{7}$$

Substituting

$$\Psi(x) = \tag{8}$$

this equation reduces to

$$\frac{d^2s}{dx^2}+\left(\frac{ds}{dx}\right)^2+\frac{2m}{\hbar^2}[E-U(x)] = 0. \tag{9}$$

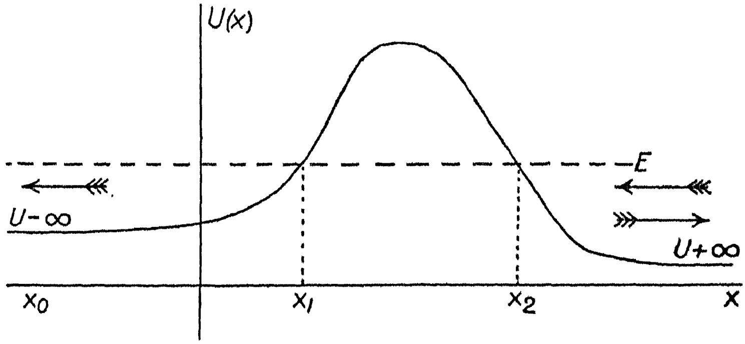

Fig. 12

This equation (9) can be solved by the method of successive approximations if the first term is small compared with the second one, that is, if

$$\left|\frac{\frac{d^2s}{dx^2}}{\left(\frac{ds}{dx}\right)^2}\right| = \left|\frac{d}{dx}\left(\frac{1}{\frac{ds}{dx}}\right)\right| \ll 1, \tag{10}$$

a condition which, as we shall see, is usually satisfied for the potential barriers which we meet in the theory of radioactive disintegration. For the first approximation we neglect the first term and write

$$\left(\frac{ds_1}{dx}\right)^2 = \frac{2m}{\hbar^2}[U(x)-E]. \tag{11}$$

Integrating, we have

$$s_1 = \pm\frac{\sqrt{(2m)}}{\hbar}\int\limits_{x_0}^{x}\sqrt{[U(x)-E]}\,dx+C. \tag{12}$$

For the second approximation we substitute in the first term of (9) from the expression (12) for s_1. We have

$$\left(\frac{ds_2}{dx}\right)^2 = \frac{2m}{\hbar^2}[U(x)-E]\mp\frac{\sqrt{(2m)}}{\hbar}\frac{d}{dx}\sqrt{[U(x)-E]} \tag{13}$$

or
$$\frac{ds_2}{dx} = \pm\frac{\sqrt{(2m)}}{\hbar}\sqrt{[U(x)-E]} - \frac{1}{2}\frac{\frac{d}{dx}\sqrt{[U(x)-E]}}{\sqrt{[U(x)-E]}}. \tag{14}$$

Integrating, we have
$$s_2 = \pm\frac{\sqrt{(2m)}}{\hbar}\int\limits_{x_0}^{x}\sqrt{[U(x)-E]}\,dx - \tfrac{1}{2}\log\sqrt{[U(x)-E]} + C. \tag{15}$$

Proceeding in the same way we see that the third approximation is already of no great importance. Thus we have, finally,
$$\Psi(x) = e^{s_2(x)} = \frac{C}{\sqrt[4]{[U(x)-E]}}\,e^{\pm\frac{\sqrt{(2m)}}{\hbar}\int_{x_0}^{x}\sqrt{[U(x)-E]}\,dx}. \tag{16}$$

The solution (15) is valid only for regions for which the condition (10) is satisfied. Using the first approximation for s we write this condition in the form,
$$\left|\frac{\hbar}{\sqrt{(2m)}}\frac{d}{dx}\left(\frac{1}{\sqrt{[U(x)-E]}}\right)\right| \ll 1. \tag{17}$$

Returning to the potential distribution, we see that the condition (17) is not satisfied near the points $x = x_1$ and $x = x_2$ where its left-hand side becomes infinite. To take the integration over these points we actually need to know the analytical form of $U(r)$, but if these regions $(x_1-\Delta x_1,\ x_1+\Delta x_1)$ and $(x_2-\Delta x_2,\ x_2+\Delta x_2)$, where $\{\sqrt{[U(x)-E]}\}^{-1}$ varies too rapidly, are small we can make the solutions on both sides satisfy the boundary conditions of continuity. On the left-hand side of the barrier we must choose the negative sign in the exponent of (16) in order to get, substituting (16) in (6), only a wave travelling from right to left, and representing the particles which have crossed the barrier. At a great distance from the barrier, on the left-hand side, the potential $U(x)$ is constant, and we have the complex expression*
$$\underset{x\ll x_1}{\Psi(x)} = \frac{C}{\sqrt[4]{(E-U_{-\infty})}}\,e^{-\frac{i\sqrt{(2m)}}{\hbar}\sqrt{(E-U_{-\infty})}(x-x_0)} \tag{18}$$
representing a wave travelling from right to left.

In the region $x_1 < x < x_2$, the difference, $U(x)-E$, becomes positive, and both solutions, apart from the arbitrary constants, are real, one of them increasing and the other decreasing rapidly with the distance.

---

* We choose for the initial point of integration x_0 a value for x at a great distance from the left-hand side of the barrier $x_0 \ll$

In order to join the solutions at the point $x = x_1$, we must take inside the barrier the general form with complex coefficients,

$$\Psi_{x_1<x<x_2}(x) = \frac{C}{\sqrt[4]{[E-U(x)]}}\left[b_+ e^{+\frac{\sqrt{(2m)}}{\hbar}\int\limits_{x_1}^{x}\sqrt{[U(x)-E]}\,dx} + b_- e^{-\frac{\sqrt{(2m)}}{\hbar}\int\limits_{x_1}^{x}\sqrt{[U(x)-E]}\,dx}\right]. \tag{19}$$

It is easy to see that the boundary conditions at $x = x_1$, (continuity of ψ and $\frac{d\psi}{dx}$), give

$$b_+ = \tfrac{1}{2}(1-i)e^{-\frac{i\sqrt{(2m)}}{\hbar}\int\limits_{x_0}^{x_1}\sqrt{[E-U(x)]}\,dx}; \quad b_- = \tfrac{1}{2}(1+i)e^{-\frac{i\sqrt{(2m)}}{\hbar}\int\limits_{x_0}^{x_1}\sqrt{[E-U(x)]}\,dx}. \tag{20}$$

At the other end of the barrier, $x = x_2$, the second term in (19) will be very small and the solution reduces to

$$\Psi_{x\sim x_2} = \frac{\frac{1}{2}C(1-i)}{\sqrt[4]{[E-U(x)]}}e^{-\frac{i\sqrt{(2m)}}{\hbar}\int\limits_{x_0}^{x_1}\sqrt{[E-U(x)]}\,dx}\,e^{+\frac{\sqrt{(2m)}}{\hbar}\int\limits_{x_1}^{x}\sqrt{[U(x)-E]}\,dx}. \tag{21}$$

To join this function with the complex solution for $x > x_2$ we must again take a linear combination of both solutions:

$$\Psi_{x_2<x}(x) = \frac{C}{\sqrt[4]{[E-U(x)]}}\left[a_+ e^{+\frac{i\sqrt{(2m)}}{\hbar}\int\limits_{x_2}^{x}\sqrt{[E-U(x)]}\,dx} + a_- e^{-\frac{i\sqrt{(2m)}}{\hbar}\int^{x}\surd[E}\right. \tag{22}$$

and the boundary conditions give

$$\begin{aligned} a_+ &= \tfrac{1}{2}(1-i)b_+ e^{\frac{\sqrt{(2m)}}{\hbar}\int\limits_{x_1}^{x_2}\sqrt{[U(x)-E]}\,dx}. \\ a_- &= \tfrac{1}{2}(1+i)b_+ e^{\frac{\sqrt{(2m)}}{\hbar}\int\limits_{x_1}^{x_2}\sqrt{[U(x)-E]}\,dx}. \end{aligned} \tag{23}$$

If x_0' is some value of x at a great distance on the right-hand side of the barrier, the expression (22) becomes

$$\Psi_{x_2 \ll x} = A_+ e^{+i\frac{\sqrt{(2m)}}{\hbar}\sqrt{[E-U_{+\infty}]}(x-x_0')} + A_- e^{-i\frac{\sqrt{(2m)}}{\hbar}\sqrt{[E-U_{+\infty}]}(x-x_0')} \tag{24}$$

where the amplitudes are given by

$$\begin{aligned} A_+ &= \frac{-iC}{2\sqrt[4]{[E-U(x)]}}e^{\frac{\sqrt{(2m)}}{\hbar}[-i\int\limits_{x_0}^{x_1}\sqrt{(E-U)}\,dx + \int\limits_{x_1}^{x_2}\sqrt{(U-E)}\,dx + i\int\limits_{x_2}^{x_0'}\sqrt{(E-U)}\,dx]} \\ A_- &= \frac{C}{2\sqrt[4]{[E-U(x)]}}e^{\frac{\sqrt{(2m)}}{\hbar}[-i\int\limits_{x_0}^{x_1}\sqrt{(E-U)}\,dx + \int\limits_{x_1}^{x_2}\sqrt{(U-E)}\,dx + i\int\limits_{x_2}^{x_0'}\sqrt{(E-U)}\,dx]} \end{aligned} \tag{25}$$

These two waves represent the incident and reflected beams of particles. The amplitude of the reflected wave must be actually slightly smaller than that of the incident wave as a part of it has crossed the barrier; in our approximate calculations we get equal amplitudes, because we have neglected terms of a small order of magnitude.

The coefficient of transparency of the barrier is given by the square of the ratio of the transmitted and incident waves:

$$G=\left|\frac{\Psi(-\infty)}{\Psi(+\infty)}\right|^2=4\sqrt{\left(\frac{E-U_{+\infty}}{E-U_{-\infty}}\right)}\,e^{-\frac{2\sqrt{(2m)}}{\hbar}\int\limits_{x_1}^{x_2}\sqrt{[U(x)-E]}\,dx}. \tag{26}$$

This is the formula we shall use in future for calculations of the transparency of the barriers surrounding radioactive nuclei. Before using this formula we must first make sure that condition (16) is fulfilled.

§ 4. General Theory of α-disintegration.

Returning to the general problem of radioactive disintegration, we shall suppose that the potential field surrounding the nucleus is spherically symmetrical and is defined by a certain function $U(r)$. This function, which has a certain finite value at the centre of the nucleus, must reach rather large values at some distance, giving rise to a barrier, and must vanish at infinity (Fig. 13).

The wave-equation for the α-particle, written in spherical polar coordinates (r, θ, ϕ) is

$$\frac{1}{r^2}\frac{\partial}{\partial r}\left(r^2\frac{\partial\psi}{\partial r}\right)+\frac{1}{r^2\sin\theta}\frac{\partial}{\partial\theta}\left(\sin\theta\frac{\partial\psi}{\partial\theta}\right)+\frac{1}{r^2\sin^2\theta}\frac{\partial^2\psi}{\partial\phi^2}+\frac{2i}{\hbar}\frac{\partial\psi}{\partial t}-\frac{2m}{\hbar^2}U(r)\psi=0 \tag{27}$$

or, if E is the energy,

$$\frac{1}{r^2}\frac{\partial}{\partial r}\left(r^2\frac{\partial\Psi}{\partial r}\right)+\frac{1}{r^2\sin\theta}\frac{\partial}{\partial\theta}\left(\sin\theta\frac{\partial\Psi}{\partial\theta}\right)+\frac{1}{r^2\sin^2\theta}\frac{\partial^2\Psi}{\partial\phi^2}+\frac{2m}{\hbar^2}[E-U(x)]\Psi=0 \tag{28}$$

where $$\psi=\Psi(r,\theta,\phi)e^{-\frac{i}{\hbar}Et}. \tag{29}$$

As the potential energy is independent of the angular coordinates θ and ϕ, we can, as is well known, write the solution of (28) in the form

$$\Psi_{E,j}=\frac{1}{r}S_j(\theta,\phi)\chi_{E,j}(r), \tag{30}$$

where $S_j(\theta, \phi)$ is a spherical harmonic of order j, where j is an integer and $\chi_{E,j}(r)$ must satisfy the equation,

$$\frac{\partial^2\chi_{E,j}(r)}{\partial r^2}+\frac{2m}{\hbar^2}\left[E-U(r)-\frac{\hbar^2}{2m}\frac{j(j+1)}{r^2}\right]\chi_{E,j}(r)=0$$

j corresponds to the azimuthal quantum-number, and the last term in the bracket represents the additional potential due to the centrifugal force.

Not every solution of our equation, however, will represent the process of spontaneous ejection of an α-particle from the space inside the potential barrier. We must satisfy some boundary conditions which arise from the physical interpretation of our solutions. First of all the function Ψ must be finite at the origin, which, from (30), is only possible if $\chi(r)$ vanishes for $r=0$. The second condition is that outside the nucleus, for very large values of r, the solution must represent particles flying out of the nucleus; this means that here we must have a *divergent wave*.

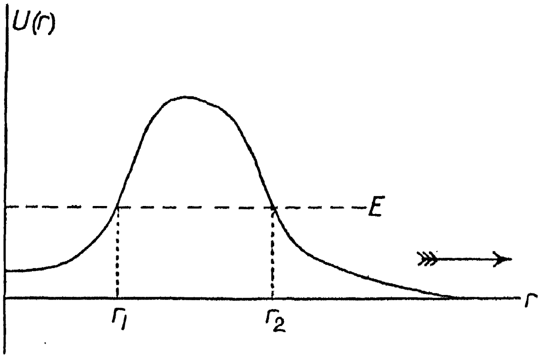

Fig. 13

If for any arbitrary value of E we proceed to construct solutions of (31), beginning with the value $\chi(0)=0$, we get, for large values of r, the expression

$$\chi_{\substack{E,j\\ r\to\infty}}=A_{E,j}e^{+\frac{i\sqrt{(2m)}}{\hbar}\sqrt{(E)}r}+\bar{A}_{E,j}e^{-\frac{i\sqrt{(2m)}}{\hbar}\sqrt{(E)}r}. \tag{32}$$

where the coefficients $A_{E,j}$ and $\bar{A}_{E,j}$ are expressed in terms of E and j. If we substitute (32) in (29) the first and second terms will give respectively a divergent and convergent wave. The condition that there shall be only a divergent wave is now

$$A_{E,j}\neq 0;\qquad \bar{A}_{E,j}=0. \tag{33}$$

For each value of the azimuthal quantum-number j the equations (33) will define a discrete set of E-values which we shall distinguish by different indices n. Thus we get a set of discrete energies $E_{n,j}$ for the escaping particle, depending on two whole numbers, n and j (radial and azimuthal quantum numbers), just as in the ordinary problem of electrons in an atom. The great difference lies in the fact that here the eigenvalues are positive, or rather, as we shall now see, complex with a positive real part.

At first sight the conditions (33) seem to show that such solutions do not exist; if $A_{E,j}$ vanishes for certain values of E, the conjugate complex quantity, $\bar{A}_{E,j}$, must vanish also. This is true if E is a real quantity as is usual in the wave mechanics. We can, however, satisfy the conditions (33) if we allow *complex values of E*† and write the

$$E_{n,j} = E^0_{n,j} + \frac{i\hbar}{2}\lambda_{n,j}.‡$$

The complex equations (33) will now give a set of values for both the real quantities E^0 and λ. In this way we come to the conclusion that the problem of radioactive decay can be solved only by using *complex eigenvalues*. We shall now discuss the physical interpretation of the solutions and the meaning of the imaginary part of the energy.

Outside the potential barrier surrounding the nucleus the solution is a divergent wave representing the flow of α-particles escaping from the nucleus. We have seen in the previous paragraph that if the potential barrier is high enough, as it always is in the radioactive nuclei, the solution on the other side of it, that is, inside the nucleus, will be very nearly a stationary wave with amplitude much greater than that of the escaping wave. Neglecting the small escaping part, we have inside the nucleus a representation of a particle oscillating between the walls surrounding it. The real part of each eigenvalue will be practically equal to an energy-level of a particle surrounded by infinitely high walls. The small leak gives rise to the additional imaginary term in the expression for the energy, but this does not affect the real part very much.

It is well known that in order to interpret the solutions of the Schrödinger equation we must construct the quantities,

$$\sigma = \psi\bar{\psi}; \qquad I = \frac{\hbar}{2mi}(\psi \operatorname{grad}\bar{\psi} - \bar{\psi}\operatorname{grad}\psi), \tag{35}$$

---

† Conjugate complex functions of the *same* complex argument do not vanish simultaneously.

‡ The reason for introducing the coefficient $\hbar/2$ in the imaginary part of the energy will appear later.

representing respectively the density and the flow of the probability for a particle to be observed at a certain point. For the ordinary solutions with real eigenvalues both these quantities are harmonic in the time, or constant, representing certain stable quantized states of the system.

For complex eigenvalues both quantities will have an aperiodic time-factor:

$$e^{\frac{i}{\hbar}\left(E^0_{n,j}+\frac{i\hbar}{2}\lambda_{n,j}\right)}\,e^{-\frac{i}{\hbar}\left(E^0_{n,j}-\frac{i\hbar}{2}\lambda_{n,j}\right)} = e^{-\lambda_{n,j}t}. \tag{36}$$

Thus the density at each point decreases exponentially with the time, the solution representing the gradual decrease of the probability, previously concentrated near the centre. The decay constant (logarithmic decrement) is given by $\lambda_{n,j}$. The complex value of the energy will not only introduce a damping time-factor, but it will also give rise to an aperiodic factor in the space coordinate. For we have

$$\underset{r\to\infty}{\chi_{E_{n,j}}(r)} = A_{n,j}\,e^{+\frac{i\sqrt{(2m)}}{\hbar}\sqrt{\left(E^0+\frac{\hbar i}{2}\lambda\right)}\,r} = A_{n,j}\,e^{\frac{i\sqrt{(2m)}}{\hbar}\sqrt{(E^0)}r}\,e^{+\frac{\lambda\sqrt{(m)}}{\sqrt{(2E^0)}}r}. \tag{37}$$

This means that the amplitude of the divergent wave gradually increases with the distance and tends to an infinite value at infinity. We always meet this effect when dealing with solutions representing a damping process; for example, in the classical solution for an electro-magnetic wave radiated by a damped oscillator. The fact that at any definite moment we have an abnormally dense flow at a great distance means that these waves were radiated long before when the amplitude of the oscillator was greater. For radioactive decay the number of particles at a great distance r from the centre must correspond to the efficiency of the source at time $t = r/v$ earlier, when it was $e^{\frac{\lambda r}{v}} = e^{\frac{\lambda r\sqrt{(m)}}{\sqrt{(2E)}}}$ times greater, which exactly corresponds to the aperiodic factor in (37). In practice this increase is of no importance. Even for the element with the shortest life, RaC′, for which $1/\lambda = 10^{-5}$ sec., the intensity of the flow will be only doubled at a distance of about 0·1 km., since

$$\frac{v}{\lambda} = \frac{10^9\ \text{cm./sec.}}{10^5\ \text{sec}^{-1}.} = 10^4\ \text{cm.} = 0{\cdot}1\ \text{km.}$$

We have seen that the divergent spherical wave will not be exactly periodic because of the damping factor. In optics such a damping would cause a broadening of the spectral line in the spectrograph. For moving particles we have to use a mass-spectrograph, and the broadening of the lines will be explained as uncertainty in the energy of the particles. Using the Fourier expansion of the damped wave, we easily get for the uncertainty in the energy (half-breadth of the line) the value

$$\Delta E \sim \hbar\lambda.$$

Remembering that the mean time T for the α-particle to stay inside the nucleus is given by the reciprocal of the decay constant, we have

$$\Delta E\,.\,T \sim \hbar. \tag{38'}$$

This is just Heisenberg's uncertainty relation for the time and energy. We can hardly expect to observe this deviation from the constant energy of α-disintegration with the known radioactive elements; the shortest period of life at present known is $T = 10^{-5}$ sec., which gives for ΔE a value of about 10^{-22} ergs, i.e. only 10^{-14} per cent. of the total energy.

The total flow through any closed surface surrounding the nucleus will be equal to the decrease of the total amount inside the surface. Taking a sphere of large radius R with its centre in the nucleus, we can write

$$\frac{\partial}{\partial t}\int \psi\bar{\psi}\,dv = \frac{\hbar}{2im}\int\left[\psi\frac{\partial\bar{\psi}}{\partial r_n} - \bar{\psi}\frac{\partial\psi}{\partial r_n}\right]dS$$

from which

$$\lambda_{n,j} = \frac{\frac{\hbar}{2im}\left(\chi\frac{\partial\bar{\chi}}{\partial r} - \bar{\chi}\frac{\partial\chi}{\partial r}\right)_{r=R}}{\int\limits_0^R \chi\bar{\chi}\,dr}. \tag{40}$$

This formula is independent of t and will be found very useful in calculating the decay constants of radioactive nuclei. It means simply that the damping coefficient is equal to the ratio of the flow to the total amount inside and is quite analogous to the classical formula used for the calculation of the damping of any radiating oscillator. For calculations of the decay constant by means of the formula (40) it is of no practical importance what value of R we take, provided that it is large enough compared with r_2. In fact, we have seen that the flow is fairly constant, only doubling its value in a distance 0·1 km. The integral in the denominator of (40) should actually be taken up to the radius R. Due to the rapid decrease of χ inside the barrier the part of the integral outside the nucleus is very small, and in practice we need integrate only inside the potential barrier.

§ 5. Application to the Real Nuclei

We shall now apply our formulae to the calculation of the decay constants for the real radioactive nuclei. The distribution of potential energy of a nuclear α-particle in the field of the rest of the nucleus is shown in Fig. 14. At distances large compared with the dimensions of the nucleus we have the Coulomb inverse square law of force, and the potential energy of the α-particles is given by , where Z is the charge-number of the disintegrating nucleus. At a certain small distance from the centre the attractive forces come into play and the potential drops down rather rapidly, attaining a practically constant value inside the nucleus. Since the exact law of the attractive forces is at present unknown, we must make some assumption about the shape of the potential curve at small distances and introduce a simplified model of the nucleus. A simple and natural approximation to the real distribution of potential inside the nucleus is obtained by substituting for the curve a rectangular trough as shown in Fig. 14. We assume that

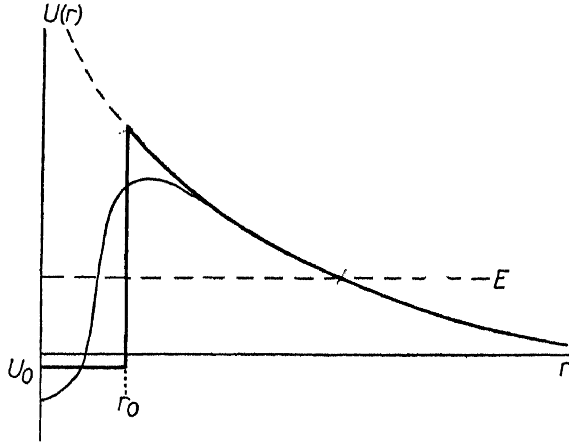

FIG. 14

$$U(r) = \frac{2(Z-2)e^2}{r} \quad (r_0 < r),$$

$$U(r) \text{ jumps from } \frac{2(Z-2)e^2}{r_0} \text{ to } U_0 \text{ at } r = r_0 \qquad (41)$$

$$U(r) = U_0 = \text{const } (r < r_0).$$

Thus our model of the nucleus is defined by two quantities, the critical radius r_0 and the value of the internal potential U_0. Both r_0 and U_0 clearly correspond to the nucleus of the product element. We notice here that such an approximation to the real form of the potential barrier will scarcely affect the value of its coefficient of transparency, as the chief part of the integral in formula (26) is taken over the region of the barrier where the deviations from the Coulomb law are very small. On the other hand, our model will give only very rough results for the calculation of the energy-levels of the α-particles inside the nucleus, since these values depend essentially on the actual shape of the potential curve.

The solution for $r < r_0$ is

$$\chi_{E,j} = AJ_{j+\frac{1}{2}}\left(\frac{\sqrt{(2m)}}{\hbar}\sqrt{(E-U_0)r}\right) \tag{42}$$

where $J_{j+\frac{1}{2}}$ is a Bessel function of order $j+\frac{1}{2}$. If $\kappa_{n,j+\frac{1}{2}}$ are roots of these functions, we have

$$E_{n,j} = \frac{\kappa^2\hbar^2}{2mr_0^2}+U_0. \tag{42$'$}$$

In the case of radial oscillations

$$\chi_{E,0} = A\sin\frac{\sqrt{(2m)}}{\hbar}\sqrt{(E-U_0)r}, \tag{43}$$

and we have simply

$$E_{n,0} = \frac{n^2\hbar^2\pi^2}{2mr_0^2}+U_0. \tag{43$'$}$$

As we have already said, these formulae can only be applied very roughly for the real nuclei.

In calculating the decay constant for our model we shall at first examine the case of radial motion. Normalizing to unity the amplitude of the wave escaping from the nucleus, we have

$$\chi_{E,0} = e^{+\frac{i\sqrt{(2m)}}{\hbar}\sqrt{(E)}r} = e^{+\frac{im}{\hbar}v_e . r}, \tag{44}$$

where v_e is the velocity of the escaping particle. According to formula (26) the square of the amplitude of the vibrations inside the barrier is given by

$$|A|^2 = 4\frac{v_e}{v_i}e^{-\frac{2\sqrt{(2m)}}{\hbar}\int\limits_{r_0}^{\frac{2(Z-2)e^2}{E}}\sqrt{\left(\frac{2(Z-2)e^2}{r}-E\right)}\,dr} \tag{45}$$

where v_i is the velocity of the α-particle oscillating inside the nucleus.

The numerator and denominator in the general expression (40) for the decay constant now become

$$\frac{\hbar}{2im}\left(\chi_{E,0}\frac{d\bar{\chi}_{E,0}}{dr}-\bar{\chi}_{E,0}\frac{d\chi_{E,0}}{dr}\right)=v_e \tag{46}$$

$$\int\limits_0^{r_0}\chi_{E,0}\bar{\chi}_{E,0}\,dr=|A|^2\int\limits_0^{r_0}\sin^2\frac{\sqrt{(2m)}}{\hbar}E\,dr=|A|^2\frac{r_0}{2} \tag{46'}$$

and we have finally,

$$\lambda_{E,0}=\frac{v_i}{2r_0}e^{-\frac{2\sqrt{(2m)}}{\hbar}\int\limits_{r_0}^{\frac{2(Z-2)e^2}{E}}\sqrt{\left(\frac{2(Z-2)e^2}{r}-E\right)}\,dr} \tag{47}$$

where the factor before the exponential can be described classically as the number of collisions per unit time of an α-particle oscillating inside the nucleus with the barrier. The integral in the exponent of (47) can be simply evaluated by means of the substitution†

$$\cos^2u=\frac{r}{\frac{2(Z-2)e^2}{E}}=\frac{r}{r^*}. \tag{48}$$

We have

$$\lambda_{E,0}=\frac{v_i}{2r_0}e^{-\frac{4e^2}{\hbar}\frac{(Z-2)}{v_e}(2u_0-\sin 2u_0)}, \tag{49}$$

where

$$\cos^2u_0=\frac{r_0}{r^*}=\frac{r_0E}{2(Z-2)e^2}. \tag{48'}$$

In radioactive nuclei the value of r_0/r^* is small. Developing the exponent of (49) in powers of r_0/r^* and taking the first two members, we get a simple formula which is very convenient for the calculation of decay constants,

$$\lambda_{E,0}=\frac{\pi\hbar}{2mr_0^2}e^{-\frac{4\pi e^2}{\hbar}\frac{(Z-2)}{v_e}+\frac{8e\sqrt{(m)}}{\hbar}\sqrt{[(Z-2)r_0]}}.$$

If the azimuthal quantum number differs from zero we have the additional potential energy due to the centrifugal force, and the expression for the decay constant must be written in the form

$$\lambda_{E,j}=\frac{\pi\hbar}{4mr_0^2}e^{-\frac{2\sqrt{(2m)}}{\hbar}\int\limits_{r_0}^{r^*}\sqrt{\left(\frac{2(Z-2)e^2}{r}+\frac{\hbar^2}{2m}\frac{j(j+1)}{r^2}-E\right)}\,dr}. \tag{51}$$

---

† $r^*=\frac{2(Z-2)e^2}{E}$ is the so-called classical radius of the nucleus, i.e. the closest distance of approach of an α-particle in classical mechanics.

In radioactive nuclei ($Z = 82, \dots 92$; $r_0 \sim 10^{-12}$ cm.) and the potential of the centrifugal forces will in general be very small compared with the Coulomb potential, the ratio σ being given by:

$$\sigma = \frac{\hbar^2}{2m}\frac{j(j+1)}{r_0^2} : \frac{2(Z-2)e^2}{r_0} \sim 0{\cdot}002j(j+1), \qquad (52)$$

and for the calculation of the integral in (51) we may develop the square root in powers of the small quantity σ. Thus we get the final [illegible]

$$\lambda_{E,j} = \frac{\pi\hbar}{2mr_0^2} e^{-\frac{4\pi e^2}{\hbar}\frac{(Z-2)}{v_e} + \frac{8e\sqrt{(m)}}{\hbar}\sqrt{[(Z-2)r_0]}.(1-\sigma)}$$

which shows that the azimuthal quantum number will only slightly affect the second member in the exponent. The value of this member for radioactive bodies is about 85; so that a calculation shows that for $j = 1$ the decay constant will be changed only by 30 per cent.

§ 6. Comparison with Experiment

The formula (50), which we shall write now in the form†

$$\log_{10}\lambda = \log_{10}\frac{\pi\hbar}{2mr_0^2} - \frac{4\pi e^2}{\hbar M}\frac{Z-2}{v} + \frac{8e\sqrt{(m)}}{\hbar M}\sqrt{(Z-2)}\sqrt{(r_0)}, \qquad (54)$$

or, putting in the numerical values for the constants,

$$\log_{10}\lambda = 20{\cdot}4652 - 1{\cdot}191 \times 10^9\frac{Z-2}{v} + 4{\cdot}084 \times 10^6\sqrt{(Z-2)}\sqrt{(r_0)}, \qquad (54')$$

corresponds to the empirical relation found between the decay constants and the velocities of α-particles for different radioactive bodies, by Geiger and Nuttall (see p. 36). We see from (54) that $\log\lambda$ depends actually not only on the velocity v of the ejected α-particle but also on the charge-number Z and the radius r_0 of the disintegrating nucleus, and therefore cannot be represented on a two-dimensional graph. The curious fact that Geiger and Nuttall could get a smooth curve by plotting simply $\log\lambda$ against v is due to the fact that the variation of Z, v, and r_0 in a radioactive series is practically monotone as we go down the series. We should expect certain anomalies in the Geiger-Nuttall graph at the points where this regularity breaks down. Fig. 10 shows that such deviations actually exist; for example, for AcX the point does not lie on the continuous curve, which is due to the fact that the velocity of the ejected α-particle is *smaller* than for the previous element RaAc, whereas, generally, the velocity increases as we go down the series. As we see from (54), $\log\lambda$ depends only slightly on the variation of the radius r_0 which comes in the last term; thus we can roughly calculate the values of the decay constant for different radioactive elements with known values of Z and v, using a certain constant value for r_0. The calculations show that taking $r_0 \sim 8\,.\,10^{-13}$ cm. we can get rather good agreement with the experimental values of λ. The systematic deviations indicate that the radius r_0 is not constant but increases slightly for heavier elements. Using the experimental data for Z, v, and λ we can calculate the values of the nuclear radii for elements of the three known radioactive families. These are given in the Tables III *a*, *b*, *c*, and in Fig. 15.

---

† We have written M for 2·303..., the factor for converting natural logari[illegible] to base 10.

TABLE III(1

Disintegrating nucleus.	(Z–2)	Effective velocity $V\alpha\left(1+\frac{4}{M}\right)\times 10^{-9}\frac{\text{cm.}}{\text{sec.}}$.	Decay constant λ sec^{-1}.	Effective nuclear radius of the product nucleus $r_0\times 10^{13}$cm.	Product nucleus.
Th	88	1·41	$1{\cdot}3\,.\,10^{-18}$	8·9	M Th$_{\text{I}}$
RaTh	88	1·63	$1{\cdot}16\,.\,10^{-8}$	8·7	ThX
ThX	86	1·68	$2{\cdot}20\,.\,10^{-6}$	8·5	ThEm
ThEm	84	1·76	$1{\cdot}27\,.\,10^{-2}$	8·3	ThA
ThA	82	1·83	4·95	8·1	ThB
ThCα_0	81	1·75	$1{\cdot}5\,.\,10^{-5}$	6·6	ThC″ (norm.)
ThCα_1		1·74	$5{\cdot}1\,.\,10^{-5}$	7·0	ThC″ (excited)
ThC′	82	2·10	$[3{\cdot}10^{+8}]$	[8·7]	ThD
U$_{\text{I}}$	90	1·44	$4{\cdot}8\,.\,10^{-18}$	9·5	UX$_{\text{I}}$
U$_{\text{II}}$	90	1·53	$[2{\cdot}10^{-13}]$	[9·3]	Io
Io	88	1·51	$2{\cdot}9\,.\,10^{-13}$	9·1	Ra
Ra	86	1·54	$1{\cdot}39\,.\,10^{-11}$	8·6	RaEm
RaEm	84	1·65	$2{\cdot}097\,.\,10^{-6}$	8·5	RaA
RaA	82	1·72	$3{\cdot}78\,.\,10^{-3}$	8·3	RaB
RaCα_0	81	1·65	$1{\cdot}34\,.\,10^{-7}$	6·3	RaC″ (norm.)
RaCα_1		1·62	$0{\cdot}44\,.\,10^{-7}$	7·5	RaC″ (excited)
RaC′	82	1·96	$4{\cdot}2\,.\,10^{+5}$	8·9	RaD
RaF	82	1·62	$5.88\,.\,10^{-8}$	7·7	RaG
Pa	89	1·58	$1{\cdot}9\,.\,10^{-12}$	8·2	Ac
RaAc	88	1·72	$4{\cdot}24\,.\,10^{-7}$	7·9	AcX
AcX	86	1·68	$7{\cdot}14\,.\,10^{-1}$	8·2	AcEm
AcEm	84	1·84	$1{\cdot}77\,.\,10^{-1}$	7·7	AcA
AcA	82	1·92	$4{\cdot}74\,.\,10^{+2}$	7·9	AcB
AcCα_0	81	1·81	$4{\cdot}79\,.\,10^{-3}$	6·9	AcC″ (norm.)
AcCα_1		1·76	$0{\cdot}96\,.\,10^{-3}$	7·3	AcC″ (excited)
AcC′	82	1·91	$[1{\cdot}10^{+3}]$	[8·3]	AcD

---

[1] See references for the Table II (p. 35).

We see that the radii vary fairly regularly for each family and increase steadily with the mass of the nucleus. The nuclei of corresponding members of the Thorium and Uranium families have nearly the same radii, while for the Actinium family the radii are considerably smaller, probably owing to the presence of an odd number of protons. We also notice the anomalously low values of the nuclear radii for the C-products of all three families, where 'forking' (α- and β-disintegration) takes place; and the anomalously large radius of the short-lived RaC′ nucleus. The knowledge of the radii is important

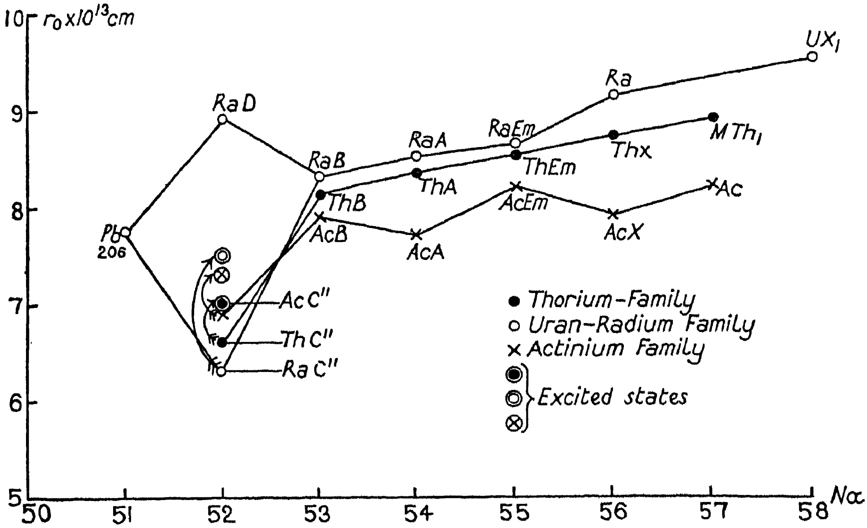

FIG. 15. Effective radii of radioactive nuclei.

for further investigations of the properties of radioactive nuclei; from the Table III we see that the excited nuclei (before γ-radiation) have radii somewhat larger than nuclei in the normal state.

§ 7. General Features of β-disintegration

The other type of spontaneous nuclear disintegration is the ejection of nuclear electrons (β-disintegration). This type of radioactive disintegration has been observed not only in heavy elements but also in certain light elements (K and Rb) which have been shown to emit β-particles of great energy, although the intensity is very small (about 500 times weaker than for UX).

The explanation of the process of β-decay presents very serious difficulties for the modern quantum theory. The chief puzzle of β-disintegration is the fact that the magnetic spectrum of the emitted β-particles is always continuous, which shows that the energy of the electrons emitted from the same substance varies within very wide limits. It has been shown that the number of electrons in the continuous spectrum is equal to the total number of disintegrated atoms, so that we actually have nuclear electrons and not secondary electrons which might be ejected from the K-L-M-shells of the atom. The energy-distribution in the β-spectra of different radioactive elements is shown in Fig. 16. The distribution has very much the same shape for different elements with an ill-defined maximum and a rather sharp upper limit;† of two neighbouring transformations (ThB and ThC; UX_1 and UX_{11}; RaB and RaC) the second always has β-particles of greater energy.

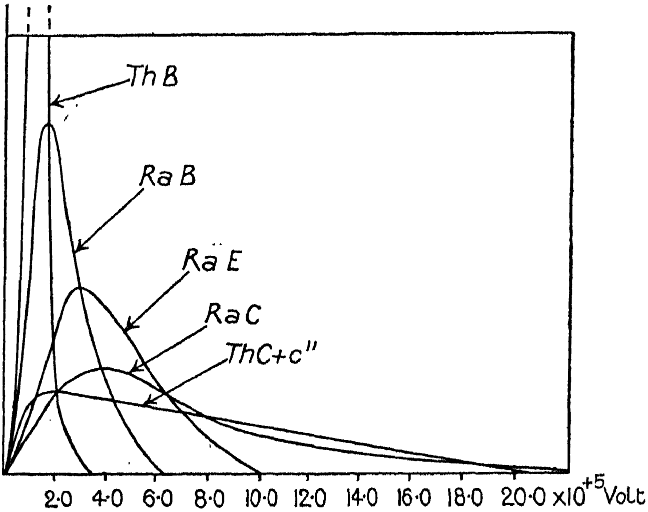

FIG. 16. Energy-spectra of β-rays.

Very careful experiments were carried out by Ellis‡ in order to prove that the continuous β-ray spectrum is not due to some secondary scattering of β-particles all originally having the same energy. Ellis measured calorimetrically the total energy produced by a known amount of the β-disintegrating element RaE. As this element shows only extremely weak γ-emission, the total measured energy divided by the number of disintegrated atoms must give the average energy of disintegration per nucleus. If the continuous β-spectrum is due to

---

† New investigations of Terroux (*Proc. Roy. Soc.*, A, vol. cxxxi, p. 90 (1931)) seem to show, however, that this upper limit does not exist, the continuous spectra extending to very high energies with exponentially decreasing intensity.

‡ C. D. Ellis and W. A. Wooster, *Proc. Roy. Soc.*, A, vol. cxvii, p. 109 (1927). These experiments have been recently repeated with great care by L. Meitner and W. Orthman (*Zs. f. Phys.*, Bd. 60, p. 143 (1930)) with the same result.

TABLE IV

Name of the element.	Mass-number M.	Charge-number Z.	Decay const.(1 λ, sec^{-1}.	Average energy of disint.		Upper limit of contin. spectra.		Notes.
				$\bar{E}\times 10^6$ erg.	$\bar{E}\times 10^{-6}$ volt.	$E_{\max}\times 10^{+6}$ erg.	$E_{\max}\times 10^{-6}$ volt.	
MTh$_{\text{I}}$	228	88	$3{\cdot}26.10^{-9}$					
MTh$_{\text{II}}$	298	89	$3{\cdot}14.10^{-5}$					
ThB	212	82	$1{\cdot}82.10^{-5}$	**0·16**	**0·1**	**0·5**	**0·3**	(2
ThC (65%)	212	83	$1{\cdot}23.10^{-4}$	(1·1)	(0·7)	(3·4)	(2·1)	(2
ThC″	208	81	$3{\cdot}61.10^{-3}$	(1·1)	(0·7)	(3·4)	(2·1)	(2
UX$_{\text{I}}$	234	90	$3{\cdot}37.10^{-7}$	0·18	(0·11)			(3
UX$_{\text{II}}$	234	91	$9{\cdot}9.10^{-8}$	0·62	(0·39)			(3
RaB	214	82	$4{\cdot}31.10^{-4}$	**0·37**	**0·23**	**1·04**	**0·65**	(4
RaC (99·96%)	214	83	$5{\cdot}92.10^{-4}$	**1·32**	**0·76**	**5·04**	**3·15**	(4
RaC″	210	81	$8{\cdot}7.10^{-3}$					
RaD	210	82	$1{\cdot}34.10^{-9}$					
RaE	210	83	$1{\cdot}66.10^{-6}$	**0·62**	**0·39**	**1·68**	**1·05**	(5
Ac	227	89	$1{\cdot}08.10^{-9}$					
AcB	211	82	$3{\cdot}21.10^{-4}$					
AcC (0·32%)	211	83	$1{\cdot}6.10^{-5}$					
AcC″	207	81	$2{\cdot}43.10^{-3}$					

[1] E. Rutherford, J. Chadwick, and C. D. Ellis, *Radiations from Radioactive Substances* (Cambridge, 1930).

[2] R. W. Gurney, *Proc. Roy. Soc.*, A, vol. cxii, p. 380 (1926).

[3] L. Meitner, *Zs. f. Phys.*, Bd. 17, p. 54 (1923).

[4] R. W. Gurney, *Proc. Roy. Soc.*, A, vol. cix, p. 540 (1925).

[5] E Madgwick, *Proc. Camb. Phil. Soc.*, vol. xxiii, p. 982 (1927).

TABLE IVA

Name of the element.	Mass-number M.	Charge-number Z.	Decay constant.(1 λ, sec^{-1}.	Energy of disintegration.	
				$\bar{E}_\beta\times 10^6$ erg.	$\bar{E}_\beta\times 10^{-6}$ volt.
K	39·41	19	$(1{\cdot}5.10^{-21})$	c. 1·5	c. 1·0
Rb	85·87	37	$(5{\cdot}0.10^{-20})$	c. 0·2	c. 0·1

[1] The decay constants were estimated by Mühlhoff, by counting the number of β-particles emitted from a given quantity of the element in question (W. Mühlhoff, *Ann. der Phys.*, Bd. 7, p. 205 (1930)). The investigations of G. v. Hevesy (*Nature*, vol. cxx, p. 838 (1927)) have shown that the β-radiation observed from K is due only to the heavier isotope, and consequently the value of λ given in the table has to be divided by the relative abundance of this isotope (factor 19). It is at present unknown which Rb isotope is the active one. It is also possible that the observed β-radiation is due to some unknown isotope present in a very small quantity (K_{40}; $Rb_{..}$)

secondary scattering, in which the β-particles lose their energy in collision with other atoms, we should expect the average energy measured by the heating effect to be equal to the maximum energy observed in the continuous β-spectrum. This is, however, not the case; the energy measured by Ellis coincides exactly with the *average* energy of the electrons in the continuous spectrum, which proves that no energy is lost in collisions and the continuity of the β-spectrum is a property of the disintegrating nucleus.

In spite of the indefinite energy of β-particles the period of decay for β-transformations is a quite definite quantity for each element. Special experiments were carried out to show that the probability of ejection of a β-particle does not depend on its energy, for a given element. A source of RaE was placed behind a screen thick enough to absorb all β-particles of the continuous spectrum except the fastest. The decrease in a given time of the number of these fast particles was observed and proved to be the same as the decrease of the total number of electrons in the continuous spectrum. This can only be the case if the probability of ejection of fast electrons is the same as for slow ones.

These results lead us to a very strange conclusion. Since there is no process compensating for the difference of energy lost by different nuclei of the same element in the ejection of a β-particle, we must deduce, according to the principle of the conservation of energy, that the internal energy of a given nucleus can take any value within a certain continuous range. This difference of energy between the nuclei, however, has not the slightest effect before or after the β-emission. The decay constants of the β-disintegrating element itself and of the neighbouring product are quite definite, and there is no trace of a continuous distribution of energy in the emission of α-particles or γ-rays. In these processes all the nuclei seem to be again completely identical, although up to the present no direct proof of this identity has been obtained.†

We could try to construct some peculiar mechanism in order to explain why these differences of internal energy, which suggests the continuous β-spectrum, have no other effect on the properties of the nucleus. However at the present state of the theory, as was pointed out by N. Bohr, we must reckon with the possibility that the continuous distribution of energy among the nuclei is fundamentally not observable, or, in other words, has no meaning in the description of the physical processes.

---

† To prove directly that the nuclei all have the same definite amount of energy we should have to measure very exactly the corresponding mass-defects (at best for an element just between two β-disintegrations, as, for example, RaE) and show that it has a definite value inside the limits of energy variation in the β-spectrum. It can, however, easily be seen that even with a modern mass-spectrograph such exact measurements are outside the limits of experimental possibility. Another and perhaps better proof of the identity of the nuclei would be the detection of intensity alternation in the band-spectra of the diatomic molecules of some radioactive body. The presence of any trace of intensity alternation ($W\uparrow\uparrow/W\uparrow\downarrow\neq 1$) in these bands would prove conclusively the identity of the nuclei. Unfortunately the band-spectra of radioactive elements have not so far been observed.

∾ *This would mean that the idea of energy and its conservation fails in dealing with processes involving the emission or capture of nuclear electrons.* This does not sound so improbable if we remember all that has been said about the peculiar properties of electrons in the nucleus. While we have no relativistic theory and only very few experimental data it is very difficult to give an explanation, but there is no doubt that the question is of fundamental importance and will lead to revolutionary changes in our present picture of the physical world. ∾

III

EXCITED STATES AND ELECTRO-MAGNETIC RADIATION OF NUCLEI

§ 1. The Spectra of the γ-rays

The spontaneous disintegration of an unstable nucleus with the ejection of α- or β-particles means a vigorous disturbance of the whole nuclear system and is very often accompanied by very hard electromagnetic radiation γ-rays. The spectroscopy of γ-rays is very difficult since the wave-lengths are so small, and only very soft γ-rays can be directly measured in the ordinary way with a crystal spectrometer. The most convenient method of γ-ray spectroscopy is the study of the photo-electrons ejected by the γ-rays from the different electron-levels of the disintegrating atom, a method developed particularly by C. D. Ellis and L. Meitner. All radioactive elements which are known to emit γ-rays also emit strong secondary β-radiation, which appears in the magnetic spectrum as a rather complicated system of lines of different energies. For β-disintegrating elements these discrete lines lie in the region of the continuous spectrum of the primary β-rays.

We must bear in mind that γ-rays of a single wave-length give rise to several lines in the β-ray spectrum corresponding to the various levels (K, L, M,...) in the atom from which they can eject an electron. Accordingly, in analysing the β-ray spectrum we must first look for lines with energy-differences equal to the energy-differences ($K-L$, $K-M$, $L-M$,...) of the atomic levels; these lines will then define a single wave-length of the γ-ray spectrum. (The process of analysis is shown in Table I.)

The question arises whether the γ-rays are emitted before or after the disintegration, i.e. whether the observed β-ray lines correspond to transitions of the disintegrating nucleus itself or of its product. To decide this it is sufficient to investigate whether the γ-rays of a given element are converted in the electron-levels of the same atom or in those of its product. Owing to the small difference between the levels of two neighbouring atoms very accurate measurements are necessary to distinguish between these two possibilities. The matter was investigated by L. Meitner, who used the γ-rays emitted by the α-disintegrating elements RaAc and AcX, for which the

TABLE I

Analysis of the secondary β-ray spectra emitted by AcX ($Z = 88$)

Energy of β-group $\times 10^6$ erg.	Intensity.	Level of origin.	Energy of the level $\times 10^6$ erg.	Energy of γ-ray $\times 10^{-6}$ volt.	Deviations %
0·0723	80	K(86)	0·1554	0·2277	0·6
0·2003	50	L_1 ,,	0·0286	0·2289	
0·2204	25	M_1 ,,	0·0071	0·2275	
0·0889	100	K ,,	0·1554	0·2443	0·6
0·2159	60	L_1 ,,	0·0286	0·2445	
0·2358	15	M_1 ,,	0·0071	0·2429	
0·0950	40	K ,,	0·1554	0·2504	1·0
0·2204	25	L_1 ,,	0·0286	0·2490	
0·2407	15	M_1 ,,	0·0071	0·2478	
0·1658	40	K ,,	0·1554	0·3212	2·0
0·2860	15	L_1 ,,	0·0286	0·3165	
0·2717	100	K ,,	0·1554	0·4361	0·2
0·3990	30	L_1 ,,	0·0286	0·4295	

charge-numbers of the original nucleus and the product differ by two, so that the difference of the levels is more easily perceptible. Meitner found that the conversion takes place in the product-atom,

TABLE II A(1

Energy $\hbar\omega \times 10^6$ erg.	Energy $\hbar\omega \times 10^{-6}$ volt.	Conversion observed in.	Relative intensity
0·0924	0·0581	L_1, L_3, M, N	(250)
0·1265	0·0795	L_1, L_3	(15)
0·205	0·129	L, M, N	(100)
0·293	0·184	K, L, M	(50)
0·387	0·243	K	(4)
0·398	0·250	K, L_1	(18)
0·508	0·319	K, L_1	(16)
0·538	0·338	K, L_1	(8)
0·649	0·408	K, L_1	(3)
0·735	0·462	K, L_1, M	(8)
1·454	0·914	K, L_1	(6)
1·543	0·970	K, L_1	(3)
2·555	1·606	K	(1)
2·619	1·646	K	(1)

D. H. Black, *Proc. Roy. Soc.*, A, vol. cvi, p. 632 (1925).

TABLE II B(1

γ-rays from $ThB \to ThC$ (β)

Energy $\hbar\omega \times 10^6$ erg.	Energy $\hbar\omega \times 10^{-6}$ volt.	Conversion observed in.	Relative intensity.
0·1188	0·0747	L_1, L_3, M_1, N_1	(60)
0·278	0·175	K	(4)
0·304	0·191	K	(20)
0·321	0·202	K	(1)
0·369	0·232	K	(30)
0·383	0·241	K, L_1, M_1, N_1	(200)
0·401	0·252	K	(4)
0·480	0·302	K, L_1, M_1	(30)
0·557	0·350	K	(1)

¹ D. H. Black, l. c.

TABLE II C(1

$$\gamma\text{-rays from}\begin{cases} ThC \to ThC' \ (\beta) \\ ThC \to ThC'' \ (\alpha) \\ ThC' \to ThD \ (\alpha) \\ ThC'' \to ThD \ (\beta) \end{cases}$$

Energy $\hbar\omega \times 10^6$ erg.	Energy $\hbar\omega \times 10^{-6}$ volt.	Conversion observed in.	Relative intensity.	Notes about origin
0·0649	0·0408	L_1, L_2, L_3, M_1, N_1, O	(v.s.)	ThCC″ (α)
0·231	0·145	K, L_1	(f.)	ThCC″ (α)
0·259	0·163	K	(f.)	ThCC″ (α)
0·283	0·178	K	(f.)	
0·310	0·195	K	(m.)	
0·335	0·211	K, L_1	(m.s.)	
0·370	0·233	K, L_1	(m.s.)	
0·386	0·243	K	(f.)	
0·402	0·253	K, L_1	(m.s.)	
0·412	0·259	K, L_1	(m.)	
0·444	0·279	K, L_1	(v.s.)	ThCC″ (α)
0·464	0·292	K, L_1	(s.)	
0·550	0·346	K	(m.f.)	
0·698	0·439	K	(f.)	ThCC″ (α)
0·762	0.479	K	(f)	ThCC″ (α)
0·822	0·517	K, L_1, M_1	(v.s.)	
0·938	0·590	K, L_1	(v.s.)	
0·997	0·627	K	(m.f.)	
1·046	0·658	K, L_1	(m.s.)	
1.250	0·786	K	(m.f.)	
1·385	0·871	K	(m.s.)	
1·420	0·893	K	(f.)	
4·212	2·649	K, L_1, M_1	(s.)	

¹ D. H. Black, l. c.

and we therefore conclude that *the γ-rays are emitted by the radioactive nucleus after the disintegration.*

Much experimental knowledge of the γ-rays of different radioactive bodies has been obtained by analysing their secondary β-ray spectra in this way. The results thus obtained are given in Tables II, III, and IV.†

TABLE III A(1

γ-rays from Ra → RaEm (α)

Energy $\hbar\omega \times 10^6$ erg.	Energy $\hbar\omega \times 10^{-6}$ volt.	Conversion observed in.	Relative intensity.
0·298	0·189	K, L, M	

[1] L. Meitner, *Zs. f. Phys.*, Bd. 26, s. 161 (1924).

TABLE

γ-rays from RaB → RaC (β)

Energy $\hbar\omega \times 10^6$ erg.	Energy $\hbar\omega \times 10^{-6}$ volt.	Conversion observed in.	Relative intensities
0·0852	0·0536	$L_1, L_2, L_3, M_1, N_1, O$	(53)
0·313	0·197	K	(2)
0·328	0·206	K	(1)
0·386	0·243	K, L_1, M_1	(25) **0·163**
0·413	0·260	K, L_1	(6)
0·439	0·276	K	(3)
0·472	0·297	K, L_1, M_1	(30) **0·313**
0·507	0·319	K	(1)
0·563	0·354	K, L_1, M_1	(40) **0·511**
0·749	0·471	K	(1)
0·766	0·482	K	(1)

[1] C. D. Ellis and W. B. Skinner, *Proc. Roy. Soc.*, A, vol. cv, p. 190 (1924).

---

† In these tables the data obtained hitherto, concerning the γ-rays from different radioactive bodies, are collected. The relative intensities, represented roughly by the relative number of electrons ejected from K-levels, are shown in the last column. Only for a few γ-lines (from RaB and RaC) are the intensities measured accurately (see p. 78); in such cases the number (heavy type) given represents the total number of transitions in question (number of γ-quanta plus the number of ejected electrons) per disintegration.

TABLE III C(1

$$\gamma\text{-rays from}\begin{cases} RaC \rightarrow RaC' \ (\beta);\ [RaC \cdot \quad RaC''] \ (\alpha);\ RaC' \rightarrow RaD \ (\alpha); \\ [RaC'' \rightarrow RaD] \ (\beta) \end{cases}$$

Energy $\hbar\omega \times 10^6$ erg.	Energy $\hbar\omega \times 10^{-6}$ volt.	Conversion observed in.	Relative intensity.	Notes about origin.
0·0937	0·0589	L_1, L_2, L_3, M_1	(6)	
0·382	0·240	K	(1)	
0·399	0·251	K	(1)	
0·437	0·275	K, L_1	(4)	
0·448	0·282	K	(2)	
0·528	0·332	K, L_1	(2)	
0·619	0·389	K, L_1	(3)	
0·682	0·429	K, L_1	(3)	
0·800	0·503	K, L_1	(1)	
0·867	0·545	K	(2)	
0·917	0·577	K	(1)	
0·937	0·589	K	(1)	
0·973	0·612	K, L_1, M_1, N_1	(30) **0·663**	
1·043	0·656	K	(5)	
1·067	0·671	K	(5)	
1·229	0·773	K, L_1	(5) **0·065**	
1·334	0·839	K	(5)	
1·496	0·941	K, L_1	(7) **0·067**	
1·590	1·000	K	(5)	
1·797	1·130	K, L_1, M_1	(13) **0·208**	
1·857	1·168	K	(3)	
1·984	1·248	K, L_1	(7) **0·063**	
2·051	1·290	K	(2)	
2·210	1.390	K, L_1	(7) **0·064**	
2·267	1·426	K, L_1	(16) **0·003**	RaCC′ (β) ?
2·290	1·440	K	(2)	
2·326	1·463	K	(2)	
2·474	1·556	K	(1)	
2·554	1·606	K	(1)	
2·614	1·644	K	(1)	
2·681	1·686	K	(1)	
2·743	1·725	K	(2)	
2·773	1·744	K	(1)	
2·827	1·778	K, L_1	(8) **0·259**	
2·886	1·815	K	(1)	
3·019	1·899	K	(1)	
3·096	1·947	K	(1)	
3·228	2·030	K	(1)	
3·282	2·064	K	(1)	
3·385	2·129	K	(1)	
3·528	2·219	K, L_1	(3) **0·074**	
3·784	2·380	K	(1)	
3·907	2·457	K	(1)	
4·015	2·525	K	(1)	
4·185	2·632	K	(1)	

---

[1] C. D. Ellis, *Proc. Camb. Phil. Soc.*, vol. xxii, p. 369 (1925).

TABLE III D(1

γ-rays from RaD -> RaE (β)

Energy $\hbar\omega \times 10^6$ erg.	Energy $\hbar\omega \times 10^{-6}$ volt.	Conversion observed in.	Relative intensity.
0·0750	0·0472	L_1, L_2, L_3, M_1, N_1	

---

[1] C. D. Ellis, *Proc. Camb. Phil. Soc.*, vol. xxi, p. 125 (1922).

TABLE IV A(1

γ-rays from Pa -> Ac (α)

Energy $\hbar\omega \times 10^6$ erg.	Energy $\hbar\omega \times 10^{-6}$ volt.	Conversion observed in.	Relative intensity.
0·1516	0·0954	L_1, M_1, N_1	(6)
0·468	0·294	K, L_1, M_1	(6)
0·515	0·324	K, L_1, M_1	(4)

---

[1] L. Meitner, *Zs. f. Phys.*, Bd. 50, s. 5 (1928).

TABLE IV B(1

γ-rays from RaAc -> AcX (α)

Energy $\hbar\omega \times 10^6$ erg.	Energy $\hbar\omega \times 10^{-6}$ volt.	Conversion observed in.	Relative intensity.
0·051	0·032	$L_1, L_3, M_1, M_2, M_5, N_1, N_6$	(2)
0·0695	0·0437	L_1, L_2, L_3, M_1	(4)
0·0847	0·0533	L_1, M_1	(4)
0·0976	0·0614	L_1, M_1, N_1	(9)
0·160	0·1007	L_1, M_1, N_1	(4)
0·2370	0·1491	K, L_1, M_1	(8)
0·311	0·1954	K, L_1, M_1	(3)
0·4036	0·2539	K, L_1, M_1	(4)
0·4485	0·2821	K, L_1	(2)
0·4773	0·3002	K, L_1	(2)

---

[1] L. Meitner, *Zs. f. Phys.*, Bd. 34, s. 807 (1925).

TABLE IV C(1

γ-rays from AcX -> AcEm (α)

Energy $\hbar\omega \times 10^6$ erg.	Energy $\hbar\omega \times 10^{-6}$ volt.	Conversion observed in.	Relative intensity.
0·228	0·143	K, L_1, M_1	(8)
0·244	0·153	K, L_1, M_1	(10)
0·249	0·157	K, L_1, M_1	(4)
0·318	0·200	K, L_1	(4)
0·427	0·269	K, L_1	(10)

---

[1] L. Meitner, l. c.

TABLE IV D[1]

$$\gamma\text{-}rays\ from \begin{cases} [AcC \rightarrow AcC'] \ (\beta) \\ AcC \rightarrow AcC'' \ (\alpha) \\ [AcC' \rightarrow AcD] \ (\alpha) \end{cases}$$

Energy $\hbar\omega \times 10^6$ erg.	Energy $\hbar\omega \times 10^{-6}$ volt.	Conversion observed in.	Relative intensity.
0·562	0·353	K, L_1, M_1	(10)
0·731	0·460	K, L_1	(5)
0·763	0·480	K, L_1	(3)

[1] L. Meitner, l. c.

We see that some elements have rather complicated γ-ray spectra, while others have only a few lines or even only one line of small energy. The disintegration of the elements RaEm, RaA, RaE,..., is proved not to be accompanied by γ-radiation or only by such weak radiation that it cannot be perceived. These facts are evidently connected with the strength of the initial excitation and the relative position of the quantum-levels in the different nuclei. We might mention here that in using the data of Tables II, II, and IV we must be very careful: γ-ray spectroscopy is as yet in an early stage and the existing data cannot be regarded as so certain as those from Rowland's Tables. It is possible that many lines are not yet registered and the big gaps (for example, in ThC between $1{\cdot}420 \times 10^{-6}$ erg and $4{\cdot}212 \times 10^{-6}$ erg) do not necessarily mean that there are no lines in between; possibly this region has not yet been investigated experimentally.

§ 2. Fine Structure of α-particles and γ-rays

Since the emission of a γ-ray is always preceded by an α- or β-disintegration of the nucleus, we interpret the γ-radiation as due to radiative transitions of the nucleus excited by the disintegration. The diagrammatic representation of the history of successive disintegrations with the emission of γ-rays is given in Fig. 17. The particle (α or β) ejected from the nucleus No. 1 may leave the product-nucleus No. 2 in an excited state, after which transitions to states of lower energy with emission of γ-rays will take place.

As the period of γ-ray emission is usually much shorter than the average life of the nucleus, the γ-rays will appear to be emitted together with the ejected particle from No. 1 and will be ascribed to No. 1, although they are actually due to transitions between the quantum states of the nucleus No. 2, and are converted in the electron-levels of the atom No. 2. In view of this it is more rational to denote a γ-ray by the names of both the disintegrating and the product-element together. With this notation γ-ThCC$''$, for instance, means the γ-ray observed in the disintegration of ThC and corresponding to the level system of the ThC$''$-nucleus.

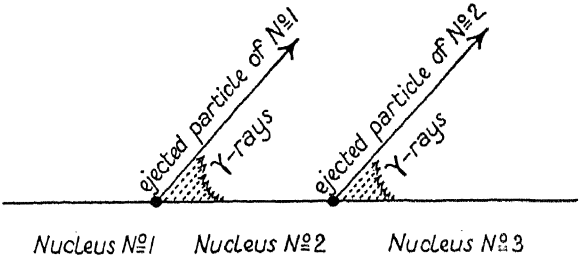

FIG. 17

If the nucleus is excited during the ejection of an α-particle the particle will evidently be emitted with smaller energy than when the nucleus is left in its normal state. We may therefore expect that bodies emitting γ-rays must have, besides the ordinary particles, several groups of particles of lower energy. The energy-differences between the different groups of these *low-speed particles* will correspond to those of the *different quantum-levels of the product-nucleus* (see the diagrammatic representation in Fig. 18). If the product-nucleus is left in an excited state, a transition to a state of lower energy can take place with emission of γ-rays. We should therefore

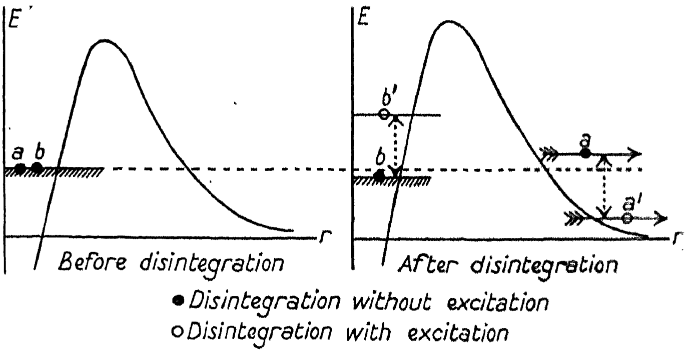
E′
a b
r
Before disintegration
E
b′
b
a
a′
r
After disintegration
● Disintegration without excitation
○ Disintegration with excitation

FIG. 18. Origin of the low-speed

expect the energies of the γ-rays emitted by the product-nucleus to agree with the energy-differences between the different groups of low-speed particles. If the excitation of the nucleus is due to the ejection of an α-particle and E_{α_0} is the energy of the ordinary α-particles emitted from a certain disintegrating element A, and E'_0, E'_1, E'_2,... are the energy-levels of the product-nucleus A', we may expect to observe besides the main group of energy E_{α_0} also slower groups of α-particles with energies

$$E_{\alpha_1} = E_{\alpha_0} - [E'_1 - E'_0];\ E_{\alpha_2} = E_{\alpha_0} - [E'_2 - E'_0];\ \ldots$$

The relative intensities of the different groups will decrease rather rapidly with their energy.

Such weak groups of α-particles with smaller energies than that of the main group have actually been observed for certain α-disintegrating bodies which emit γ-rays. Using a strong magnetic field Rosenblum succeeded in showing that the magnetic spectrum of ThC α-particles consists of five very close groups, referred to by Rosenblum as the 'fine structure of α-rays'. The groups of smaller energy are very weak.† The energy-differences and relative intensities of different groups as measured by Rosenblum are given in the first two columns of Table V A.

TABLE V A

Low speed α-particles of ThC[1]

Name of the group.	Energy-differences $(E_{\alpha_0} - E_{\alpha_n}) \times 10^6$ erg.	Energy-differences $(E_{\alpha_0} - E_{\alpha_n}) \times 10^{-6}$ volt.	Relative intensity $I_{\alpha_n}/I_{\alpha_0}$.
α_0	—	—	1
α_1	0·0646	0·0406	3·3
α_2	0·522	0·328	0·1
α_3	0·735	0·462	0·02
α_4	0·768	0·483	0·07

[1] G. Rosenblum, *C. R.*, vol. cxc, p. 1124 (1930); *Journal de physique*, vol. i, p. 438 (1930). The notation is different from Rosenblum's. The lines are numbered in the order of decreasing energies and not of relative intensities.

From what has been said above we should expect to find in the γ-ray spectrum emitted during the disintegration of ThC lines with energies equal to the differences between the levels as given in Table VA. Inspection of the table of γ-rays from ThCC′+CC″+C″D (p. 59) shows that such lines actually exist (0·0649; 0·231; 0·259; 0·444; 0·698; $0{\cdot}762 \times 10^{-6}$ erg).† They agree well with the energy-differences between the different α-particle groups. As the energies of the γ-rays are measured more accurately than those of the different fine-structure groups, it is more rational to construct the exact level scheme using these values. The balanced values of the energy levels are given in Table VB and also in Fig. 19. The agreement between the calculated and observed energies for the γ-rays can be seen from Table VC.

---

† These groups cannot be explained as α-particles escaping from the different excited levels of the ThC nucleus. As we shall see in the next paragraph, such particles can only be observed for elements with very short life, while the disintegration period corresponding to the different groups of α-particles of ThC is about six hours.

TABLE VB

Level.	Energy $\times 10^6$ erg. From γ-rays.	Energy $\times 10^6$ erg. From α-rays structure.
A	0·0000	0·0000
B	0·0644	0·0646 ± 0·0012
C	0·502	0·522 ± 0·020
D	0·731	0·735 ± 0·015
E	0·758	0·768 ± 0·015

TABLE VC

Transition.	Energy-differences from levels $\times 10^6$ erg.	Energy of γ-quanta observed $\times 10^6$ erg.	
B–A	0·0644	0·0641	+0·0003
D–C	0·229	0·227	+0·002
E–C	0·256	0·255	+0·001
C–B	0·438	0·440	−0·002
E–B	0·694	0·694	0·000
E–A	0·758	0·758	0·000

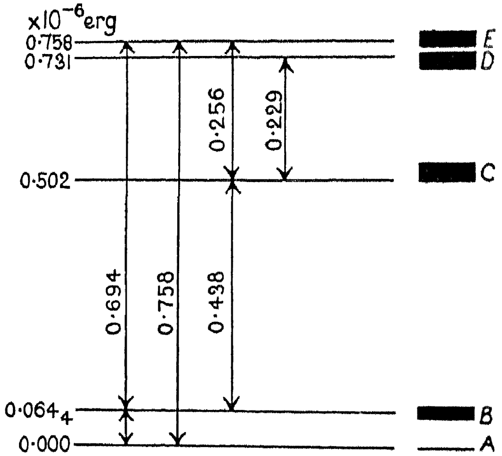

FIG. 19. Level-scheme of the ThC″ nucleus.

---

† These lines are calculated as due to ThC″ β-transformation and consequently converted in the atoms of ThD. Thus we must introduce a correction: $-0{\cdot}0036 . 10^{-6}$ erg for the *K*-level and $-0{\cdot}0008 . 10^{-6}$ erg for the *L*-level. In Table VC already corrected values of $\hbar\omega$ are given.

We see that the agreement within the given level scheme and also between the values of the energies obtained from the γ-ray lines and the α-ray fine structure is very good. Three γ-rays are missing; this may be due to their small intensity or simply to the incompleteness of the present γ-ray tables. The relative intensity of the different low-energy groups will evidently be defined by the ratio of the corresponding decay constants. Using formula (50) of Chap. II we may write

$$\frac{I_{\alpha_n}}{I_{\alpha_0}} = e^{-\frac{2\pi e^2\sqrt{(2m)}}{h}(Z-2)\left[\frac{1}{\sqrt{E\alpha_n}}-\frac{1}{\sqrt{E\alpha_0}}\right]+\frac{8e\sqrt{m}}{h}(Z-2)\left[\sqrt{r_0^{(n)}}-\sqrt{r_0}\right]}, \tag{1}$$

where $r_0^{(n)}$ is the radius of the nucleus in the nth excited state. Putting $r_0^{(n)} = r_0$ this formula gives a decrease of intensity of the different ThC groups somewhat more rapid than that observed. This shows that we must ascribe to the nucleus in an excited state a radius greater than that for a normal state, which is quite reasonable. The radii of the ThC″ nucleus in its normal and excited states are shown in Table VI.

TABLE VI

Radii of excited ThC″ nucleus

Level excited.	Excitation energy $\times 10^6$ erg.	$r_0 \times 10^{13}$ cm.
Normal	0·000	6·6
B	0·064	7·0
C	0·502	6·9
D	0·731	6·9
E	0·758	7·3

Up to the present ThC is the only element for which measurements of the low-speed groups of α-particles have been made. The investigations of Rutherford and his collaborators† by a new precise differential method for range measurement give evidence of the existence of a similar fine structure for the α-particles of RaC and AcC (Fig. 20). For all three *C*-products the curves show the existence of groups of α-particles with energy slightly smaller than the normal. The analysis of such curves in order to define the exact position of the different groups can give us only very rough data and more detailed investigations by the method of magnetic deflexion are necessary.

---

† E. Rutherford, F. Ward, and C. Wynn-Williams, *Proc. Roy. Soc.*, A, vol. cxxix, p. 211 (1930).

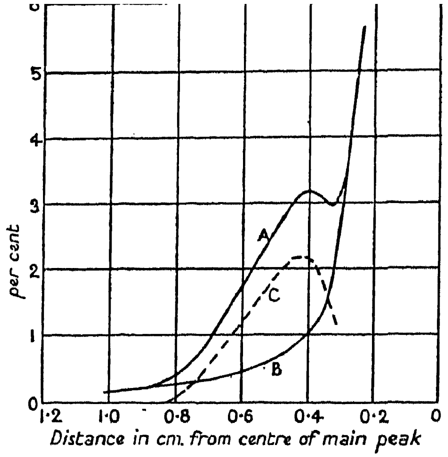

FIG. 20 *a*. Fine-structure of *ThC*-α-rays.

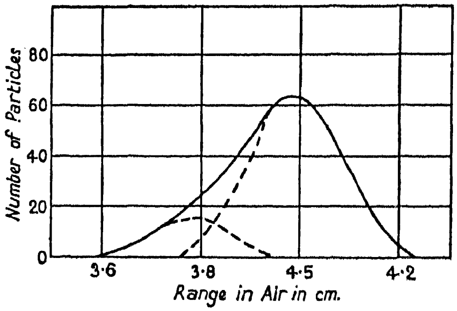

FIG. 20 *b*. Fine-structure of *RaC*-α-rays.

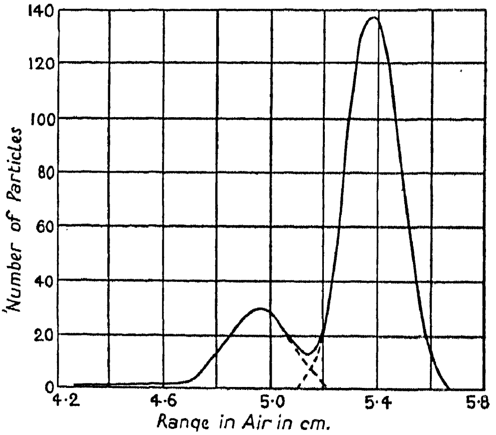

FIG. 20 *c*. Fine-structure of *AcC*-α-rays.

For ThC the range distribution curve as observed by Rutherford is just the curve we should expect from Rosenblum's exact values of the velocities and intensities of the different groups. The analysis of the range spectra for RaC and AcC suggests besides the main group ($R_0 = 4{\cdot}05_5$ cm. and $5{\cdot}41_1$ cm.) the existence of low-speed groups: $R_0 = 3{\cdot}86_8$ cm. for RaC, and $R_0 = 4{\cdot}99_1$ cm. for AcC. The corresponding energy differences are $0{\cdot}27 \times 10^{-6}$ erg for RaC and $0{\cdot}54 \times 10^{-6}$ erg for AcC. The corresponding γ-rays can hardly be expected to be found in the spectrum of the RaC mixture as the number of α-disintegrating atoms is only 0·04 per cent. of the whole, and the lines will be very weak. In the case of AcC, for which the percentage of α-disintegrating atoms is 99·7 per cent., the line must be fairly strong and may fit with the line $0{\cdot}562 \times 10^{-6}$ erg from the table of γ-rays of the AcC mixture.

We should expect the existence of low-speed α-particles for all α-disintegrating elements which emit strong γ-radiation such as RaAc, AcX, though owing to experimental difficulties these groups have not yet been observed.† On the other hand, for elements with very weak γ-radiation such as Ra, Po, or for those which show no perceptible radiation such as RaEm, RaA, the groups of low-speed α-particles must be extremely weak. The occurrence or non-occurrence of excitation by the α-disintegration is evidently due to a rather complicated interaction between the different constituent parts of the nucleus.

∾ Very strong γ-radiation is observed as a rule for β-disintegrating elements. There are again some exceptions; RaEF, for example, shows no trace of γ-radiation. Owing to our ignorance of the behaviour of the nuclear electrons and the process of β-decay the problem of the excitation of the nucleus by the ejection of a β-particle cannot be solved at present. The experimental fact that the energy of the γ-rays from β-disintegrating nuclei never exceeds the upper limit of the continuous β-spectrum shows a close connexion between the excitation of the different nuclear levels and the energy distribution among the β-particles in the continuous spectrum. ∾

§ 3. Long Range α-particles and γ-rays

We have spoken hitherto of the excited states of the nucleus as a whole. Since the nucleus consists of many particles of different kinds we may consider different kinds of excited states due to the excitation of an α-particle, or of a proton, or to the simultaneous excitation of several nuclear particles, although owing to the strong interaction between the parts of the nucleus this division is rather rough. We should expect the differences between the energy levels due to the excitation of an α-particle to be smaller than those corresponding to the excitation of a proton, owing to the greater mass of the α-particle. The diagrammatic representation of the two sets of levels‡ is given in Fig. 21; the fundamental level E^0_α and E^0_p of each system is defined as the difference between the energies of binding (mass-defects) of the original nucleus in the state of lowest energy and the product-nucleus after the emission of the corresponding nuclear particle. We must keep in mind that, owing to the interaction of the particles, the energies of the excited states, when more than one particle is excited, are not exactly equal to the sum of the energies of excitation of each particle separately.

---

† Quite recently a complex-structure of α-rays from RaAc has been found by I. Curie (*C.R.*, vol. cxcii, p. 1102 (1931)), who was able to show that the α-radiation of this element consists of two groups (of about equal intensity) $0{\cdot}28\times10^6$ volt apart, in good agreement with the γ-ray $0{\cdot}282\times10^6$ volt of RaAc.

‡ For radioactive substances the fundamental α-level E^0_α is positive (corresponding to the possibility of spontaneous α-disintegration), while the fundamental proton-level E^0_p has a large negative value.

If the nucleus is in an excited state a transition can take place to a level of lower energy, the energy-difference being emitted in the form of γ-rays. There is, however, the possibility of an alternative process in which an excited particle, if its energy is sufficiently large, will cross the potential barrier surrounding the nucleus and escape with the energy of the excited level. We should, therefore, observe several groups of *high-speed particles* due to the disintegration of the excited nucleus. As the fundamental proton level in radioactive nuclei is very deep a proton would have to be very highly excited before it could be ejected; on the other hand, the fundamental, and consequently all excited levels of a nuclear α-particle, have positive energies. It would be incorrect to say that the actually observed high-speed α-groups correspond entirely to the excited α-levels of the nucleus, as owing to the very strong interaction we should expect the following process. Suppose there is a proton in a certain excited level $E_p^{(n)}$, perhaps even of negative energy (see Fig. 21); it can happen that the proton in falling to a lower level $E_p^{(m)}$ will, instead of radiating energy, give it to an α-particle, which is just going to leave the nucleus from a level of energy $E_\alpha^{(n')}$, say. The α-particle will be ejected with the energy $E_\alpha^{n'}+E_p^n-E_p^m$, just as if there existed an α-level of

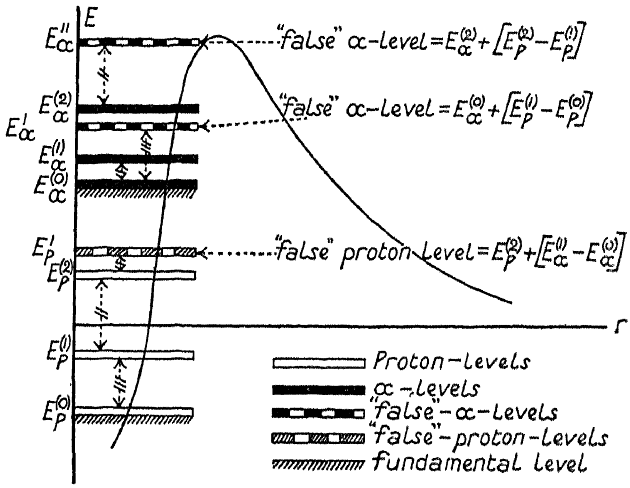

FIG. 21. Origin of high-speed α-groups.

this energy, which we may call a 'false α-level'. Such processes, which may be compared with those which give rise to low-speed α-particles, make the scheme of α-groups very complicated. Owing to the strong interaction the probability of emission of such groups is very great, and it is practically impossible to distinguish between the true and 'false' levels until the nature of the different quantum states of the nucleus is more exactly known. The high-speed α-groups do, however, give us the complete system of all possible excited states of the nucleus.

If now $E_\alpha^{(n)}$ is the energy of an excited α-level (true or 'false'), $\lambda^{(n)}$ the corresponding decay constant and $\kappa_{n,m}$ the probability of a transition from the nth to the mth level, the relative number of α-particles in the nth high-speed group will be

$$N^{(n)} = p^{(n)} \frac{\lambda^{(n)}}{\sum_{m=0}^{n-1} \kappa_{n,m}} \tag{2}$$

where $p^{(n)}$ is the percentage of nuclei with an α-particle in the excited nth level. The relative number of high-speed α-particles will be rather small owing partly to the fact that even for these energies the decay constant λ is still much smaller than the probability of transition, and partly to the small number of α-particles in excited states of very high energy.

The high-speed groups have been actually detected in the α-radiation of certain radioactive elements with a very short period of life. The range-spectra of these groups in ThC′ and RaC′ are shown in Figs. 22 *a*, *b*.[†] From this distribution only two groups for ThC′ ($R_0^I = 9{\cdot}77$ cm. and $R_0^{II} = 11{\cdot}57$ cm.) and one group for RaC′ ($R_0^I = 9{\cdot}03$ cm.) can be definitely established, but it is certain that also several weaker groups are present.[‡] The differences between the energies of the high-speed groups and that of the normal group are given in the fifth column of Table VII A, B. These energy-values give us directly the position of the different excited levels of the

---

[†] Nimmo and Feather, *Proc. Roy. Soc.*, A, vol. cxxii, p. 668 (1929).

[‡] Quite recently the high-speed groups of RaC′ have been investigated by Rutherford, Ward, and Lewis (*Proc. Roy. Soc.*, A, vol. cxxxi, p. 684 (1931)). In addition to one previously known group eight more could be traced. The energy-differences between these groups and the normal one are: 1·00; 2·32; 2·80; 3·09; 3·50; 3·74; 4·11; 4·52; $4{\cdot}77 \times 10^{-6}$ erg. Although the nuclear levels indicated by these groups fit well with several known γ-rays of RaC′, one has not yet succeeded in the identification of all possible transitions with the observed γ-spectra.

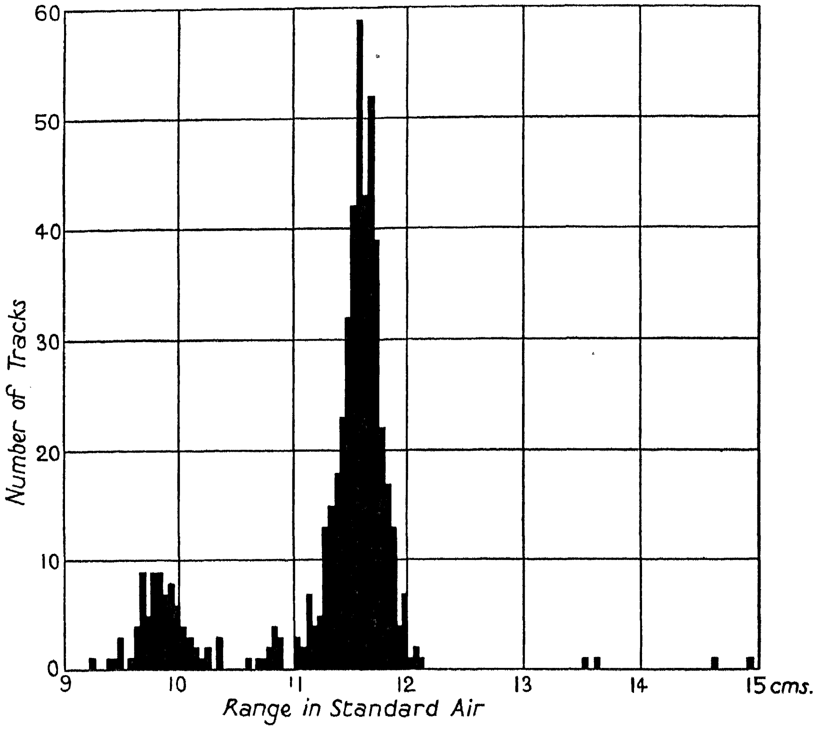

FIG. 22 *a*. Long-range α-particles from *ThC′*.

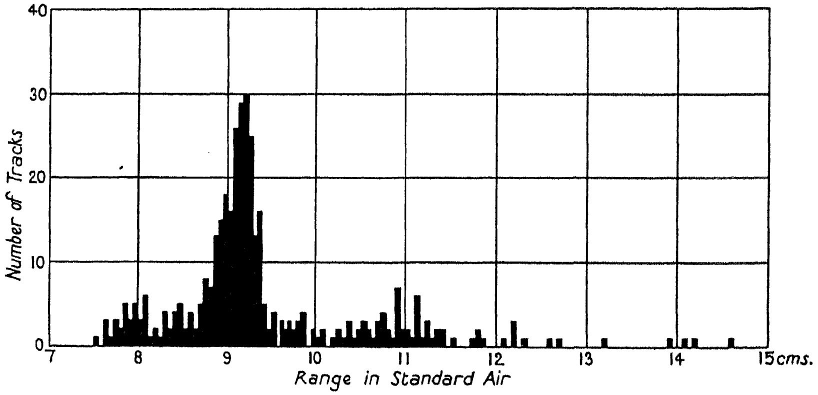

FIG. 22 *b*. Long-range α-particles from *RaC′*.

nuclei of the C′-products. From what was said above we should expect the existence of γ-rays 1·30 and $3{\cdot}01 \times 10^{-6}$ erg for ThC′ and of a γ-ray $2{\cdot}36 \times 10^{-6}$ erg for RaC′.

TABLE VII A

High-speed particles from ThC′.

Name of the group.	Range R_0 cm.	Energy $\times 10^6$ erg.	Energy-difference.		Relative number.
			$\times 10^6$ erg.	$\times 10^{-6}$ volt.	
Normal α_0	8·487	13·99	—	—	1
α^I	9·77	15·29	1·30	0·82	65×10^{-6}
α^{II}	11·57	17·00	3·01	1·90	180×10^{-6}

TABLE VII B

High-speed particles from RaC′.

Name of the group.	Range R_0 cm.	Energy $\times 10^6$ erg.	Energy-difference.		Relative number.
			$\times 10^6$ erg.	$\times 10^{-6}$ volt.	
Normal α_0	6·854	12·20	—	—	1
α^I	9·03	14·56	2·36	1·49	12×10^{-6}

The identification of the energy-differences between the different groups of high-speed α-particles with those of the lines of the γ-spectra is difficult owing to the uncertainty in estimating the energy of the α-particles from the range measurements. The ThC′-difference $E_{\alpha^I} - E_{\alpha_0} = 1{\cdot}30 \times 10^{-6}$ erg may fit with the γ-line $1{\cdot}385 \times 10^{-6}$ erg, while the two other differences $E_{\alpha^{II}} - E_{\alpha_0} = 3{\cdot}01 \times 10^{-6}$ erg and fall in a region of the γ-spectrum which has not yet been investigated. R. H. Fowler has discussed the possibility that the RaC′-difference $E_{\alpha^I} - E_{\alpha_0} = 2{\cdot}36 \times 10^{-6}$ erg may fit with the RaC γ-line $2{\cdot}267 \times 10^{-6}$ erg. As this line evidently corresponds to a forbidden transition of the RaC′-nucleus (see p. 79) it would be possible to account for the fact that the E_{α^I} group of RaC′ is much stronger than all the other groups. This question cannot be decided, however, until more accurate measurements of the energies of the high-speed α-groups have been carried out.

The energy-levels as obtained from the analysis of low-speed and high-speed α-particles are at present the only data which are at all reliable. Of course, it is possible to construct a tentative nuclear level scheme, using the combination principle, in order to account for the observed γ-lines. Such a scheme, based only on numerical agreement, is very uncertain and also not unique, so that no great reliance can be placed on it. A typical example of such a scheme is shown in Fig. 23, classifying ten lines of the RaCC′+RaCC″+RaC′D+RaC″D γ-spectra in five levels; all ten possible transitions between the given levels can be found in Table III c, agreeing with an accuracy of 0·3 per cent. or less. If the level scheme shown in Fig. 23 is correct it ought to give the levels of the excited RaC′ nucleus.

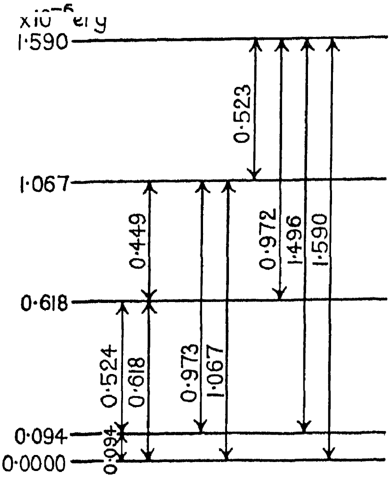

FIG. 23. Level scheme of RaC′ nucleus (doubtful!).

§ 4. Probability of γ-emission

We shall now consider more closely the question of the probabilities of the different radiative transitions of the excited nucleus. The light quanta emitted by any radiating system can have different values of the angular momentum greater than zero ($j_q = |\mathbf{j}_q| = 1, 2, 3,...$).† If, as for γ-rays, the wave-length λ of the emitted radiation is large compared with the dimensions r_0 of the radiating system, the probability of emission of such quanta will decrease rapidly [r

with increasing angular momentum, so that only transitions giving rise to light quanta with angular momentum unity will be of any importance.‡ If **i** and **i**′ are the angular momenta of the *nucleus* before and after emission respectively, we have

$$\mathbf{j}_q = \mathbf{i}' - \mathbf{i}. \tag{3}$$

From what has been said about the possible values of the angular momenta of the emitted γ-quanta, the following selection rules for the nuclear radiative transitions may be obtained. The transition $i \to i \pm 1$ is possible as it corresponds to light-quanta with unit angular momentum; while transitions $i \to i + x$ $(x \gg 1)$, corresponding to the emission of light quanta with larger angular momentum, are very weak. Transitions between two states with equal i are allowed for all values of i except zero, as if $i = i' > 0$ the vector equation (3) always allows the possibility of non-zero angular momenta. Therefore, in the γ-radiation from nuclei only transitions with $\Delta i = \pm 1$ and $\Delta i = 0$ (for $i \neq 0$) may be expected to be observed; the lines corresponding to $|\Delta i| > 1$ are too weak, and those corresponding to $i = i' = 0$ are excluded. The probability of a radiative transition between the mth and nth levels is, as is well known, given by the

---

† It can be shown that light quanta with zero angular momentum do not exist.

‡ The wave-length of the hardest γ-rays ($\lambda \sim 5 \times 10^{-11}$ cm.) is still sixty times greater than the nuclear radius ($r_0 \sim 10^{-12}$cm.), so that the probability of a transition giving rise to quanta with angular momentum two is more than a thousand times smaller than that of a transition with emission of quanta with angular momentum unity.

$$\kappa_{n,m} = \frac{4}{3}\frac{z^2e^2\omega_{n,m}^2}{\hbar c^3}|r_{n,m}|^2 < \frac{2}{3}\frac{z^2e^2}{c^3\hbar^2 m}(\hbar\omega_{n,m})^2, \tag{4}$$

where $\omega_{n,m}$ is the frequency of the emitted γ-ray, and ze, $r_{n,m}$ are the charge and matrix element of the radius vector of the radiating particle respectively. Since we do not know the wave-functions representing the motion of a radiating nuclear particle we can obtain from the formula (4) only the upper limit for the transition-probability. We must, however, always remember that the actual values of κ may be much smaller than the calculated upper limit.

A more or less direct estimation of the transition probabilities for excited nuclei can be carried out for nuclei for which the high-speed α-groups have been observed. From formula (2) we have

$$\kappa_n = \sum_{m=0}^{n-1} \kappa_{n,m} = p^{(n)}\frac{\lambda^{(n)}}{N^{(n)}}, \tag{2'}$$

where $\lambda^{(n)}$ can be calculated from the known energy of the high-speed particles and $N^{(n)}$ can be directly observed. From the measurements of the intensities of the γ-lines (see, for example, Table VIII) we conclude that the excitation $p^{(n)}$ of the levels corresponding to the main high-speed groups of ThC′ and RaC′ is strong and of the order of magnitude unity. For the α-particles of two groups of ThC′ and one

---

† From the general wave-mechanical relation:

$$\sum_{m=0}^{n-1} \frac{2m\omega_{n,m}}{\hbar}|r_{n,m}|^2 = 1 \text{ it follows that: } |r_{n,m}|^2 < \frac{\hbar}{2m\omega_{n,m}}.$$

of RaC′ we calculate the decay constants to be

$$\lambda = 3\times 10^{10};\ 5\times 10^{12};\ 7\times 10^{9};\ \text{sec}^{-1}.$$

Using the values of $N^{(n)}$ from the Tables VII A, B and putting $p^{(n)} \sim 1$ we obtain for the transition probabilities of the γ-lines corresponding to the high-speed groups $\kappa \sim 5\times 10^{14}$; 3×10^{16} for ThC′ and $\kappa \sim 6\times 10^{14}$ for RaC′. The corresponding upper limits given by (4) are $< 6\times 10^{15} < 3\times 10^{16}$ and 2×10^{16}. We see that the actual values are rather smaller than the calculated upper limit. Probably the comparatively small transition probabilities from the levels in question give the reason why the high-speed α-groups corresponding to these levels are much more intense than the others.

§ 5. Secondary Electrons ejected from the Atom during Disintegration

Energy may also be liberated from an excited nucleus in another way; it may be communicated to one of the extra-nuclear electrons. Then, instead of a γ-ray, an electron will be emitted from the atom with energy equal to that of the excited nucleus minus the ionization energy of the atomic level from which the electron has been ejected. As we have seen, such discrete groups of secondary electrons are actually observed in radioactive transformations and they supply us with one of the best methods of investigation of the excited states of the nucleus. The interaction between the extra-nuclear electron and the excited nucleus, which gives rise to the process of emission, will be essentially different for large and small distances of the electron from the nucleus. For distances large compared with the dimensions of the nucleus the interaction may be treated as due to the electro-magnetic radiation field of the nucleus, and we may consider the so-called *internal conversion of γ-rays* in the electron-shells of the atom in which they are emitted as a kind of photo-electric effect. By the general theory of perturbations the probability of ejection due to such an interaction is given by

$$\kappa_1^{(e)} = \frac{1}{\hbar}\left| \int W\psi_{e_1}\bar{\psi}_{e_2}\,dv \right|^2 \quad r \gg r_0, \tag{5}$$

where ψ_{e_1} and ψ_{e_2} are the wave-functions for the electron in a stable orbit and the ejected electron respectively and W is the perturbing term in the wave-equation due to the electro-magnetic field of the radiation from the nucleus. If W_n corresponds to the field due to the emission of one quantum per unit time the formula (5) may be

written in the form
$$\kappa_1^{(e)} = \kappa_\omega^{(r)} K(\omega) \tag{5$'$}$$

$$K(\omega) = \frac{1}{\hbar}\left|\int W_n \psi_{e_1} \bar{\psi}_{e_2}\, dv\right|^2, \tag{5$''$}$$

and $K(\omega)$ may be called the coefficient for the internal photoelectric effect, or internal conversion coefficient of the γ-ray. To indicate in which electron-level the conversion has taken place we must add a further index: ${}^{K}K(\omega)$; ${}^{L_1}K(\omega)$; ${}^{L_2}K(\omega)$;.... The value of the internal conversion coefficient can be calculated from (5″) if we substitute for ψ_{e_1} and ψ_{e_2} the corresponding solutions of the relativistic wave-equation. For hard γ-rays, with energy large compared with $m_e c^2 (= 0{\cdot}54 \times 10^{-6}$ erg) we obtain the formula†

$${}^{K}K(\omega) = \frac{1}{Zp}\alpha^2(2\alpha)^{2\sqrt{(1-\alpha^2)}} \frac{|\Gamma\{\sqrt{(1-\alpha^2)}-i\alpha\}|^2}{\Gamma\{1+2\sqrt{(1-\alpha^2)}\}} e^{-2\alpha \arccos \alpha}, \tag{6}$$

where
$$\alpha = \frac{Ze^2}{\hbar c} \text{ and } p = \frac{\left(\frac{v}{c}\right)}{\sqrt{\left[1-\left(\frac{v}{c}\right)^2\right]}}, \tag{6$'$}$$

and Z is the charge-number of the nucleus in question.

If the distance between the electron and the nucleus is comparable with the nuclear radius the formula (6) can no longer be applied, as the electron comes into the region where the interaction is unknown. The contribution to the total probability of ejection due to the interaction at small distances may be roughly estimated from the formula

$$\kappa_2^{(e)} = \frac{1}{\hbar}\left|\int V_{n,e} \psi_n \bar{\psi}_{n'} \psi_{e_1} \bar{\psi}_{e_2}\, dv\right|^2 \text{ for } r \sim r_0, \tag{7}$$

where $V_{n,e}$ is the interaction energy of the nuclear excited particle and the electron at small distances, and ψ_n, $\psi_{n'}$ are the wave-functions for the normal and excited states of the nuclear particle. As we do not know the functions ψ_n, $\psi_{n'}$, nor even whether the integral (7) may be applied for strong interaction inside the nucleus, this part of the probability cannot at present be estimated theoretically. We can only say that this probability will be proportional to the values of $|\psi_{e_1}|^2$ and $|\psi_{e_2}|^2$ inside the nucleus.

Thus, we can conclude that the probability will be small if one or both of the electron wave-functions has the quantum-number $l > 0$, as then their product vanishes when $r = 0$. Thus, the ejection due to collision will be mainly from the K-levels of the atom, and the ejected electron will have no angular momentum. This leads us to the following exclusion principle: *The ejection of an extra-nuclear electron due to collision may take place only for nuclear transitions for which the change of angular quantum-number for the nucleus is* $\Delta i = 0, \pm 1$. *This exclusion principle is equivalent to that for radiative transitions, except that the transition,* $i = 0 \rightarrow i = 0$, *is allowed.*

---

† I am indebted to H. Casimir for this formula.

The total probability of ejection of an electron is given by the sum of both probabilities

$$\kappa^{(e)} = \kappa_{\omega}^{(r)} K(\omega) + \kappa_{2}^{(e)}. \tag{8}$$

As we cannot yet calculate the value of $\kappa_2^{(e)}$, experiment must decide which of these two probabilities is the more important in radioactive nuclei.

For this purpose we can use the results of Ellis,[†] who measured the number of γ-quanta and electrons ejected from the K-level during the disintegration of RaB and RaC. His results are given in Table VIII.

TABLE VIII

Internal conversion of RaC γ-lines

$\hbar\omega \times 10^6$ erg.	Number of γ-quanta (per disintegration).	Number of electrons from K-level.	Ratio.	$^{\kappa}K(\omega)$ calculated.
0·973	0·658	0·00401	0·0061	0·00046
1·229	0·065	0·00031	0·0048	0·00037
1·496	0·067	0·00041	0·0061	0·00033
1·797	0·206	0·00128	0·0062	0·00028
1·984	0·063	0·00036	0·0057	0·00026
2·210	0·064	0·00009	0·0014	0·00024
2·267	0·000 (!)	0·0025	∞	0·00023
2·827	0·258	0·00041	0·0016	0·00018
3·528	0·074	0·00010	0·0013	0·00016

If the ejection of electrons is mainly due to internal conversion (i.e. if $\kappa^{r} K \gg \kappa_2^{(e)}$) the ratio of the number of ejected electrons to the number of γ-quanta must give directly the value of the internal conversion coefficient. These ratios are given in the fourth column of Table VIII, while the values calculated from formula (6) are given in the fifth. We see that the observed ratios are about twenty times larger than the calculated coefficients, which proves that the majority of the secondary electrons are due to direct collisional ejections ($\kappa_2^{(e)}$).

[†] Ellis and Aston, *Proc. Roy. Soc.*, A, vol. cxxix, p. 180 (1930).

For hard γ-rays, therefore, the internal conversion is unimportant compared with the ejection due to collision.

In Table VIII we observe one peculiar line, 2·267, which is fairly strong in the secondary β-ray spectrum but completely absent from the γ-ray spectrum. This means that the corresponding radiative transition of the nucleus is not allowed; this, as we have seen, happens only for the transition $i = 0 \rightarrow i = 0$. We have already mentioned that this line possibly represents the transition from an excited level of the RaC′ nucleus corresponding to a very strong group of long-range α-particles.

§ 6. The Anomalous Absorption of γ-rays

The absorption of hard γ-rays in matter is mainly due to the Compton-scattering by the extra-nuclear electrons. As the energy of hard γ-rays is much greater than the binding-energy of the electrons in an atom, the 'Klein-Nishina formula'[†] for the scattering by free electrons may be applied in this case. We have, therefore, for the absorption-coefficient σ the expression:

$$\sigma = n\sigma_{\epsilon} = 4{\cdot}96\,.\,10^{-25}n\left[\frac{1+\alpha}{\alpha^2}\left\{\frac{2(1+\alpha)}{1+2\alpha}-\tfrac{1}{2}lg(1+2\alpha)\right\}-\right.$$

$$\left.-\frac{1}{\alpha}lg(1+2\alpha)-\frac{1+3\alpha}{(1+2\alpha)^2}\right], \qquad (9)$$

where

$$\alpha = \frac{\hbar\omega}{mc^2} \qquad (9')$$

and n is the total number of electrons per c.c. of the absorbing substance.

Recently the validity of this formula for hard γ-rays has been investigated by several authors.[†] Their results agree in that the absorption-coefficients of the lighter elements fit well with the formula (9), whereas for the heavier elements they find an additional absorption, increasing rapidly with the charge-number.

We shall discuss here the results of the recent measurements of Meitner and Hupfeld and of Jacobsen. Their results do not agree with respect to the finer details of the dependence of the anomalous absorption on the charge-number.

[†] O. Klein and Y. Nishina, *Zs. f. Phys.*, Bd. 52, p. 853 (1929).

[‡] G. T. Tarrant, *Proc. Roy. Soc.*, A, vol. cxxviii, p. 345 (1930); C. Y. Chao, *Proc. Nat. Acad. Amer.*, vol. xvi, p. 431 (1930); L. Meitner and H. Hupfeld, *Zs. f. Phys.*, Bd. 67, p. 147 (1931); J. Jacobsen, *Zs. f. Phys.*, Bd. 70, p. 145 (1931).

In Fig. 24 the absorption-coefficient per electron σ_ϵ for the γ-rays of ThC (filtered through 4 cm. of lead and consisting practically of only one γ-line of energy $\hbar\omega = 4{\cdot}212 \,.\, 10^{-6}$ erg) in different elements is plotted against the charge-number. The values of Meitner do not lie on a smooth curve; in particular they show a marked discontinuity between Mg and Al, the reality of which was checked by especially careful experiments. On the other hand Jacobsen's values lie on a rather smooth curve. The theoretical value of σ_ϵ for the γ-rays used in these experiments is $\sigma_\epsilon = 1{\cdot}235 \,.\, 10^{-25}$, and we see that for the heavy elements the anomaly goes up to 40 per cent.

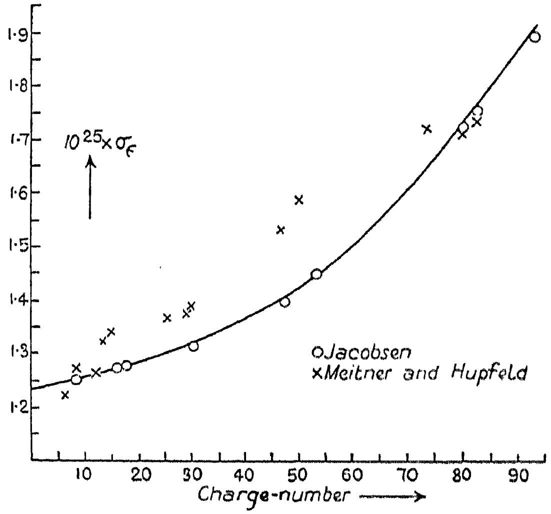

Fig. 24

The experiments with the somewhat softer radiation from RaC (filtered through 4 cm. of lead but still rather inhomogeneous and with an average energy of $\overline{\hbar\omega} = 2{\cdot}9 \,.\, 10^{-6}$ erg) seem to show no deviations for the elements up to *Zn* ($Z = 30$) and deviations of only 30 per cent. for lead.

The experiments do not decide whether the anomaly is due to an additional scattering, or to the transformations of the γ-quanta into some other kind of energy. The recent experiments of Gray† seem to show that for the elements for which anomalous absorption has been observed, the scattering is nevertheless normal, but these experiments are not quite conclusive.

The theoretical interpretation of the observed anomalies is at present not at all clear; we do not even know whether they originate in the electronic shells of the atom (photo-electric effect), or if the effect must be ascribed to the nucleus. To decide this it would be very important to know whether the effect varies continuously or not with the charge-number, as an irregular variation would point definitely to a nuclear origin of the anomalous absorption. But, as we have seen, on just this point the experimental data do not agree with one another.

---

† Gray, *Proc. Roy. Soc.*, A, vol. cxxx, p. 524 (1931).

However, it seems very improbable that the ordinary photo-electric effect should play an important part for the hard γ-rays used. This is also shown by the fact that the additional absorption observed is greater in the case of ThC γ-rays than in the case of the much softer γ-rays from RaC, as the probability of the photo-electric effect must be expected to decrease with increasing energy of the light-quanta.

Turning to the nucleus we shall first discuss the possibility of treating the effect as due to the scattering of γ-radiation by the heavy nuclear particles. The absorption-coefficient per nucleus must then be given by the expression:

$$\sigma_n = \frac{8\pi}{3} N^2 \left\{ \frac{2\omega (ze)^2}{c^2} \sum_n \frac{(E_n - E_0)}{(E_n - E_0)^2 - (\hbar\omega)^2} |r_{n,0}|^2 \right\}^2, \tag{10}$$

where ze and N are the charge and the number of the active particles (per nucleus) and E_0, $E_1 \ldots E_n$ the energies of the different quantum states of the nucleus in question. An upper limit for the matrix-element of the amplitude $|r_{n,0}|$ can be deduced from the general wave-mechanical relation

$$\sum_n \frac{2m(E_n - E_0)}{\hbar^2} |r_{n,0}|^2 = 1.$$

We get, therefore:

$$|r_{n,0}|^2 < \frac{\hbar^2}{2m(E_n - E_0)}$$

and formula (10) becomes

$$\sigma_n < \frac{8\pi}{3} N^2 \left\{ \frac{(ze)^2}{mc^2} \sum_n \frac{(\hbar\omega)^2}{(E_n - E_0)^2 - (\hbar\omega)^2} \right\}^2. \tag{10'}$$

Assuming that the active particles are α-particles, we put $z = 2$; $N \sim 50$, and get with $\hbar\omega = 4{\cdot}212 \,.\, 10^{-6}$ erg (assuming, further, that there is no resonance) for the nuclear scattering a value about 1600 times smaller than that observed. Of course, we can get much greater values of σ_n by assuming that the energy of the γ-quanta is very near to one of the energy-levels (E_n-E_0) of the nucleus; calculation shows that in order to explain the observed absorption in this way we must have $[\hbar\omega-(E_n-E_0)]/\hbar\omega \sim \frac{1}{100}$. The supposition that this is really so for all the elements for which the effect has been observed is, however, highly improbable.

∾ The other possibility is to ascribe the additional absorption to the nuclear electrons. Such an explanation, however plausible, cannot at present be treated theoretically on account of our ignorance of the behaviour of the electrons in the nucleus. We will only point out that, as the principle of conservation of energy does not seem to be applicable to nuclear processes involving the electrons, it is not impossible that the energy of the γ-rays is not scattered but is directly absorbed by the nuclear electrons and disappears without leaving any trace. ∾

IV

ARTIFICIAL EXCITATION AND TRANSFORMATION OF NUCLEI

§ 1. Anomalous Scattering of α-particles

In this chapter we shall deal with phenomena that occur when atoms are bombarded by particles of very great energy which penetrate very close to the nucleus. For such experiments the α-particles emitted by different radioactive bodies are generally used as they have more energy than any other particles at present obtainable in the laboratory. Very recently attempts have been made to prepare artificially strong beams of rapidly moving particles by accelerating ionized atoms in a very strong electric field ($0{\cdot}3\times 10^6$ volts). We should expect the probability of observing the disturbance of a nuclear system by fast particles to be greatest for light elements, where, owing to the small electric charge, the Coulomb repulsive forces acting on the incident α-particles are comparatively small. If a beam of particles falls on a light nucleus surrounded by a potential barrier not very high compared with the energy of the incident particle, a certain proportion of the particles will be able to penetrate the potential barrier and reach the interior of the nucleus. We shall now discuss what happens to these particles. They can either escape from the nucleus again without losing energy (elastic collision), or they can give up some of their energy to the nucleus. The first process is responsible for deviations from the ordinary scattering formula for a Coulomb field of force (anomalous scattering), the second causes certain changes in the nucleus of the bombarded element (artificial excitation or disintegration of nuclei).

We shall deal first with anomalous scattering. It is well known that if a stream of charged particles, such as α-particles, is scattered by an inverse square law centre of force, both classical mechanics and wave mechanics predict that the scattering is according to Rutherford's law. This states that the effective cross-section which must be hit by a particle for it to be scattered in a solid angle $d\omega$ is equal to

$$\left(\frac{ZZ'e^2}{4E}\right)^2 \operatorname{cosec}^4\tfrac{1}{2}\theta\, d\omega, \tag{1}$$

where Z and Z' are the charge-numbers of the scattering nucleus and the particle respectively, E the energy of the incident particle, and θ the angle of scattering.

As we have seen, it is found that the scattering of α-particles by the heavier elements conforms exactly to this law. We deduce that the field of these nuclei is that of the inverse square down to the smallest distance to which these particles penetrate. For the light elements, however, Rutherford and Chadwick have found deviations from this law. For sufficiently slow particles the law is obeyed, but as the energy increases the scattering falls below that predicted by the law and then rises above it. Rutherford and Chadwick deduced that the inverse square law does not hold up to the very small distances to which such particles can penetrate; they have estimated the radius at which the law begins to break down.

In order to explain the anomalous scattering we must calculate the amplitude of the wave scattered from the nucleus when the plane wave which represents the incident α-particles falls on it. A rough approximation to the scattering law may be obtained in the following way from the wave-equation:† each element of volume is supposed to scatter a wavelet, and these wavelets interfere to form the resultant scattered wave. The amplitude of the wavelet, scattered by an element of volume *dxdydz*, at a distance r from it is

(2)

times the amplitude of the incident wave at that point, where $U(x,y,z)$ is the potential energy of the particle in the field of the nucleus. The wavelet has the same phase as the incident wave if U is positive and the opposite phase if U is negative. If U is the potential for a Coulomb field then the resultant of all the wavelets is a scattered wave of amplitude

$$\frac{1}{r}\frac{ZZ'e^2}{4E}\operatorname{cosec}^2\tfrac{1}{2}\theta \qquad (3)$$

which leads directly to Rutherford's law. In the actual nuclei certain non-Coulomb forces must come into play at small distances, and deviations from Rutherford's law may be expected. If, however, the potential barrier is high enough compared with the energy of the α-particle the amplitude of the incident wave will drop almost to zero at distances for which the departure from the inverse square law is appreciable, so that the deviations from Rutherford's law will be small. If, on the other hand, the amplitude of the incident wave is appreciable inside the nucleus, the wavelets scattered by this region will cause deviations from the law. To calculate the scattering exactly we should have to know the precise form of the field inside the nucleus. We can see that the generally adopted form of the nuclear potential distribution will explain qualitatively the deviations from Rutherford's law. In the region where the Coulomb law holds the potential U is positive, dropping down at small distances ($r < r_0$) and reaching negative values (for light elements) inside the nucleus. Therefore, the wave scattered by the inside of the nucleus will have the opposite phase to that scattered in the region where the inverse square law holds. Thus, in the region where the two waves have amplitudes of the same order of magnitude it is clear that the scattering will be *less* than that given by Rutherford's formula. For incident particles of still greater energy, when the internal attractive field accounts for the greater part of the total scattering, we should expect the scattering to be greater than that given by Rutherford's formula, because the field in the nucleus is greater than it would be at the same distance from the centre if the nucleus were a point charge. It is found experimentally that the ratio of the observed scattering to that given by Rutherford's formula for a given angle falls to a minimum and then rises again (see Fig. 25 *a, b, c*).[†]

---

† This method is due to N. F. Mott.

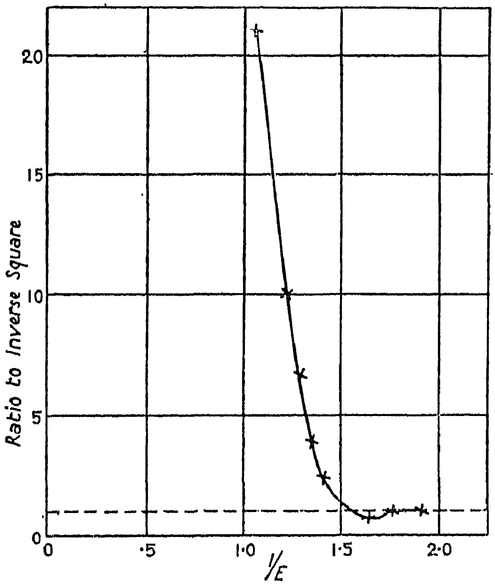

Fig. 25 *a*. Scattering of α-particles by Helium.

[†] Rutherford and Chadwick, *Phil. Mag.*, vol. 1, p. 889 (1925); vol. iv, p. 605 (1927).

The most striking deviations from Rutherford's law are shown by the two lightest elements, hydrogen and helium. For these elements the scattering for fast α-particles is as much as 20 times as great as that given by Rutherford's formula, while for heavier elements, such as Mg and Al, only the beginning of the ascending part of the curve can be observed.

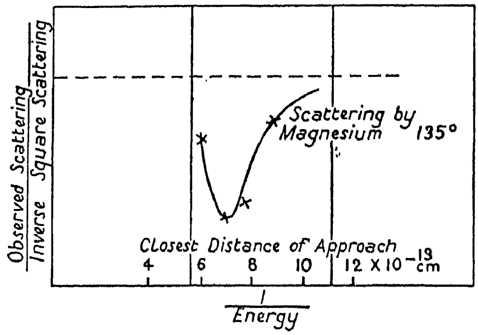

FIG. 25 *b*

We see, therefore, that it is possible to explain qualitatively the observed anomalies in the scattering of α-particles by light nuclei.

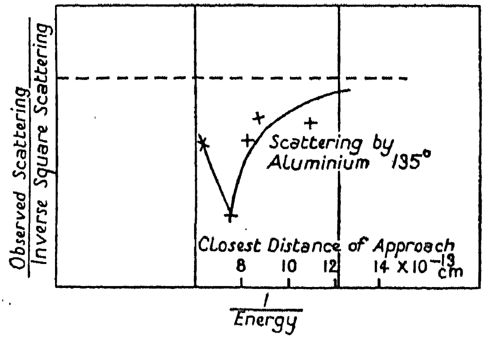

FIG. 25 *c*

At present, however, so little is known about the exact distribution of the potential energy of an α-particle inside the nucleus, that it is useless to try to account quantitatively for the observed deviations.

§ 2. General Theory of Inelastic Collisions

We shall now investigate the inelastic collisions of α-particles with atomic nuclei, when the particle may lose part of its energy, giving rise to certain changes in the nuclear structure. We must distinguish between two different cases:

(A) The nucleus is excited by the collision and a radiative transition can take place to a state of lower energy (artificial excitation of γ-rays).

(B) One of the constituents of the nucleus is ejected during the collision, and the nucleus is changed to that of another element (artificial transformation).

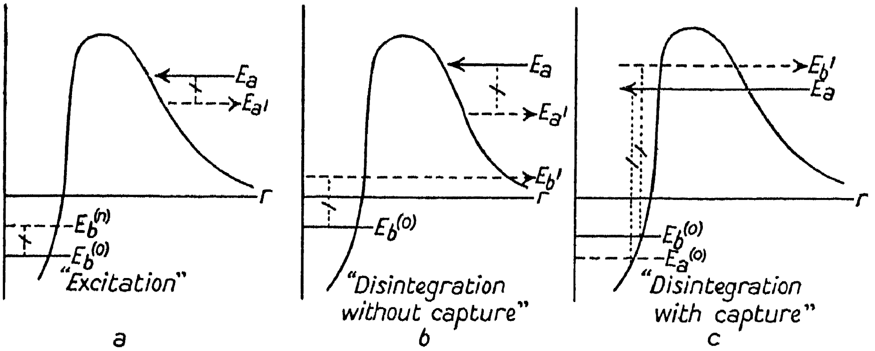

FIG. 26 *a*, *b*, *c*. Types of inelastic collisions with nucleus.

The incident particle can either escape with the rest of the energy or be captured by the nucleus.† The different kinds of inelastic collisions are represented diagrammatically in Fig. 26 *a*, *b*, *c*. Here E_a, $E_{a'}$, $E_a^{(n)}$ denote the energies of the original α-particle before and after a collision without capture and after a collision with capture on the *n*th level; $E_b^{(0)}$, $E_b^{(n)}$, $E_{b'}$ are the energies of the normal and excited states of the nucleus and of the ejected nuclear particle. In the two cases of artificial disintegration (Fig. 26 *b*, *c*) we have for the energy of the ejected nuclear particle the relations:

$$E_{b'} = E_a + [E_b^{(0)} - E_{a'}] + \delta \quad \text{(continuous-spectrum)} \tag{4}$$

$$E_{b'} = E_a + [E_b^{(0)} - E_a^{(n)}] + \delta \quad \text{(line-spectrum)}, \tag{5}$$

where the small correction δ is the recoil energy of the resulting nucleus.

---

† We must notice that the processes of excitation and artificial disintegration can sometimes overlap. If, in the process of excitation, the excited level of the nuclear particle has positive energy the particle can cross the potential barrier and escape, instead of making a transition with radiation. Also, when the nucleus disintegrates the incident α-particle may be captured in one of the excited levels and can fall to the normal level with the emission of a γ-ray.

The probabilities of these different processes are given by the transition probabilities of the system consisting of the α-particle and nuclear particle from the initial state to another state of equal energy. According to the general theory of perturbations in wave mechanics the probability of such a transition is given by the expression

$$W = C\left|\int V(r_{a,b})\psi_a\psi_b\psi_{a'}\psi_{b'}\,d\Omega_a d\Omega_b\right|^2, \tag{6}$$

where $V(r_{a,b})$ is the mutual potential energy of the two particles at a distance $r_{a,b}$ apart, and ψ_a, ψ_b, $\psi_{a'}$, $\psi_{b'}$ are the wave-functions corresponding to the initial and final states of the two particles. We must notice that this formula (6) may be applied only when the probability of the process concerned is small compared with unity. If for certain processes the value calculated from (6) is not small this means that the interaction energy is large and the formula may not be applied. In such cases the exact solution of the problem must be found. The value of the coefficient C depends on the method of normalizing the wave-functions.

If the wave-function ψ belongs to a discrete negative eigenvalue of the energy it is normalized in the usual way:

$$\int \psi\bar{\psi}\,d\Omega = 1. \tag{7}$$

This means actually that the probability of finding the particle *somewhere* is unity. If ψ corresponds to a positive eigenvalue belonging to the continuous spectrum, this normalization loses its meaning, since the integral diverges at infinity. We then use the condition that the flow per unit area across a surface at infinity must be unity. In the different problems of interaction of an incident α-particle with a nucleus, different values of the coefficient C must be taken in the formula (6), according to how many of the four functions belong to the discrete and how many to the continuous spectrum. The value of C for the most important case, where two ψ's belong to negative and two to positive eigenvalues, is $C = \frac{1}{\hbar^2}$.

We shall require three different types of wave-functions:

(A) The wave-function corresponding to a particle in the nucleus on a stable level of negative energy. Such a function represents a stationary wave of practically constant amplitude inside the potential hole of the nuclear model and decreasing exponentially for $r > r_0$ to zero as r tends to infinity. The normalized wave-function may be

$$\psi_{r<r_0} = \frac{1}{\sqrt{\Omega}}\,\omega\, e^{i\frac{E}{\hbar}t}; \quad |\omega|^2 \sim 1,$$

$$\psi_{r_0>r} = 0,$$

where Ω is the volume of the nucleus and ω represents a periodic function depending on the particular nuclear model used, but always of the order of magnitude unity.

(B) The normalized wave-function representing a particle of positive energy E and angular momentum j, ejected from the nucleus:

$$\psi = \frac{1}{r}\,\chi_j(r) Y_j(\phi,\theta)\, e^{i\frac{E}{\hbar}t},$$

where $\chi_j(r)$ are the solutions of the corresponding wave-equation which have at infinity the asymptotic expression

$$\chi_{r\to\infty} = \frac{1}{\sqrt{(4\pi v)}} \sin\left(\frac{\sqrt{(2mE)}}{\hbar}\,r+\alpha\right). \tag{10}$$

(C) The wave-function representing a parallel beam of particles at infinity, i.e. the plane wave

$$\psi_{r\geqslant r_0} = A \sin\left(\frac{\sqrt{(2mE)}}{\hbar}\,x+\alpha\right) e^{i\frac{E}{\hbar}t}, \tag{11}$$

where the direction of the particle is along the x-axis. This is normalized to represent unit flow across unit cross-section of the beam. It is well known that this expression can be expanded as a series of spherical waves, corresponding to particles with different angular momenta j relative to the nucleus:

$$\psi_{r\geqslant r_0} = A \sum_{j=0}^{\infty} \frac{\sqrt{(\pi)}\hbar}{\sqrt{(2mE)}} \sqrt{(2j+1)}\,\frac{1}{r} \sin\left(\frac{\sqrt{(2mE)}}{\hbar}\,r+\alpha_j\right) Y_j(\phi,\theta)\, e^{i\frac{E}{\hbar}t}. \tag{12}$$

Thus, the effect of a plane wave may be considered to be due to a set of spherical waves of different j and corresponding to a flow:

$$A^2 \frac{\pi\hbar^2}{2mE}(2j+1). \tag{13}$$

The solution near the nucleus may be written in the form

$$\psi = A \sum_{j=0}^{\infty} \frac{\sqrt{(\pi)}\hbar}{\sqrt{(2mE)}} \sqrt{(2j+1)}\,\frac{1}{r}\,\chi_j(r) Y_j(\phi,\theta)\, e^{i\frac{E}{\hbar}t}, \tag{14}$$

where $\chi_j(r)$ has the asymptotic expression

$$\chi_j(r)_{r\to\infty} = \frac{1}{\sqrt{(4\pi v)}} \sin\left(\frac{\sqrt{(2mE)}}{\hbar}\,r+\alpha_j\right). \tag{15}$$

The total probability of disintegration due to one incident α-particle per sec. per cm. is

$$W = \sum_{j,j'} \frac{\pi\hbar^2}{2mE}(2j+1)W_{j,j'}, \tag{16}$$

where $\frac{\pi\hbar^2}{2mE}(2j+1)$ may be called the number of collisions per sec. with angular momentum j and $W_{j,j'}$, calculated from normalized spherical waves, the probability of disintegration per collision. The functions $\chi_j(r)$ are the solutions of the equation

$$\frac{\partial^2\chi_j(r)}{\partial r^2}+\frac{2m}{\hbar^2}[E-U_j(r)]\chi_j(r) = 0 \tag{17}$$

where

$$U_j(r) = U(r)+\frac{\hbar^2}{2m}\frac{j(j+1)}{r^2}; \quad E > 0. \tag{18}$$

The only essential boundary condition for the stationary waves with positive energy is

$$\neq \infty \qquad \text{or} \qquad \chi(0) = 0, \tag{19}$$

and we start constructing our solutions from this. Finite solutions are evidently possible for any value of the energy, in contrast to the corresponding problem of disintegration, where the condition that the solution shall represent a divergent wave can be satisfied only for certain discrete values of E. Starting from the value $\chi = 0$ at the centre we must continue the solution through the potential barrier to outside the nucleus. Inside the nucleus, where the kinetic energy is positive, we have, as for spontaneous disintegration, a stationary wave of nearly constant amplitude A. At the inner boundary of the potential barrier this solution must join continuously with the solution corresponding to the 'region of negative kinetic energy'; this solution may be written:

$$\chi_{r_1<r<r_2} = A_+ e^{\frac{1}{\hbar}\int\limits_{r_1}^{r}\sqrt{[U_j(r)-E]}\,dr} + A_- e^{-\frac{1}{\hbar}\int\limits_{r_1}^{r}\sqrt{[U_j(r)-E]}\,dr}. \tag{20}$$

The coefficients A_+ and A_- must be determined from the boundary conditions at $r = r_1$, in the same way as in Chap. II. We see easily that for an arbitrary value of E both coefficients are of the same order of magnitude as A. Inside the potential barrier ($r_1 < r < r_2$) the first member of (20) increases and the second decreases very rapidly, so that, to determine the amplitude of the stationary wave outside the nucleus from the boundary conditions at $r = r_2$, we need only use the first term, and the ratio of the amplitude outside to that inside will be of the order

$$Ae^{\frac{1}{\hbar}\int\limits_{r_1}^{r_2}\sqrt{[U_j(r)-E]}\,dr}.$$

In special cases, when E has a value very near the real part of one of the eigenvalues of the nuclear model, the coefficient A_- in (20) will vanish, as may easily be seen by comparing the solution with those of Chap. II. Thus the ratio of the amplitude outside to that inside is of the order

$$Ae^{-\frac{1}{\hbar}\int\limits_{r_1}^{r_2}\sqrt{[U_j(r)-E]}\,dr}.$$

As the solution $\chi(r)$ outside is always normalized to unity we have for the region inside the nucleus in general

$$\underset{r<r_0}{\chi(r)} \sim e^{-\frac{1}{\hbar}\int\limits_{r_1}^{r_2}\sqrt{[U_j(r)-E]}\,dr}, \tag{23}$$

and in the case of resonance

$$\underset{r<r_0}{\chi(r)} \sim e^{+\frac{1}{\hbar}\int\limits_{r_1}^{r_2}\sqrt{[U_j(r)-E]}\,dr}. \tag{24}$$

§ 3. Excitation of Nuclei by Collision with α-particles

When a nucleus is excited by collision with an incident particle the general shape of the four wave-functions in the interaction integral (6) is shown in Fig. 27. The wave-functions representing both the normal and the excited states of the nuclear particle practically vanish at distances greater than the internal radius r_0 of the potential barrier. On the other hand, the wave-functions representing the incident and reflected particles decrease very rapidly inside the external radius $\left(=\dfrac{Zz_a e^2}{E_a}\right)$ of the barrier. Hence, it is clear that the main part of the integral (6) will be due to the interaction of the particles at comparatively large distances, and we may tacitly assume a Coulomb interaction between the particles, and write

$$I = \int \frac{z_a z_b e^2}{\sqrt{(\mathbf{r}_a-\mathbf{r}_b)^2}} \psi_a \psi_{a'} \psi_b \psi_{b'}\, d\Omega_a d\Omega_b, \tag{25}$$

where z_a, z_b, $\mathbf{r}_a$, and $\mathbf{r}_b$ are the charge-numbers and radius vectors of the incident and nuclear particle. As far as $|\mathbf{r}_a| \gg |\mathbf{r}_b|$ we may expand the Coulomb potential in a series:

$$\frac{1}{\sqrt{(\mathbf{r}_a-\mathbf{r}_b)^2}} = \frac{1}{r_a} + \frac{(\mathbf{r}_a \cdot \mathbf{r}_b)}{r_a^3} + \dots \quad (r_a = |\mathbf{r}_a|), \tag{26}$$

and the integral becomes

$$I = z_a z_b e^2 \left[\int \frac{1}{r_a} \psi_a \psi_{a'} \, d\Omega_a \int \psi_b \psi_{b'} \, d\Omega_b + \int \frac{\mathbf{r}_a}{r_a^3} \psi_a \psi_{a'} \, d\Omega_a \int \mathbf{r}_b \psi_b \psi_{b'} \, d\Omega_b \right]. \tag{27}$$

The second integral in the first member in brackets vanishes (owing to the orthogonality of ψ_b and $\psi_{b'}$) and the second integral in the second member is simply the matrix-element $\underset{n,m}{r_b}$ of the radius vector of the nuclear particle. Integrating over the angles in (27) we get finally

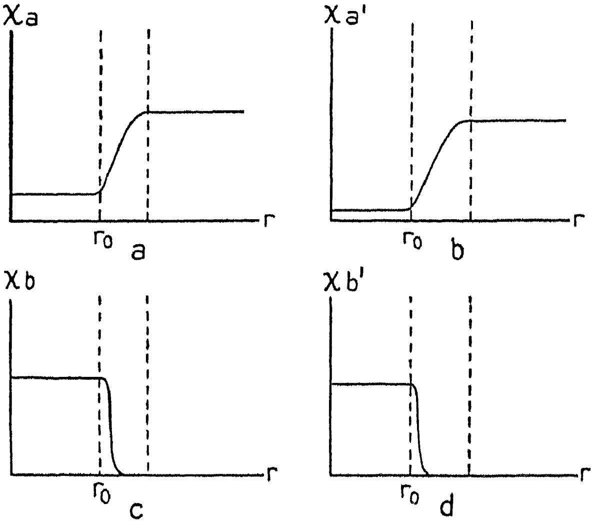

FIG. 27

$$I = z_a z_b e^2 \underset{n,m}{r_b} \int_0^\infty \frac{1}{r_a^2} \chi_a \chi_{a'} \, dr_a, \tag{28}$$

the main part of the integral being due to the integration in the region $r_0 < r$.

The solutions χ_a and $\chi_{a'}$ are given by hypergeometric and have the asymptotic expressions:

$$\begin{aligned} \chi_a_{r\to\infty} &= a \sin\frac{1}{\hbar}\sqrt{(2mE_a)}(r-r^*) \\ \chi_a_{r\to\infty} &= a_1 \sin\frac{1}{\hbar}\sqrt{(2mE_{a'})}(r-r^*) \end{aligned} \qquad r^* \gg r_0. \tag{29}$$

We have already seen that for finite distances from the nucleus we can write the solutions approximately in the form

$$\begin{aligned} \chi_a(r) &= a \sin\left(\frac{1}{\hbar}\int\limits_{r^*}^{r} \sqrt{\{2m[E-U(r)]\}}\,dr + C\right) \\ \chi_{a'}(r) &= a' \sin\left(\frac{1}{\hbar}\int\limits_{r^*}^{r} \sqrt{\{2m[E'-U(r)]\}}\,dr + C'\right). \end{aligned} \tag{30}$$

In the region most important for the integration, just outside the upper limit of the barrier, both functions are rapidly oscillating, and the evaluation of the integral is somewhat difficult. To make the approximate evaluation of the integral possible we must change the path of integration in the following manner:[†] we represent the solution $\chi_a(r)$ as the sum of two exponential functions so that the integral (28) becomes

$$I = z_a z_b e^2 {r_b}_{m,n}\left[C\int\limits_0^\infty \frac{dr}{r^2} e^{+\frac{i}{\hbar}\int\limits_{r^*}^{r}\sqrt{\{2m[E-U(r)]\}}dr} \sin\frac{1}{\hbar}\int\limits_{r^*}^{r}\sqrt{\{2m[E'-U(r)]\}}\,dr + \right.$$

$$\left. + C'\int\limits_0^\infty \frac{dr}{r^2} e^{-\frac{i}{\hbar}\int\limits_{r^*}^{r}\sqrt{\{2m[E-U(r)]\}}\,dr} \sin\frac{1}{\hbar}\int\limits_{r^*}^{r}\sqrt{\{2m[E'-U(r)]\}}\,dr\right]. \tag{31}$$

Both expressions under the integral sign in (31) vanish as $r \to \infty$ owing to the factor $\frac{1}{r^2}$. On the other hand, the integrand in the first member vanishes exponentially for $r \to +i\infty$ and that in the second member for $r \to -i\infty$. We choose, therefore, the paths of integration shown in Fig. 28 and integrate the first member in the upper part of the complex r-plane and the second one in the lower part.

We can easily see that with such a path of integration the value of the whole integral is determined except for a constant factor by

---

I am indebted to L. Landau for the development of this method.

the value of the integrand on the positive part of the imaginary axis in the neighbourhood of the origin, that is, by the expression:

$$e^{-\frac{1}{\hbar}\int\limits_{r^*}^{0}\sqrt{\{2m[U(r)-E]\}}\,dr}\sin\frac{1}{\hbar}\int\limits_{r^*}^{0}\sqrt{\{2m[E'-U(r)]\}}\,dr$$

$$\sim e^{-\frac{1}{\hbar}\int\limits_{r^*}^{0}\sqrt{[2m(U-E)]}\,dr+\frac{1}{\hbar}\int\limits_{r^*}^{0}\sqrt{[2m(U-E')]}\,dr} \tag{32}$$

if the exponents are sufficiently large.

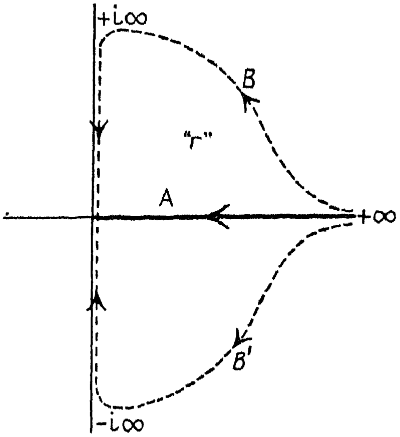

FIG. 28

The evaluation of the constant coefficient in the integral (29) is rather difficult, and we shall content ourselves with having found the dependence of the probability on the energy:

$$W=I^2\sim Ae^{-\frac{2}{\hbar}\left[\int\limits_{r^*}^{0}\qquad\qquad-\int\limits_{r^*}^{0}\sqrt{[2m(U-E')]}\,dr\right]}, \tag{33}$$

or, evaluating the integrals in the exponents in the same way as in the theory of α-disintegration (p. 49):

$$W=Ae^{-\frac{2\pi e^2\sqrt{(2m)}Z}{\hbar}\left(\frac{1}{\sqrt{E'}}-\frac{1}{\sqrt{E}}\right)}.$$

We see that the probability of excitation of a given nuclear level decreases exponentially as the energy $E_0=E-E'$ of the level increases.

The probability decreases also very rapidly with the charge-number of the nucleus, so that we can only expect to observe it for the light elements.

If the excited level of the nucleus is positive, the excited particle can cross the potential barrier and escape from the nucleus; i.e. disintegration without capture of the incident α-particle. As can be seen from the mass-defect curves (see p. 16) the average energy of binding of an α-particle in the nucleus is about 10×10^{-6} erg, so that in order to eject the nuclear α-particle without the capture of an incident one the bombarding α-particles must have energy greater than this. Even in this case the energies, both of the reflected and ejected α-particles, will be rather low and the probability of disintegration very small; in fact, such processes have not yet been observed. The same can be said of the ejection of nuclear protons, although it is not impossible that for certain elements (perhaps B) the energy conditions are especially favourable and the process of ejection of a proton without the capture of an incident α-particle could be observed. As the energy of the reflected α-particle can vary from E_{α_0} to zero the ejected protons have a continuous energy-distribution between zero and $E_{\alpha_0} - E_p^{(0)}$.

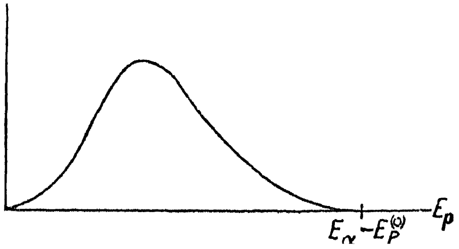

FIG. 29

In order to obtain the probability of disintegration of this kind we have to multiply formula (34) with a factor representing the probability for a proton of energy E_{α_0} $E_{\alpha'} - E_p$ to cross the corresponding potential barrier. We have

$$W = Be^{-\frac{2\pi e^2\sqrt{(2m_\alpha)}Z}{\hbar}\left(\frac{1}{\sqrt{E_{\alpha'}}} - \frac{1}{\sqrt{E_\alpha}}\right) - \frac{\pi e^2\sqrt{(2m_p)}}{\hbar}\frac{Z}{\sqrt{E_p}}}, \tag{35}$$

where B depends on the direction of ejection of the proton. From the formula (35) it can be seen that the intensity in the continuous proton-spectrum vanishes at both the upper and lower limits and reaches a maximum for a value about two-thirds of the upper limit (see Fig. 29). There seems to be some indication of the existence of continuous spectra of low-speed protons in the disintegration of certain elements.

§ 4. Transformation of Nuclei by Collision with α-particles

We shall now investigate in some detail the process of ejection of a nuclear particle when the incident particle is captured. The general shape of the graph of the four wave-functions under the integral sign in (6) is shown diagrammatically in Fig. 30. It is easy to see that the product of the four functions will vanish at all points of the six-dimensional coordinate space, over which the integral must be taken, which correspond to positions of either the a-particle or the b-particle outside the nucleus, i.e. for $r_a > r_0$ or $r_b > r_0$. Thus the integration is taken only over the inside part of the nucleus. The four wave-functions can be represented inside the nucleus by

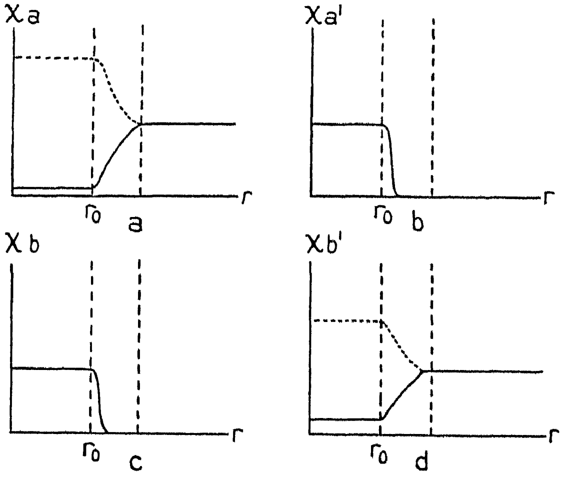

Fig. 30

$$\psi_a = \frac{1}{\sqrt{(\pi v_i)}r_0}\omega_a e^{-\frac{1}{\hbar}I_{j,a}} e^{i\frac{Ea}{\hbar}t}; \qquad \psi_{a'} = \frac{1}{\sqrt{\Omega}}\omega_{a'} e^{i\frac{Ea'}{\hbar}t}; \tag{36}$$

$$\psi_b = \frac{1}{\sqrt{\Omega}}\omega_b e^{i\frac{Eb}{\hbar}t}; \qquad \psi_{b'} = \frac{1}{\sqrt{(\pi v_i)}r_0}\omega_b e^{-\frac{1}{\hbar}I_{j,b'}} e^{i\frac{Eb'}{\hbar}t}; \tag{36'}$$

so that the probability of transformation per collision becomes

$$W_{j,j'} = \frac{1}{\hbar^2}\left[\frac{1}{\sqrt{(\pi v_a)}}\frac{1}{\sqrt{(\pi v_b)}} e^{-\frac{1}{\hbar}I_{j,a}} e^{-\frac{1}{\hbar}I_{j,b'}} \frac{1}{\Omega r_0^2}\int V(r_{a,b})\omega_a\omega_{a'}\omega_b\omega_{b'}\, d\Omega_a d\Omega_b\right]^2 \tag{37}$$

or

$$W_{j,j'} \sim \frac{\overline{V}^2}{K_a K_b} e^{-\frac{2}{\hbar}I_{j,a}} e^{-\frac{2}{\hbar}I_{j,b'}}, \tag{38}$$

where
$$\overline{V} = \frac{1}{\Omega^2}\int V(r_{a,b})\omega_a\omega_{a'}\omega_b\omega_{b'}\,d\Omega_a d\Omega_b \tag{39}$$

represents a certain average of the mutual potential energy of the two particles inside the nucleus and

$$K_a \sim \tfrac{1}{2}m_a v_a^2; \qquad K_b \sim \tfrac{1}{2}m_b v_b^2 \tag{39'}$$

the corresponding kinetic energies. Multiplying by the number of b-particles in the nucleus and the number of particles in the incident wave with momentum j we get, for the total probability of disintegration with capture,

$$W = \sum_{j,j'} \frac{\pi\hbar^2}{2mE}(2j+1)N_b W_{j,j'} = \frac{\pi\hbar^2}{2mE}N_b \sum_{j,j'}(2j+1)\left(\frac{\overline{V}^2}{K_a K_b}\right)e^{-\frac{2}{\hbar}I_{j,a}}e^{-\frac{2}{\hbar}I_{j',b'}} \tag{40}$$

where the sum must be taken over all values of j_a, and the corresponding possible values of j'_b which, from the law of conservation of angular momentum must satisfy the conditions

$$j_a + j_{b'} \geqslant |j_n - j'_n|$$
$$|j_a - j_{b'}| \leqslant j_n + j'_n,$$

where j_n and j'_n are the values of the angular momentum (spin) of the nucleus before and after disintegration.

As we do not know the actual conditions in the nucleus the value of the coefficient in formula (40) cannot be estimated exactly. However, from the fact that the intra-nuclear interactions as obtained from the mass defects are of the same order as the kinetic energy of the α-particles we can expect that the value of the coefficient will be not very much different from unity.

Evaluating the integrals in the exponents of (40) in the same way as in the theory of spontaneous α-disintegration we get finally:

$$W \sim \frac{\pi\hbar^2}{2mE}N_b \sum_{j,j'}(2j+1)e^{-\frac{\pi e^2\sqrt{(2m_a)}Zz_a}{\hbar\sqrt{E_a}} + \frac{4e\sqrt{(2m_a)}}{\hbar}\sqrt{[Zz_a r_0]}(1+\sigma_j)} \times$$
$$\times e^{-\frac{\pi e^2\sqrt{(2m_b)}Zz_b}{\hbar\sqrt{E_b}} + \frac{4e\sqrt{(2m_b)}}{\hbar}\sqrt{[(Z+z_a-z_b)z_b r_0]}(1+\sigma_j)}. \tag{42}$$

It can be seen that in the conditions under which disintegration of light nuclei takes place the probability of disintegration decreases very rapidly with j and j' so that in practice the first member in the expression is important. As the main part of the disintegration is due to the first harmonic of the incident α-wave we must expect that the ejected protons will be equally distributed in all directions;

this, as we shall see later, is in good agreement with the experimental data.

From what has been said (p. 88) about the region of validity of the perturbation formula (6) it may only be applied when one of the exponential factors occurring is small; it is not applicable, for example, when the energy of the incident α-particle and the ejected proton are both greater than the corresponding maximum value of the potential energy in the barrier.

If the energy of either the incident a-particle or ejected b-particle coincides with a corresponding excited level of the nucleus we should expect a resonance phenomenon, i.e. a large increase in the probability of disintegration, as one of the functions χ_a or χ'_b will have much larger values than in other cases (see p. 91). The values of χ in the resonance case are shown in Fig. 30 by dotted lines. In the two cases of resonance the formulae (38) become†

$$\begin{aligned} W_{j,j'} &= \frac{\bar{V}^2}{K_a K_b} e^{+\frac{2}{\hbar}I_{j,a}-\frac{2}{\hbar}I_{j',b'}} && \text{for } I_{j,a} < I_{j',b} \\ W_{j,j'} &= 1 && \text{for } I_{j,a} > I_{j',b'} \end{aligned} \tag{43}$$

and

$$\begin{aligned} W_{j,j'} &= \frac{\bar{V}^2}{K_a K_b} e^{-\frac{2}{\hbar}I_{j,a}+\frac{2}{\hbar}I_{j',b'}} && \text{for } I_{j,a} > I_{j',b'} \\ W_{j,j'} &= 1 && \text{for } I_{j,a} < I_{j',b'}. \end{aligned} \tag{44}$$

These formulae may be applied only when the values of the exponents are negative. Otherwise they have no physical meaning, since they give values greater than unity for the probability of transformation per collision; in such cases we must evidently assume that this probability is unity.

We have already seen that, owing to the strong interaction of the nuclear elements, the two kinds of levels corresponding to either excited a- or excited b-particles are practically indistinguishable. It is therefore more reasonable to say that *resonance will occur if the energy of the incident a-particle coincides with one of the excited states of the whole nucleus* (original nucleus plus a-particle); or, if the reader prefers, if the energy of the incident a-particle coincides with one of the excited 'real' or 'false' a-levels in the nucleus (see p. 70). With this terminology we can express simply the physical meaning of the formulae (33) and (34). If the a-particle falls on the nucleus with the resonance-value of the energy it will always penetrate inside the nucleus; the probability of penetration per collision is unity. Now two possibilities are open; either the a-particle will escape again with its original energy, with a probability depending on $I_{j,a}$, or another particle will be ejected, with a probability depending on $I_{j,b}$. If the probability for the a-particle to escape is the greater ($I_{j,a} < I_{j,b}$) the percentage of ejected b-particles will evidently be given by the ratio $e^{-I_b}/e^{-I_a} = e^{I_a - I_b}$, in accordance with the formula (33). If the ejection of the b-particle is more probable than the rejection of the a-particle ($I_{ja} > I_{jb}$) evidently a b-particle will be ejected for every collision and $W = 1$.

---

† From what was said on p. 91 we must, in the case of resonance, change the sign in the exponential in the expression for χ.

§ 5. Comparison with Experiment

The excitation of nuclei by collision with incident α-particles was recently investigated by Bothe and Becker,† who succeeded in observing rather hard γ-radiation from a number of light elements bombarded with α-particles from polonium. We must distinguish between two different kinds of artificial γ-rays:

(1) those which arise from the pure excitation of the bombarded nucleus when the incident α-particle is reflected;

(2) those which are emitted in a disintegration when the incident α-particle is captured on one of the higher levels of the nucleus.

The most characteristic example of γ-emission of the first kind is that of Be-nuclei, which, although they emit strong γ-radiation, have never been observed to disintegrate. Of all the light elements, beryllium shows the strongest γ-radiation, and its properties have been investigated rather thoroughly. It is fairly homogeneous with an absorption coefficient 0·5 cm.$^{-1}$ in lead. Direct measurements of the energy of the γ-rays emitted during artificial excitation have not yet been made.

The energy of the emitted γ-rays does not depend (within the limits of error) on the energy of the incident particles; this would be expected, as the γ-rays in question correspond to transitions between quite definite energy-levels of the nucleus. On the other hand, the intensity of the γ-radiation depends very much on the energy of the α-particles and decreases very rapidly with it. In Fig. 31 the number of emitted γ-quanta is plotted against the range of the incident α-particles. The dotted curve is obtained by differentiation and represents directly the number of emitted γ-quanta due to α-particles of a given range.

---

† Bothe and Becker, *Zs. f. Phys.*, vol. lxvi, p. 289 (1930).

A theoretical formula for the probability of excitation was developed in § 3. As the coefficient in the formula (34) cannot be evaluated exactly, it gives only the relative probabilities for α-particles of different energies. We have:

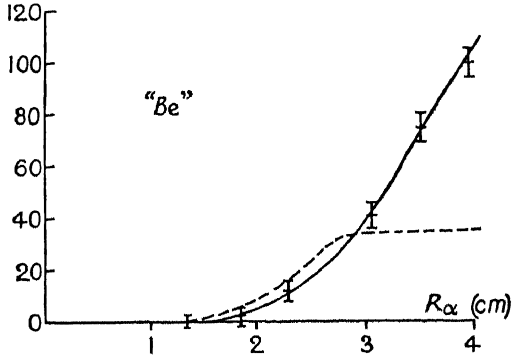

FIG. 31

$$\frac{W_1}{W_2} = e^{-\frac{2\pi e^2\sqrt{(2m_\alpha)}\,Z}{\hbar}\left(\frac{1}{\sqrt{E_{\alpha_1}}}-\frac{1}{\sqrt{E_{\alpha_2}}}\right)}. \tag{45}$$

For large values of E_α, when the energy of the α-particles is greater than the height of the potential barrier surrounding the beryllium nucleus, the expression (45) becomes unity and the theoretical curve runs parallel to the E axis. As can be seen from the figure, the agreement between theory and experiment is quite reasonable.

The results of Bothe and Becker for other elements are shown in Fig. 32, where the intensity of the artificial γ-radiation (expressed roughly as the number of γ-quanta per α-particle) is plotted against the charge-number of the nucleus. We notice that except for the two lightest elements (Li and Be) the excitation of γ-rays has been observed only for elements which show artificial disintegration. Although we ascribe the γ-rays from Li and Be to pure excitation, we must keep in mind the possibility of the other process which can occur in the disintegrable nuclei. If the incident α-particle is captured on one of the higher energy-levels of the product-nucleus, the proton ejected will have smaller energy than if it were captured on the normal level. This energy-difference must, however, be emitted later on in the form of γ-radiation. It is very plausible that the γ-rays observed from boron, aluminium, and some other disintegrable elements are of this kind.

We shall now study the experimental results on the artificial disintegration of the elements which have been most thoroughly investigated, in order to test the results of our general theoretical considerations. These elements are nitrogen, boron, and aluminium.

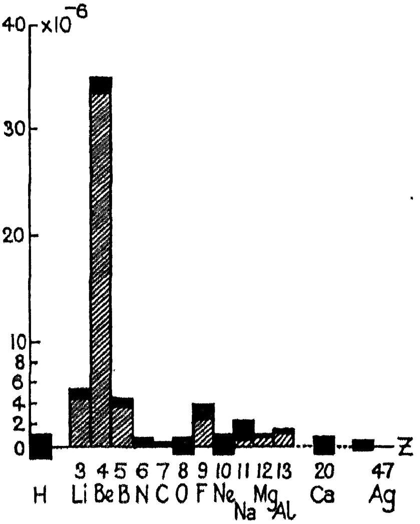

FIG. 32

Nitrogen. Nitrogen, the first element disintegrated, was investigated by Rutherford and Chadwick,† who used the α-particles of RaC′. The results of their experiments are shown in Fig. 33. As in these experiments thick layers of the matter to be disintegrated were used, the range-distribution diagram of the ejected protons is rather spread out. The energy of the ejected protons for each initial energy of the incident α-particles is given by the maximum observed range. We have the values given in the following table for the balance of energy in the disintegration.

TABLE I

ϕ	R_α(cm.).	R_p(cm.).	$E_\alpha \times 10^6$ erg.	$E_p \times 10^6$ erg.	$E_n \times 10^6$ erg.	$\Delta E \times 10^6$ erg.
0°	8·5	51	14·0	11·5	0·7	−1·8
0°	6·9	40	12·2	9·8	0·6	−1·8
0°	5·9	34	11·1	8·8	0·5	−1·8
0°	4·8	27	9·6	7·6	0·5	−1·5

---

† E. Rutherford and J. Chadwick, *Phil. Mag.*, vol. xlii, p. 809 (1921).

We see that in the disintegration of nitrogen energy is always lost; $\Delta E = -1{\cdot}7 \,.\, 10^{-6}$ erg $= -1{\cdot}1 \,.\, 10^{6}$ volt.

From these experiments it is impossible to decide whether the protons belong to a discrete group arising from 'collisions with capture' or whether they belong to the continuous spectrum; it is also not impossible that there are several discrete groups of protons, as these would be difficult to detect from the observed range-distribution.

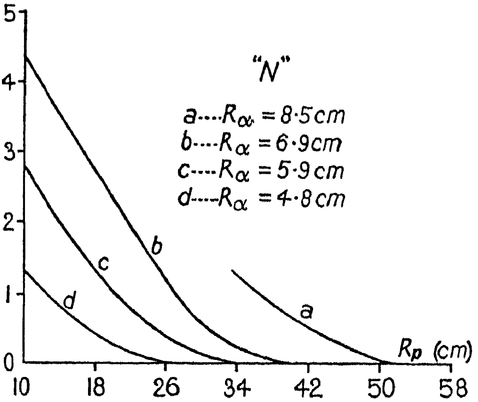

Fig. 33

Direct observations of the process of artificial disintegration of nitrogen have been made by Blackett in a Wilson chamber.[†] He succeeded in obtaining eight photographs of disintegrations. The fact that we can only see two tracks after the collision suggests that the α-particle has been captured by the nucleus during the process of ejection of a proton. Measurement of the angles shows that one track is due to a particle of unit mass (proton) and the other to a particle three units heavier than the nitrogen nucleus (the product nucleus after the ejection of a proton and capture of an α-particle). Thus we can conclude certainly that in the disintegration of nitrogen an α-particle is captured; evidently the conditions necessary for the existence of a continuous spectrum (see p. 87) are not fulfilled for nitrogen. Blackett gives the value $\Delta E = -2{\cdot}3 \,.\, 10^{-6}$ erg in satisfactory agreement with the data of Rutherford and Chadwick. The existence of only one group of protons ejected from nitrogen seems to prove that in this case the incident α-particle is always captured on the normal level (we shall see that in B and Al α-particles producing disintegration are sometimes captured on one of the excited levels). This is in good agreement with the results of Bothe, who could find no traces of γ-radiation in the disintegration of nitrogen (compare Fig. 32).

The number of protons ejected from N by α-particles of different initial ranges is shown in Fig. 34; the dotted curve (obtained by differentiation) represents the relative probability of disintegration for a given energy of the α-particle. It can be seen from the figure that the curve is in general agreement with the theoretical predictions; the probability increases first very rapidly with the energy of the α-particles, and for greater energies (greater than the height of the barrier) tends to a constant value.

[†] P. M. S. Blackett, *Proc. Roy. Soc.*, A, vol. cvii, p. 349 (1925).

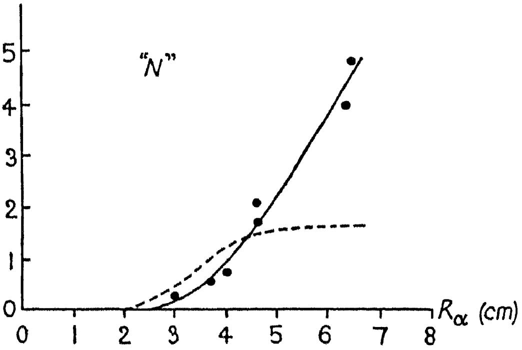

FIG. 34

Boron. The artificial disintegration of boron has been carefully investigated by Bothe and Fränz,[†] who used α-particles from Po and some from RaC′. The protons ejected from boron present three distinct groups, as shown in Fig. 35. We do not know whether all three observed groups are due to the most abundant isotope B_{11},[‡] but there seem to be certain indications that this is not so (see p. 114). From the observed ranges we find that for groups I and II the balance of energy is positive, so that both these groups are due to disintegrations with capture. For the group III the balance of energy is negative, and consequently this group may be due to disintegrations without capture; as we shall see, the peculiar behaviour of this group makes it very probable that it belongs to the continuous spectrum.

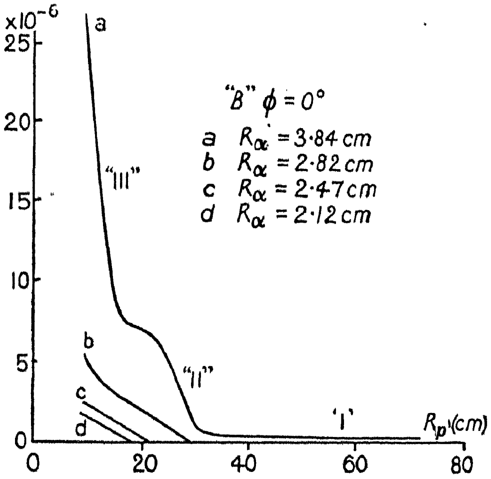

FIG. 35

As we have seen, the velocity of the ejected protons must decrease with the angle ϕ of ejection (owing to the varying energy taken by the recoil nucleus) and the range-distribution diagram will be different for different angles of observation. In fact, for a direction nearly opposite to that of the incident α-particles ($\phi = 153°$) the group III can already scarcely be detected, while the ranges of the groups I and II are considerably reduced. The variation of the range-distribution of the three groups of protons, with the direction of emission, is shown in Figs. 36 *a*, *b*, *c*, where the experimental curve is divided into three parts.

[†] Bothe and Fränz, *Zs. f. Phys.*, Bd. 49, s. 1 (1928); Fränz, ibid., Bd. 63, s. 370 (1930); Bothe, ibid., Bd. 63, s. 381 (1930).

[‡] Boron has two isotopes B_{11} and B_{10} with relative abundance 4 : 1.

We observe a striking difference between the first figure and the other two. The protons of group III seem to be ejected chiefly in the forward direction; this is strong evidence that we are dealing here with the continuous spectrum (see p. 95). On the other hand, for groups I and II the ranges gradually decrease with the angle ϕ, while the intensity is practically constant. We see that the protons of these groups are distributed fairly uniformly in all directions; this is just what we should expect from our theoretical considerations for the protons ejected in disintegrations with capture of the incident α-particle.

From the observed ranges in different directions we can calculate the corresponding velocities v of the protons in the different groups. We have:

TABLE II

ϕ	0°	153°
R_p (cm.)	74	33
$v_p \times 10^{-9}\ \frac{\text{cm.}}{\text{sec.}}$	4·2	3·2

B-Group I

ϕ	0°	7·5°	30°	52·5°	106°	153°
R_p (cm.)	33	32	29	27	20	15
$v_p \times 10^{-9}\ \frac{\text{cm.}}{\text{sec.}}$	3·2	3·2	3·1	3·0	2·7	2·4

B-Group II

ϕ	0°
R_p (cm.)	*c.* 20
$v_p \times 10^{-9}\ \frac{\text{cm.}}{\text{sec.}}$	*c.* 2·6

B-Group III

The velocity of the incident α-particles of polonium is $1{\cdot}59 . 10^9 \frac{\text{cm.}}{\text{sec.}}$. For a disintegration with capture of the incident particle it can easily be shown from the law of conservation of momentum that the velocities of protons ejected in different directions must be equal to one another in a coordinate system moving with the centre of mass of the system.

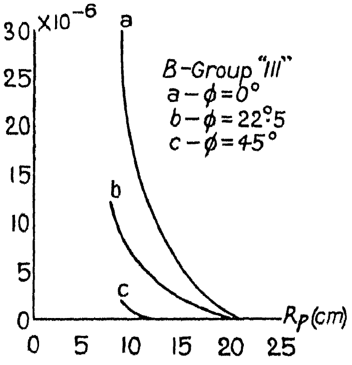

FIG. 36 *a*

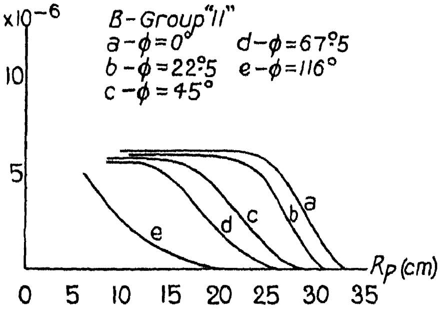

FIG. 36 *b*

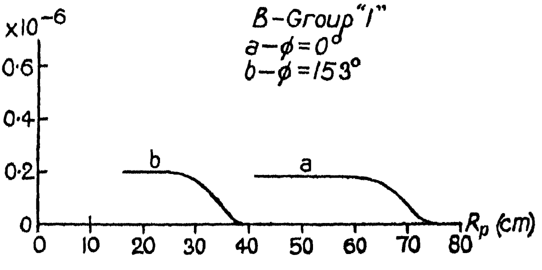

FIG. 36 *c*

If an α-particle of polonium ($v = 1{\cdot}59 . 10^9 \frac{\text{cm.}}{\text{sec.}}$) collides with the nucleus of one of the boron isotopes B_{11} or B_{10}, the centre of mass of the system will move with velocity $\frac{4}{4+11} \times \qquad = 0{\cdot}42 . 10^9 \frac{\text{cm.}}{\text{sec.}}$

or $\frac{}{4+10} . 1{\cdot}59 . 10^9 = 0{\cdot}45$. If we plot the velocities of the ejected protons in polar coordinates the points must lie on the circles with centres $0{\cdot}42 \times 10^9$ or $0{\cdot}45 \times 10^9$, according to the isotope from which the proton is ejected. Fig. 37 shows that this condition is satisfied rather well for both groups I and II, although the experimental

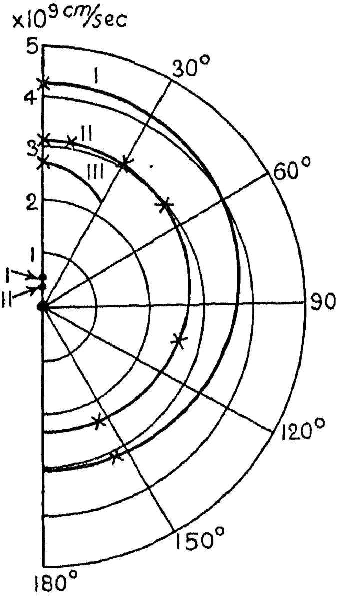

FIG. 37. Velocity-distribution diagram for disintegration of Boron.

accuracy is not sufficient to distinguish whether these groups are due to the same or different isotopes of boron. For group II we obtain 0·38.10⁹, and for I, 0·52.10⁹ (from two points only!); the deviations from the calculated values must evidently be due to the inaccuracy of the Geiger relation between velocity and range.

If the energy of the incident α-particles is reduced, the range-distribution diagram rapidly changes. The maximum ranges of the three groups will decrease and the intensity of each will be quickly lowered. These conditions are shown in Fig. 35. The groups II and I very soon disappear as the energy of the α-particles is decreased, while the group III can be observed considerably longer. The balance of energy for the three groups is given in the following table:

TABLE III

Group.	ϕ	R_α (cm.).	R_p (cm.).	$E_\alpha \times 10^6$ erg.	$E_p \times 10^6$ erg.	$E_n \times 10^6$ erg.	$\Delta E \times 10^6$ erg.
III	0°	3·84	c. 20	c. 8·36	c. 6·2	c. 0·4	c. −1·8
II	0°	3·84	33	8·36	8·6	0·6	+0·8
		2·82	29	6.83	7·9	0·6	+1·7
		2·47	22	6·25	6·6	0·5	+0·8
		2·12	18	5·66	5·7	0·4	+0·4
I	0°	3·84	74	8·36	14·7	1·1	+7·4

Thus we may deduce that the balance of energy for the different groups is

$$\Delta E_{\rm I} = +7{\cdot}4\times 10^{-6}\,\text{erg} = +4{\cdot}7\times 10^{6}\,\text{volt.}$$
$$E_{\rm II} = +0{\cdot}9\times 10^{-6}\,\text{erg} = +0{\cdot}6\times 10^{6}\,\text{volt.}$$
$$= -1{\cdot}8\times 10^{-6}\,\text{erg} = -1{\cdot}1\times 10^{6}\,\text{volt.}$$

The value $\Delta E_{\rm III}$ must give directly the energy of binding of the proton in the boron nucleus (provided the group III is actually the continuous spectrum), the values $\Delta E_{\rm I}$ and $\Delta E_{\rm II}$ the differences between the fundamental level of the proton and the excited and fundamental levels of the α-particle. If the α-particle is captured on an excited level a transition to the normal level with the emission of γ-radiation must take place. Such γ-radiation was actually observed in the disintegration of boron by Bothe. The absorption coefficient of the γ-rays observed is 0·7 cm.$^{-1}$ (in lead) which gives an energy of about $1{\cdot}6 \,.\, 10^{-6}$ erg. The fact that this energy is considerably smaller than the value of ΔE_{I} is evidently to be explained by the supposition that the transition to the normal state occurs in several steps.

Aluminium. Rutherford and Chadwick[†] found that the protons ejected from aluminium belong to two different groups. The α-particles from RaC′ give rise in aluminium to protons with ranges 90 cm. and 56 cm. (in the forward direction), the long-range group being rather weak. Both groups appear to be discrete and have to be ascribed to the process of capture of the incident α-particle on the normal and one of the excited energy-levels. These two groups of protons have energies $16{\cdot}5 \times 10^{-6}$ erg and $12{\cdot}2 \times 10^{-6}$ erg, which, taking into account the recoil energy of the nucleus, give for the balance of energy in the two cases:

$$\Delta E_{\mathrm{I}} = +4{\cdot}8 \times 10^{-6}\,\text{erg} = +3{\cdot}0 \times 10^{6}\,\text{volt}.$$
$$\Delta E_{\mathrm{II}} = +0{\cdot}4 \times 10^{-6}\,\text{erg} = +0{\cdot}25 \times 10^{6}\,\text{volt}.$$

No continuous spectrum has been with any certainty observed for aluminium, although some faint traces of it seem to be observed in the forward direction.

Very interesting experiments on the disintegration of aluminium have been made by Pose,[‡] who succeeded in observing the phenomenon of resonance disintegration discussed in a previous paragraph. The idea of the experiments is briefly as follows. If a homogeneous beam of α-particles falls on a foil of the element to be disintegrated, and the foil is thick enough to stop all the α-particles, then in the different layers of the foil there will be α-particles with energies varying from the initial value to zero. The groups of protons resulting from disintegrations with capture will not be very distinct; there will be an overlapping, as protons will be ejected in different layers of the foil by α-particles with different energies.[§] Suppose now that for a certain energy of the α-particle, between the initial value and zero, resonance can occur. The result will be a large increase of production of protons in a certain layer of the foil where the α-particles have this particular energy. We shall therefore expect to observe a rather well-defined group of protons in the otherwise indistinct spectrum. The range of this group of protons will not change if the energy of the incident α-particles is decreased, but will suddenly disappear if this energy becomes smaller than the resonance value. In investigating the range-distribution of the protons ejected by the α-particles of Po from a thick foil of aluminium, Pose has actually found two such groups with ranges 58 cm. and 47·5 cm. (in the forward direction). If the energy of the incident α-particles is reduced by means of different filters, these groups disappear one after the other. The results of these experiments are shown in Fig. 38. We see that the range and intensity of the ordinary group III decrease regularly with the energy of the α-particles, while the groups I and II behave quite differently, as we should expect for the resonance groups. The group I scarcely changes in intensity if the range of the incident α-particles is decreased from 3·63 cm. to 2·9 cm., and it completely disappears if the range R_α is less than 2·9 cm. We observe the same effect for the group II, which disappears between $R_\alpha = 2\cdot5$ cm. and $R_\alpha = 2\cdot16$ cm. From this we conclude that the ranges of the α-particles producing these two resonance effects have as lower limits $2\cdot9 < R_{\alpha,\mathrm{I}} < 3\cdot63$; $2\cdot16 < R_{\alpha,\mathrm{II}} < 2\cdot5$.

[†] Rutherford and Chadwick, *Proc. Camb. Phil. Soc.*, vol. xxv, p. 186 (1929).

[‡] M. Pose, *Zs. f. Phys.*, Bd. 64, s. 1 (1929); Bd. 67, s. 194 (1931).

[§] The main part of the protons will come from the surface of the foil as the probability of disintegration decreases with the velocity of the α-particle.

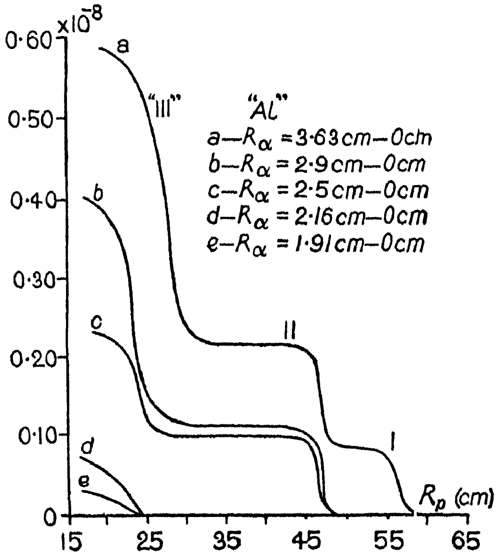

FIG. 38

Another set of experiments has been made to estimate the upper limits of the resonance energies. If the initial velocity of the α-particles is kept constant and the thickness of the aluminium foil reduced, the α-particles inside the foil will have ranges from 3·63 cm. to a certain minimum value easily found from the thickness of foil used. By taking thinner and thinner foils this lower limit of the energy of the α-particles is increased. It can be seen from the curves in Fig. 39 that with such an arrangement the groups I and II disappear if there are no α-particles with ranges smaller than certain values. Thus we have $3{\cdot}02 < R_{\alpha, \mathrm{I}} < 3{\cdot}48$ and $1{\cdot}78 < R_{\alpha, \mathrm{II}} < 2{\cdot}39$. Taking into account these two limits we have that the ranges of the α-particles for which resonance occurs are:

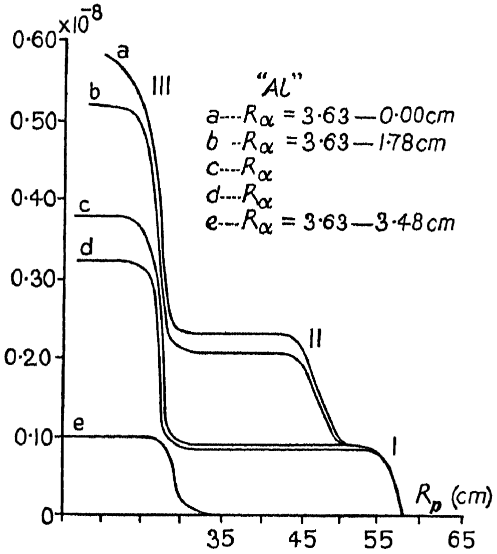

FIG. 39

$$R_{\alpha, \mathrm{I}} = 3{\cdot}25 \text{ cm.} \pm 0{\cdot}24 \text{ cm.}$$
$$R_{\alpha, \mathrm{II}} = 2{\cdot}28 \text{ cm.} \pm 0{\cdot}12 \text{ cm.}$$

From these ranges we deduce the energies of the α-particles producing resonance to be $(7{\cdot}5 \pm 0{\cdot}4)10^{-6}$ erg and $(5{\cdot}9 \pm 0{\cdot}2)10^{-6}$ erg. The ranges of the corresponding groups of protons with ranges 58 cm. and 47·5 cm. are $12{\cdot}5 \times 10^{-6}$ erg and $10{\cdot}9 \times 10^{-6}$ erg. Introducing the correction for the recoil of the nucleus, we get for the balance of energy in the two cases:

$$\Delta E_{\mathrm{I}} = +5{\cdot}4 \times 10^{-6}\,\text{erg} = +3{\cdot}4 \times 10^{6}\,\text{volt.}$$
$$\Delta E_{\mathrm{II}} = +5{\cdot}4 \times 10^{-6}\,\text{erg} = +3{\cdot}4 \times 10^{6}\,\text{volt.}$$

We see that the balance of energy for both observed resonance lines is the same as that for the ordinary group I of aluminium (p. 117); they must therefore be ascribed to disintegrations with capture of the α-particle in the fundamental level.[†]

We should also expect the existence of resonance groups due to the capture of α-particles on the first excited level and having the same balance of energy as the ordinary group II. Such groups, however, have not yet been observed, owing to the small ranges.

Very careful investigations of the artificial disintegration of light elements by Po α-particles have been recently published by Chadwick, Constable, and Pollard.[‡] These experiments confirmed in general the previous results on boron, nitrogen, and aluminium, and also provided fresh data on some other elements. The deviations from the Geiger law connecting energy and range for protons have been taken into account, which makes the values for the balance of energy given in this work more reliable. The results obtained are given in Table VI.

TABLE IV

Disintegration of light elements by α-particles of Polonium
$(R_\alpha = 3{\cdot}8)$; $E_\alpha = 8{\cdot}36 \,.\, 10^{-6}$ erg.

Name of the element.	Mass-number M.	Charge-number Z.	Direction of ejected proton ϕ.	Range of the proton R_p (cm.).	Energy balance.		Notes.
					$\Delta E \times 10^6$ erg.	$\Delta E \times 10^{-6}$ volt.	
B	10; 11	5	0°	$\begin{cases} 76 \\ 32 \end{cases}$	+5·1 +0·3	+3·2 +0·2	And indications of the group $R_p = 20$ cm.
N	14	7	0°	17·5	−2·1	−1·3	Single group.
F	19	9	0°	55	+2·9	+1·8	And indications of several slower groups.
Na	23	11	0°	44	+1·6	+1·0	And indications of several slower groups.
Al	27	13	0°	$\begin{cases} 65 \\ 32 \end{cases}$	+3·7 −0·2	+2·3 −0·1	And indications of the group $R_p = 15$ cm.
P	31	15	90°	31	+0·8	+0·5	Single group.

Very few data on the disintegration of other light elements are at present available. Some time ago Rutherford and Chadwick[§] succeeded in disintegrating almost all the light elements up to $Z = 20$, by using very fast α-particles of RaC′. The probability of disintegration, and also the energy of the ejected protons, decreases very rapidly as the charge of the nucleus increases.

[†] Prof. L. Meitner informs me however, that recent experiments done in her laboratory show no trace of resonance-phenomena in aluminium as observed by Pose.

[‡] J. Chadwick, J. E. R. Constable, and E. C. Pollard, *Roy. Soc. Proc.*, A, vol. cxxx, p. 463 (1931).

[§] E. Rutherford and J. Chadwick, *Proc. Phys. Soc. Lond.*, vol. xxxvi, p. 417 (1924).

§ 6. Balance of Energy in Artificial Transformations

Examination of the data at present available shows first that the most intense artificial disintegration, both as regards range and the number of the ejected protons, is observed with elements of atomic weight different from $4n$. The only exceptions to this rule are the lightest elements, lithium ($4n+3$, $4n+2$) and beryllium ($4n+1$). As for these elements the potential barriers preventing the α-particle from getting into the nucleus and the proton from escaping are very low (lower than the energy of the α-particles used), we must deduce that the failure to disintegrate these elements is due to unfavourable energy conditions, connected in some way with the behaviour of the mass-defect curve near the beginning (see p. 113).

On the other hand, the elements of the $4n$-type are very difficult to disintegrate. The lightest known elements of this type, He(4), C(12), O(16), show no trace of disintegration, while the heavier elements, for which the main isotope is of the $4n$-type (Ne, Mg, Si, S), send out only a few protons of very short range. We could ascribe this small effect to the disintegration of isotopes of higher order mixed in small quantities with the main isotope; but the fact that the protons observed from these elements have a very small balance of energy compared with those from other elements not of the $4n$-type, makes it more reasonable to suppose that we have to deal with the disintegration of the isotope of the $4n$-type itself. This receives strong confirmation from the fact that argon, in which both isotopes are of the $4n$-type, is also disintegrated. As we shall see, this hypothesis is also rendered plausible from the analysis of the general shape of the mass-defect curve for light elements.

No elements with atomic number greater than 19 have so far been disintegrated; this does not, however, give us any definite information about the energy conditions necessary for nuclear transformations, as for nuclei with larger charge-numbers the probability of disintegration is very small, due to the height of potential barrier.

We shall now compare the data for the energy of binding of light nuclei obtained from the study of artificial disintegration with the mass-defect measurements. In Fig. 40 the energies of binding of light nuclei (considered as built up of α-particles, protons, and electrons), as obtained from the measured mass-defects, are indicated by the dotted circles (⊙). Smooth curves are drawn through the observed points corresponding to the same types of nuclei, and the black dots indicate the hypothetical energy of binding of the nuclei for which the mass-defect has not been measured. The curve $4n+4$ is drawn on the assumption that all possible protons and electrons are not bound into α-particles, so that more than three loose protons can exist; in the same way we can construct the curves $4n+5$, $4n+6$,.... We must notice that the curves of Fig. 40 keep their formal meaning for the analysis of the energy conditions in nuclear transformations, even if the hypothesis that the nucleus is built up from α-particles as a whole is wrong.

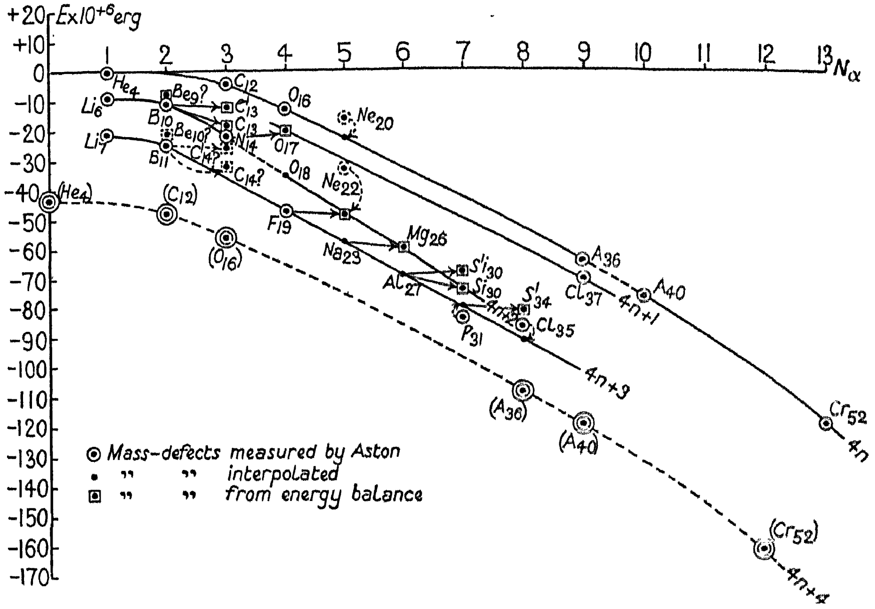

FIG. 40. Mass-defect curve for light elements from direct measurements and from the energy-balance in artificial transformations.

The balance of energy as obtained from artificial disintegration gives us directly the difference between the energy of binding of the original nucleus and that of the product of disintegration. The largest value of the balance of energy for disintegrations with capture of an α-particle gives us the fundamental energy-level of the product-nucleus, while the smaller discrete values of the balance of energy give the excited levels. The balance of energy corresponding to the upper limit of the continuous spectrum gives the energy of binding of a nucleus containing one proton less than the original one. The energies of binding obtained in this way are indicated in Fig. 40 by little squares, while the arrows indicate the transformation by which the nucleus in question has been obtained.†

From the diagram we see immediately that the conditions are very unfavourable for the ejection of protons for the lighter elements of the $4n$-type, and disintegration can be expected only with α-particles of enormous energy. For example, in order to eject a proton from oxygen, α-particles with energy much greater than 9.10^{-6} erg are necessary for 'disintegrations with capture' and much greater than 19.10^{-6} erg for 'disintegrations without capture'. For heavier elements of this type the distance between the $4n+4$ and $4n+3$ curves decreases, and we should expect disintegration to be possible, although the balance of energy is still rather small. We see from the figure that if we actually ascribe the observed disintegration of Ne, Mg, Si, S to the main isotopes of the $4n$-type, the points for the products of disintegration (Na_{23}, Al_{27}, P_{31}) fit reasonably with the $4n+3$ curve.

The data for disintegration of elements of the $4n+3$ type (Li_7, B_{11}, F_{19}, Na_{23}, Al_{27}, P_{32}) help us to construct the energy-curve for nuclei of the $4n+2$ type, for which the mass-defect measurements give very little information. For $N_\alpha > 3$ this curve varies in the same way as the $4n+3$ curve.

Some difficulties have been met in deciding to which of the two isotopes of boron we should ascribe the observed disintegrations. If we ascribe the observed continuous distribution of protons (assuming that it is really continuous) to the more frequent isotope B_{11}, the point for the product of disintegration, Be_{10}, must lie just under the point for B_{11}. As the same product will be obtained from the disintegration of Li_7 with capture of an α-particle, we see from the diagram that Li_7 should easily be disintegrated, even with a positive balance of energy. Since the disintegration of Li_7 has never been observed, we are forced to ascribe the observed continuous spectrum to the disintegration of B_{10} (with the product-nucleus C_{13}). Then Li_6 should be easily disintegrable, but owing to its comparatively small abundance the effect would be very weak. Moreover, we should expect a large loss of energy in the disintegration of Be_7, which agrees with the experimental data. We meet a similar difficulty with the groups of protons I and II from boron. If we ascribe the group I to B_{10}, with the product C_{13}, there is an irregularity in the $4n+1$ curve. If, however, we ascribe this group to B_{11}, the point for the product, C_{14} will lie deeper than the point for N_{14}. As C_{14} differs from N_{14} by one electron only, it would be difficult to understand why the N_{14} nucleus does not capture an electron, from the K-shell, say, and so transform itself into the more stable nucleus C_{14}.

---

† As we have seen, we cannot be certain from which boron isotope the observed proton groups are ejected; therefore both possibilities are indicated in the figure.

All these difficulties in interpretation are due to the incompleteness of the available experimental material, and a more detailed study of mass-defects and artificial disintegration of light elements will enable us to find the true shape of the energy-curves. In spite of the incompleteness of our knowledge we can already make some predictions, based on the energy-curves, about the possibility of disintegrating a given element. Specially interesting conclusions can be drawn concerning the possibility of disintegrating light elements by collisions with protons, with the ejection of α-particles. For example, we can see from the curves that a large gain of energy may be expected when an α-particle is ejected and a proton captured by the lighter nuclei of the $4n+3$ type (Li_7, B_{11}, Fl_{19}), whereas with nuclei of the type this would mean a loss of energy.